OBSERVATION OF COSMIC RAY ANISOTROPY ABOVE TEV ENERGIES IN ICECUBE

Simona Toscano *on behalf of the* **IceCube collaboration**

3rd Roma International Conference on Astro-particle Physics

25-27 May 2011
Roma Italy

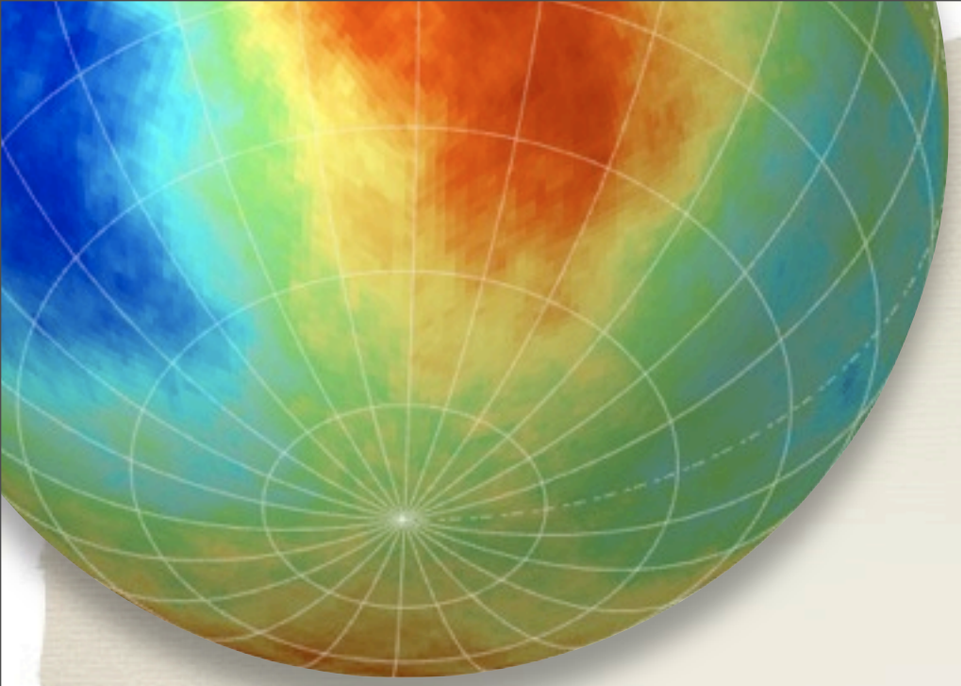

Outline

- The **IceCube** detector
- Energy dependence of the **large scale anisotropy** *(paper in preparation)*:
  - preliminary results at 20 and 400 TeV.
  - solar dipole
- **Medium and small scale** structures (submitted to ApJ, **arXiv:1105.2326**):
  - analysis
  - systematics
- Conclusions

Bartol Research Inst, Univ of Delaware, USA
University of Alaska Anchorage, USA
Pennsylvania State University, USA
University of Wisconsin-Madison, USA
University of Wisconsin-River Falls, USA
LBNL, Berkeley, USA
UC Berkeley, USA
UC Irvine, USA

Universität Mainz, Germany
DESY Zeuthen, Germany
Universität Wuppertal, Germany
Universität Dortmund, Germany
Humboldt Universität, Germany
TWTH Aachen, Germany
Universität Bonn, Germany
Ruhr-Universität, Bochum, Germany
MPI, Heidelberg, Germany

Uppsala Universitet, Sweden
Stockholm Universitet, Sweden

Imperial College, London, UK
University of Oxford, UK

Université Libre de Bruxelles, Belgium
Vrije Universiteit Brussel, Belgium
Université de Mons, Belgium
Universiteit Gent, Belgium

EPFL, Lausanne, Switzerland

University of Alberta, Canada

Chiba University, Japan

Univ. of Alabama, USA
Clark-Atlanta University, USA
Georgia Tech
Ohio State University
Univ. of Maryland, USA
University of Kansas, USA
Southern Univ. and A&M College,
Baton Rouge, LA, USA

University of the West Indies, Barbados

University of Canterbury,
Christchurch, New Zealand

IceCube Collaboration

10 countries
36 institutions
~260 collaborators

The IceCube detector

➡ **G. Sullivan** - *Status and Recent Results from the IceCube km^3 Neutrino Detector* (tomorrow Plenary)
➡ **T. DeYoung** - *Particle physics in ice with IceCube DeepCore* (today next Parallel session)

- **86 strings**
- **5160 DOMs**
- **17 m vertical spacing**
- **125 m between strings**

Digital Optical Module

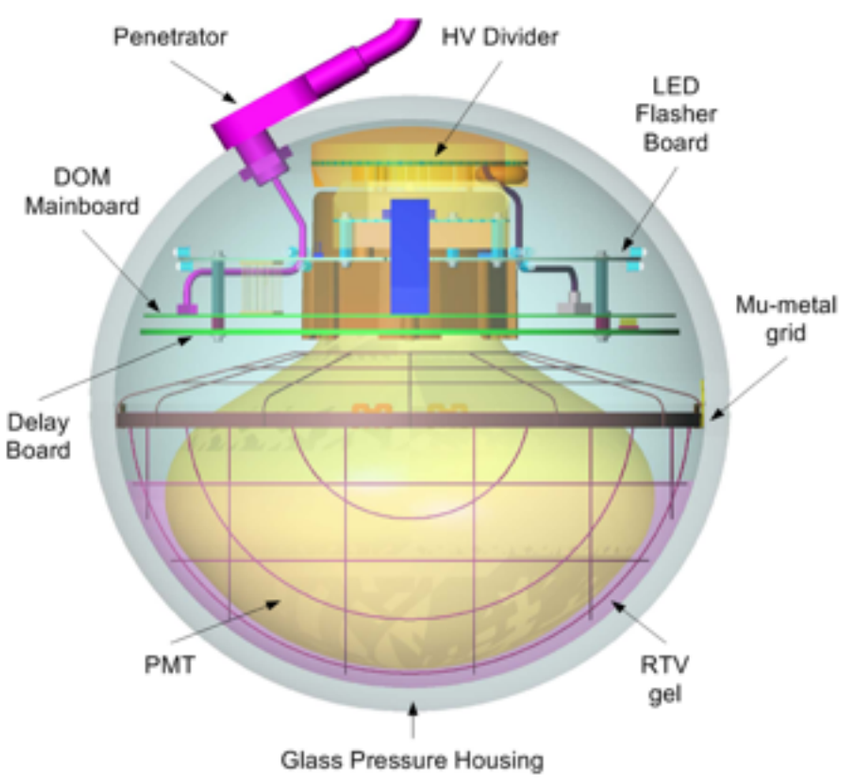

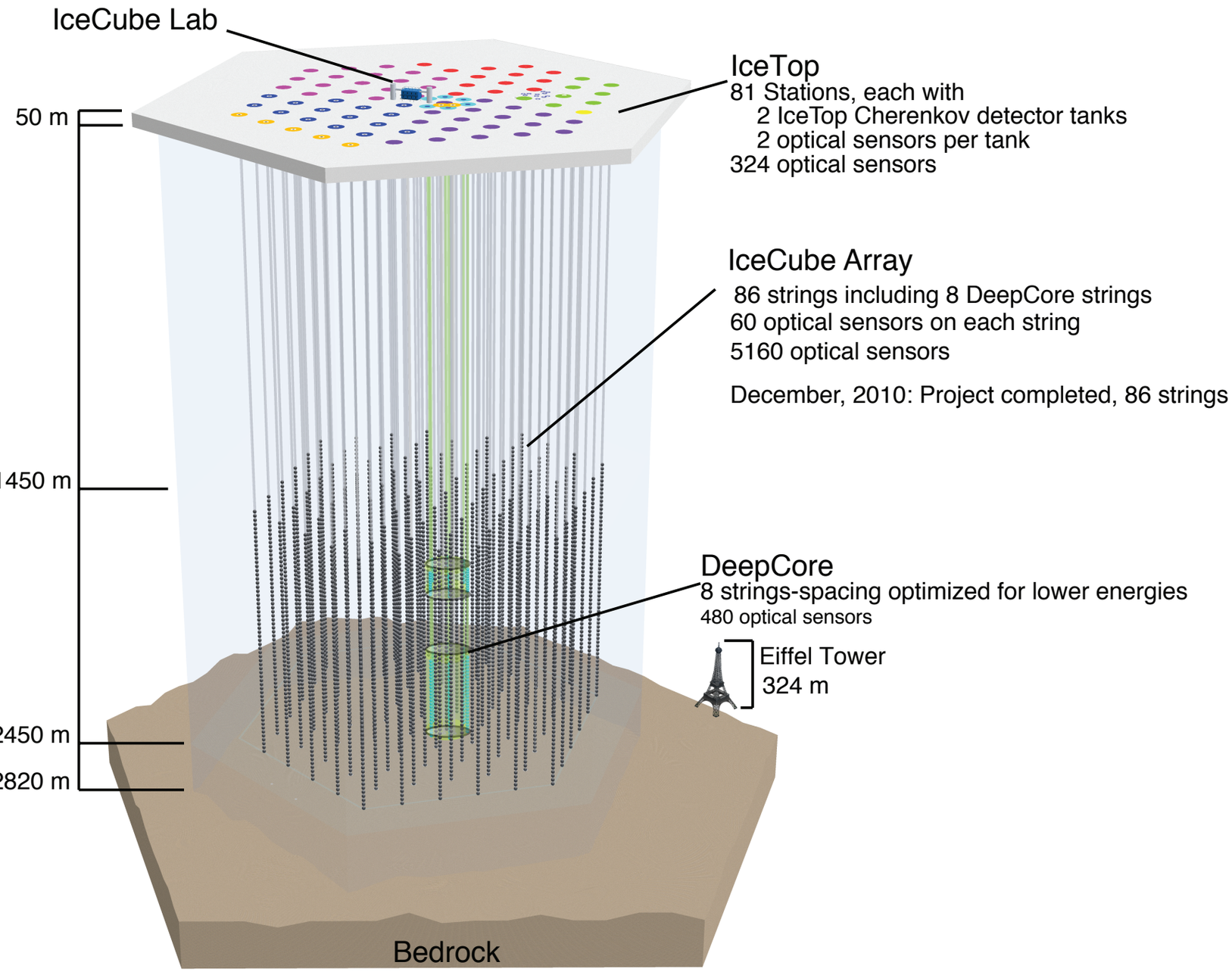

IC59 configuration

Season 2008-2009

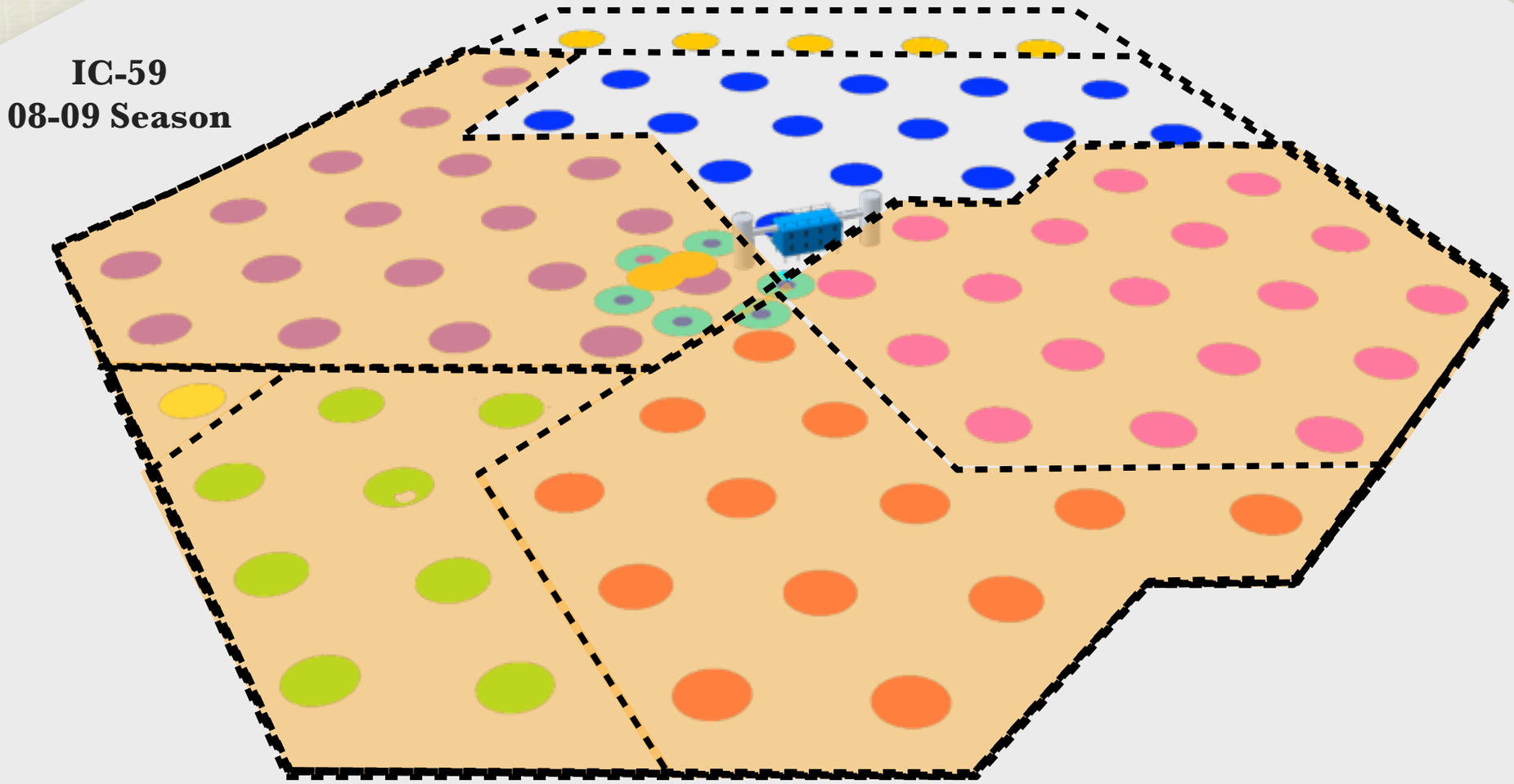

Construction finished on December 2010

Cosmic rays in IceCube

IceCube tries to identify cosmic ray sources by their neutrino signal, but it also allows for a study of the *cosmic ray flux* itself, as the detector is sensitive to *downward going muons* produced in cosmic ray air showers in the southern hemisphere.

By detecting downgoing muons, IceCube can study the *arrival direction distribution of cosmic rays* in the energy range ~10 TeV to several 100 TeV and produce a cosmic ray sky map of the southern sky.

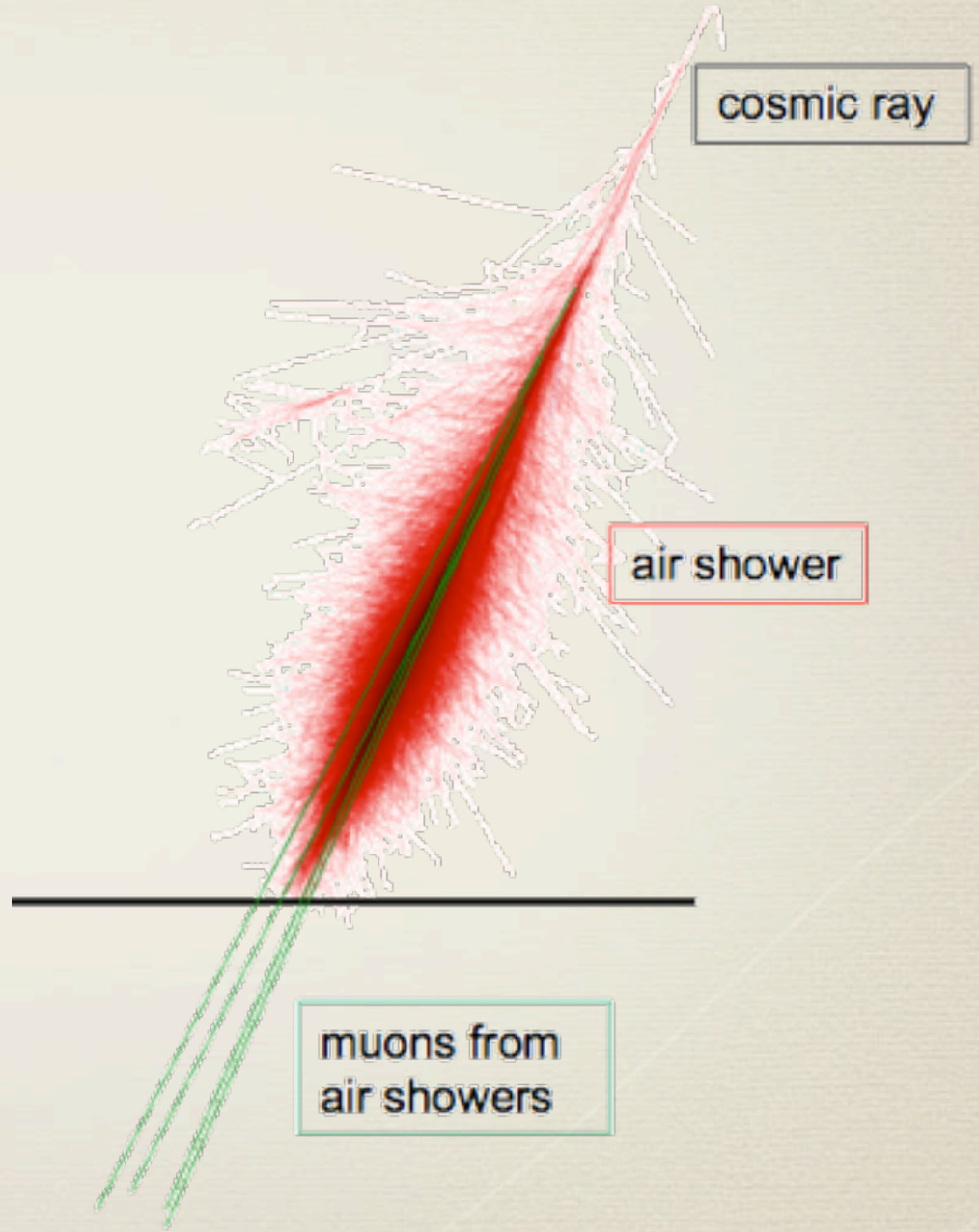

Data set

- IceCube collects billions of down-going muons generated in CR air showers
- **32 billion** of events collected between May 2008/May 2009 with **20 TeV** median energy

IceCube-59	Level 1 "Muon Filter"	DST
Live Time	96%	96%
Trigger rate	22 Hz	1.4 kHz
N_{events}	8.0×10^{8}	3.2×10^{10}
Angular resolution	<1°	3°
Energy resolution	$\Delta \log_{10}(E) = 0.3$	$\Delta \log_{10}(E) = 0.5$

Observation of the CRs large scale anisotropy

There have been several observations of *large-scale, part- per-mille anisotropy* in cosmic ray arrival directions between 0.1 and 100 TeV.

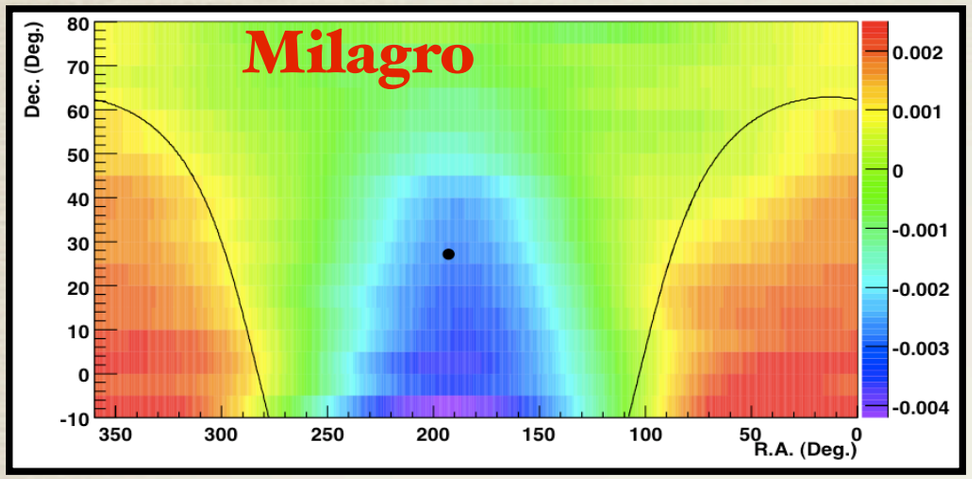

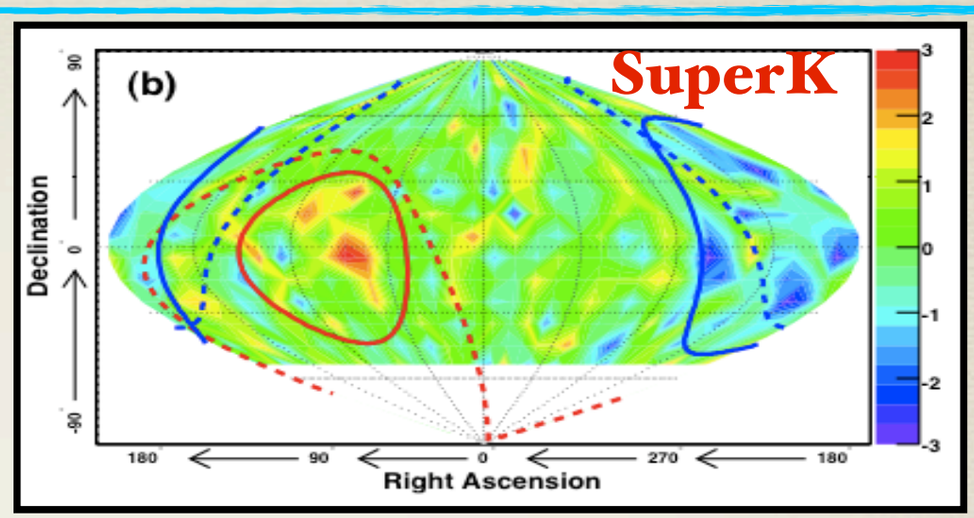

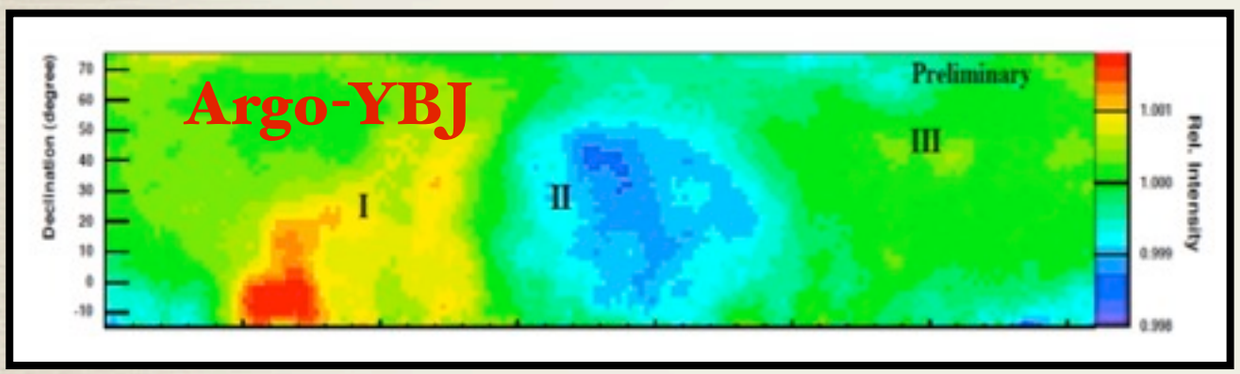

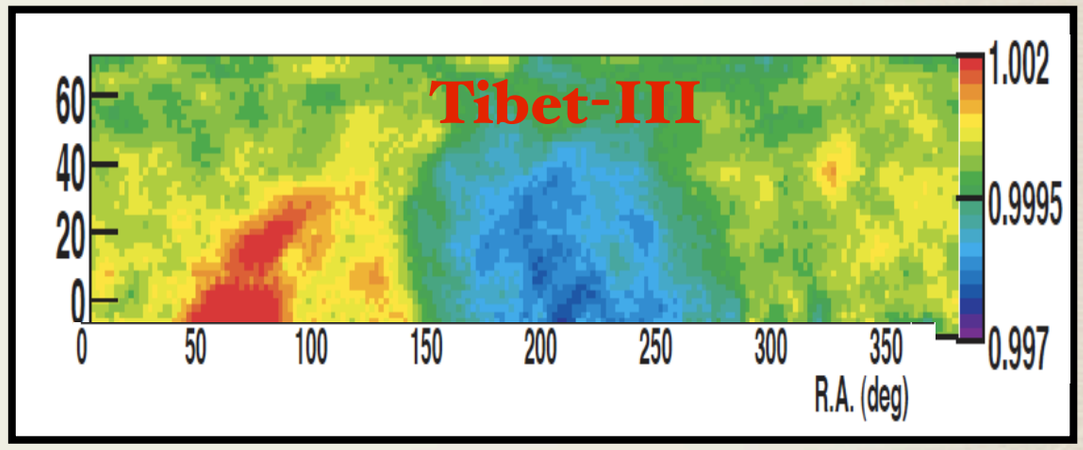

Northern Sky

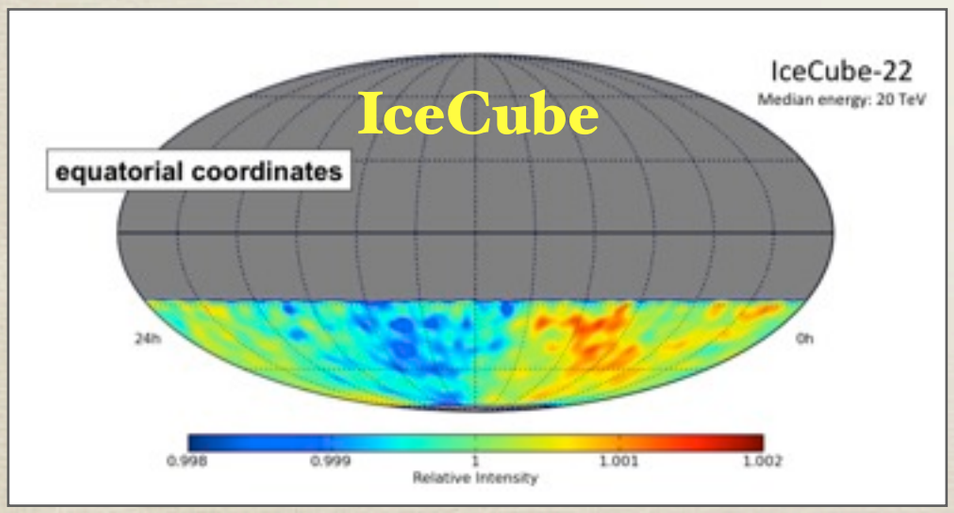

Southern Sky

Tibet ASγ	M. Amenomori et al., Astrophys. J 626 (2005) L29
SuperK	G. Guillian et al., Phys. Rev. D 75 (2007) 062003
Milagro	A. Abdo et al., Astrophys. J. 698 (2009) 2121
ARGO-YBJ	S. Vernetto, Proc. 31st ICRC, 2009
EAS-Top	M. Aglietta, Astrophys. J. 692 (2009) L130
IceCube	R. Abbasi *et al*, Astrophys. J. 718 (2010) L194

Large scale anisotropy

✳IceCube observed a large scale anisotropy at 10^{-3} level for the first time in the Southern Sky.

✳The anisotropy appears to be a continuation of large scale structures observed in the Northern Hemisphere.

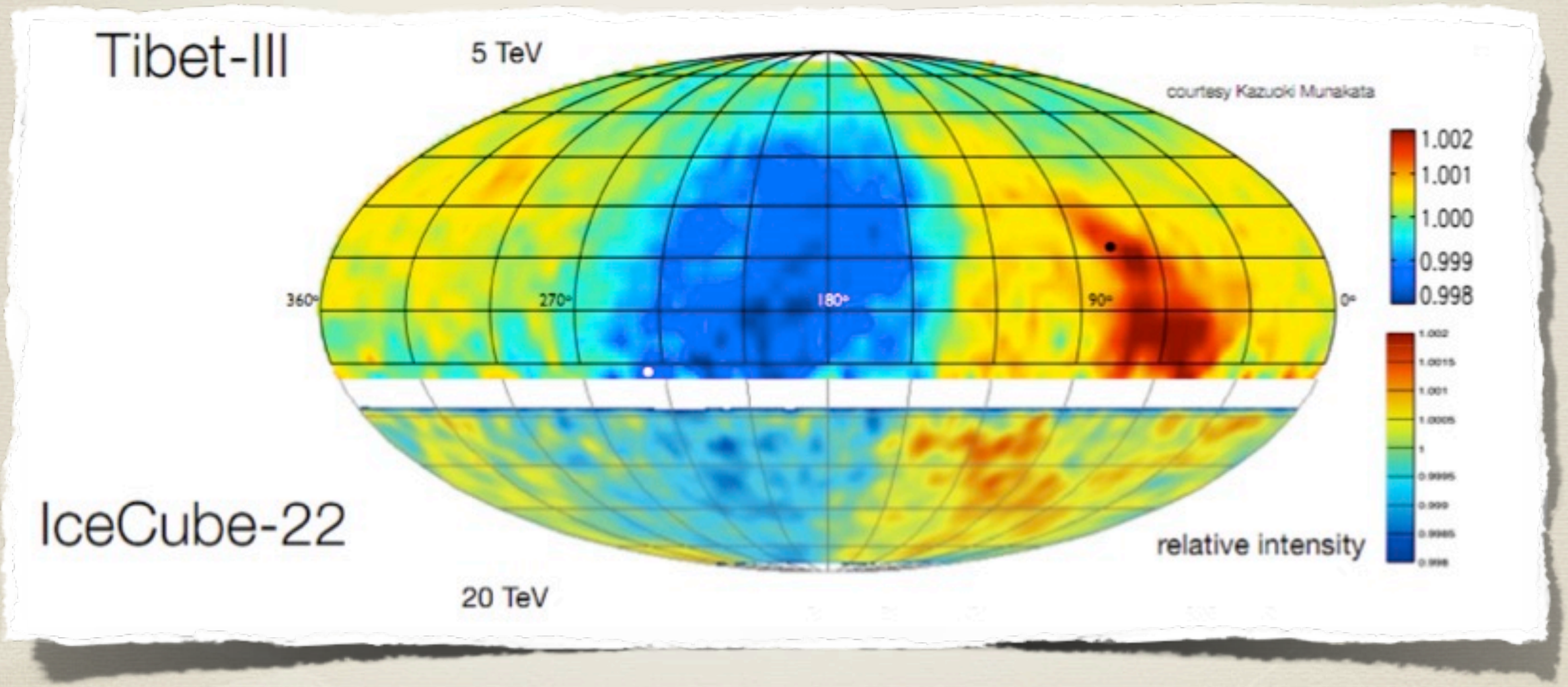

Relative intensity of the cosmic ray event rate in equatorial coordinates: for each declination belt of width 3°, the plot shows the number of events relative to the average number of events in the belt.

Energy dependence of the anisotropy

300 TeV

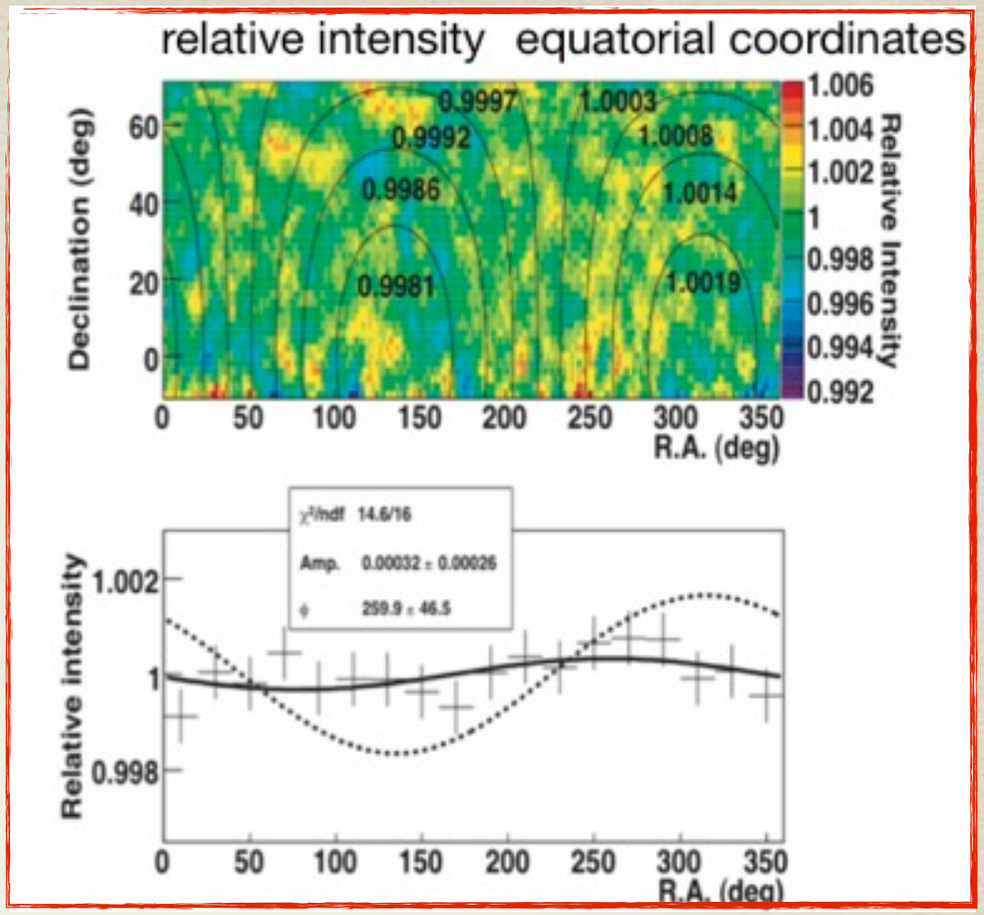

Tibet - III

Amenomori et al., Science Vol. 314, pp. 439, 2006

Amplitude: (3.2±2.6)×10^{-4}

consistent with **no anisotropy**

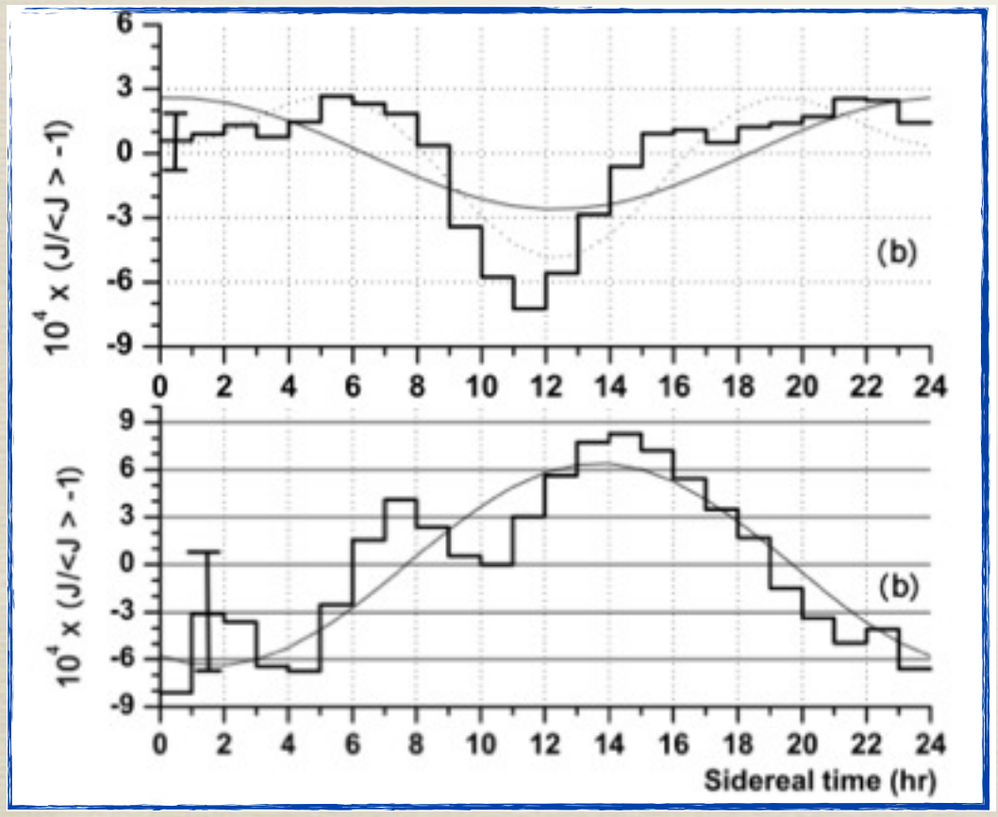

110 TeV

370 TeV

EAS-Top

Aglietta et al., ApJ 692, L130, 2009

Amplitude (370 TeV): (6.4±2.5)×10^{-4}

low significance, still not conclusive.

Relative Intensity

Equatorial sky maps in HEALPix with NSide= 16, ***pix resol ~ 3°***

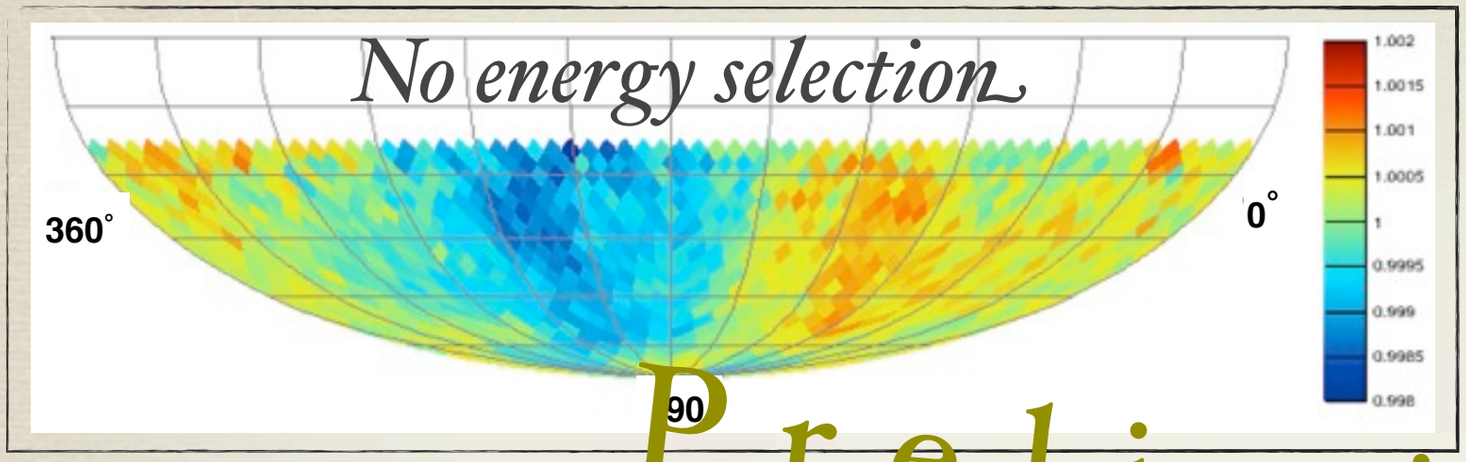

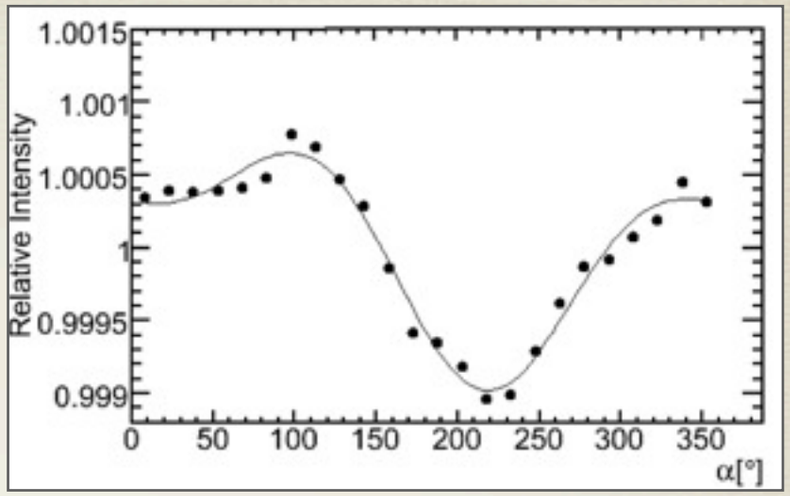

Preliminary

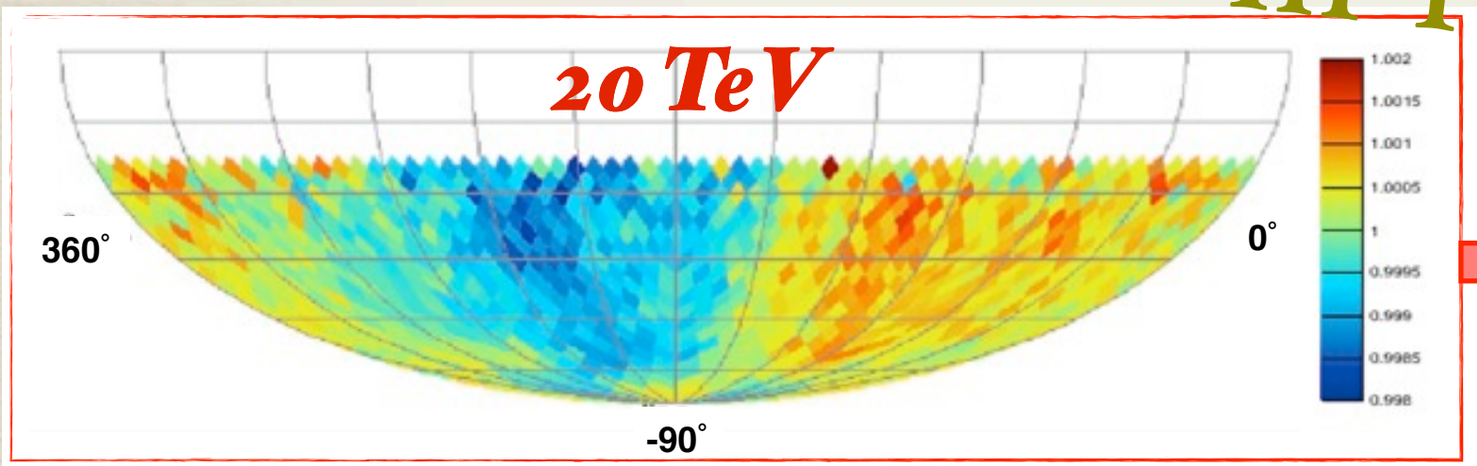

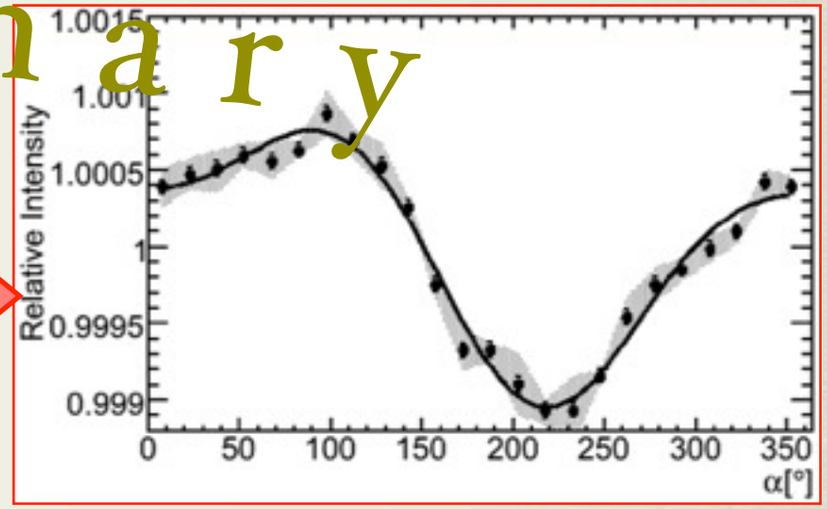

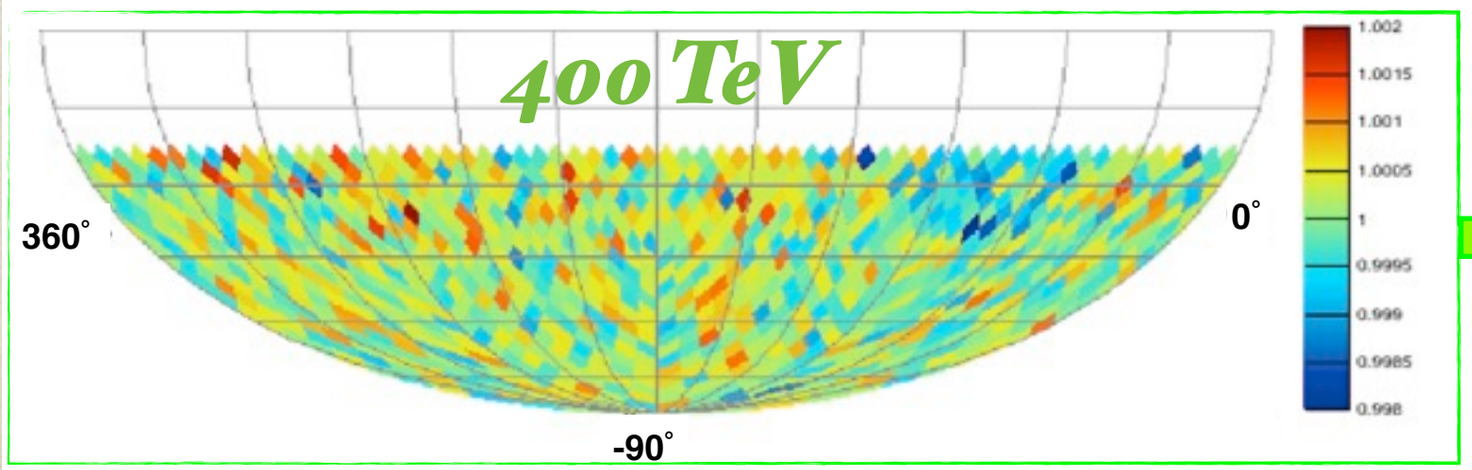

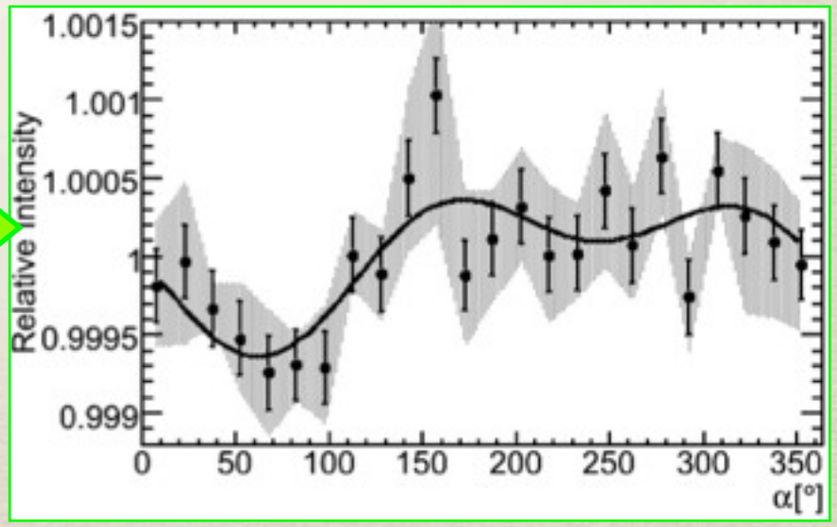

Earth's motion around the Sun: the **Solar dipole**

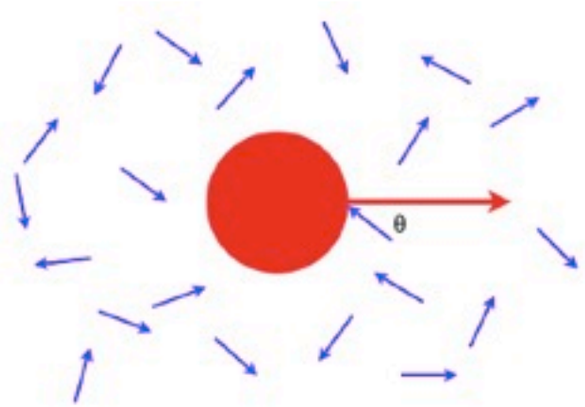

$$\frac{\Delta I}{I} = (\gamma + 2)\frac{v}{c}\cos\theta$$

v = 29.8 ± 0.5 km/s

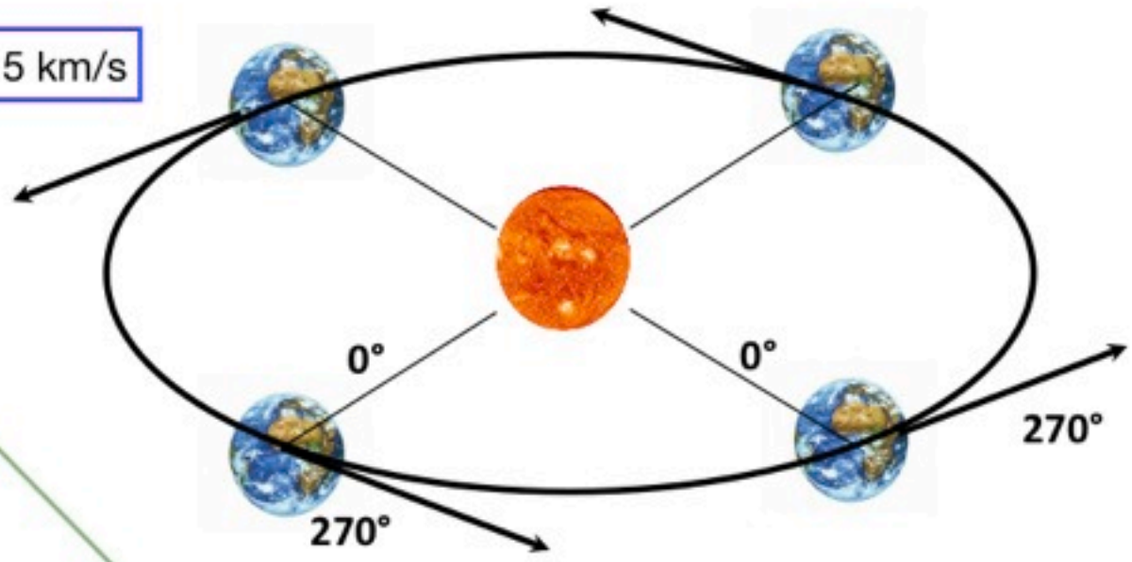

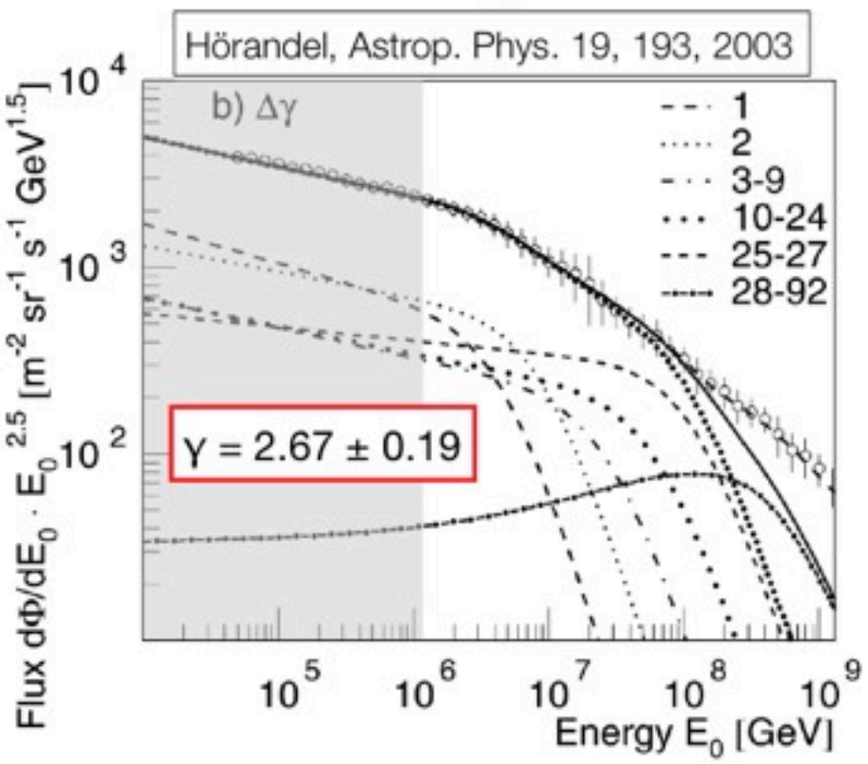

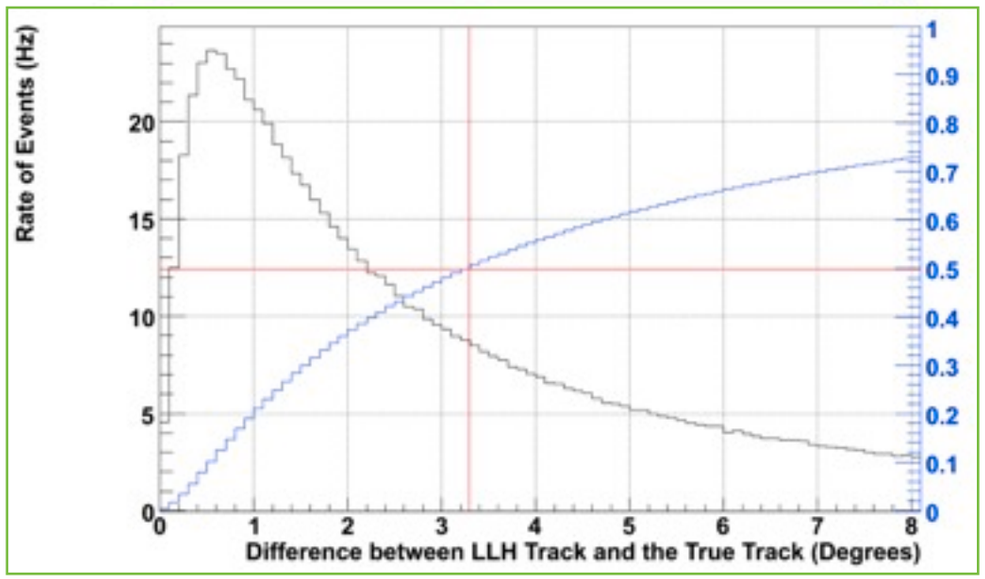

Energy dependence of the Solar dipole

✳ IceCube observes the Solar dipole in both energy bins. The observed amplitude is compatible with the expectations within the stat. and sys. uncertainties.

✳ The observation of the solar dipole supports the observation of the sidereal anisotropy in cosmic ray arrival direction.

relative intensity Vs. $(\alpha[^\circ] - \alpha_{SUN}[^\circ])$

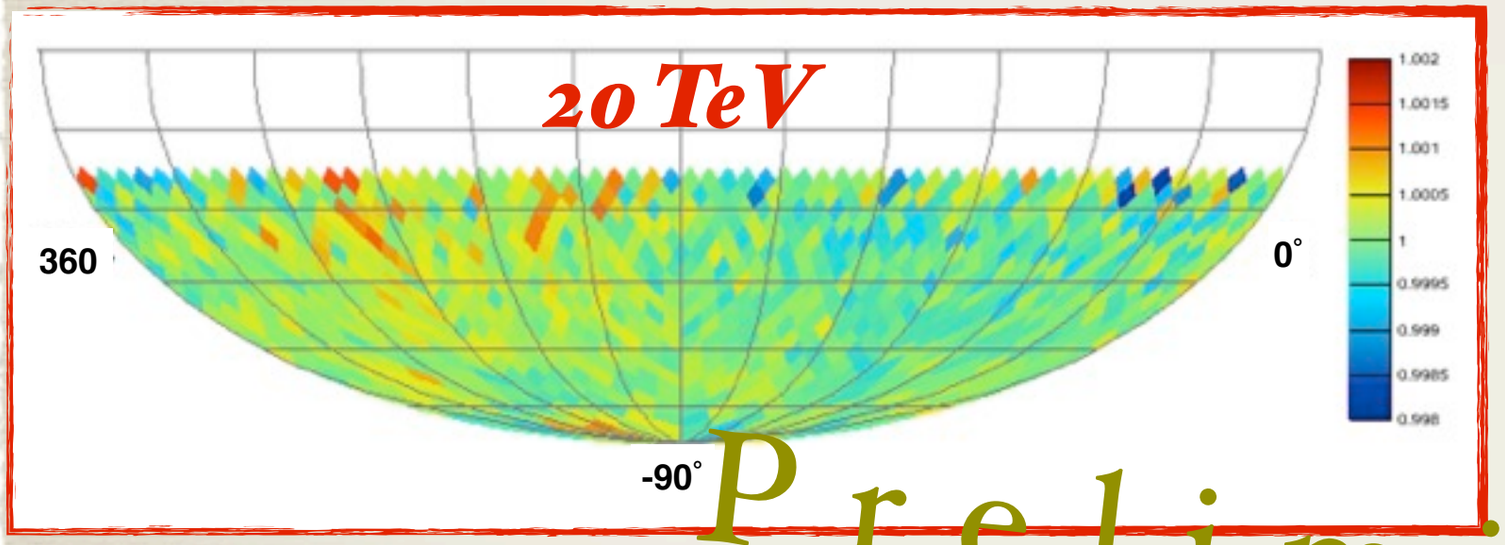

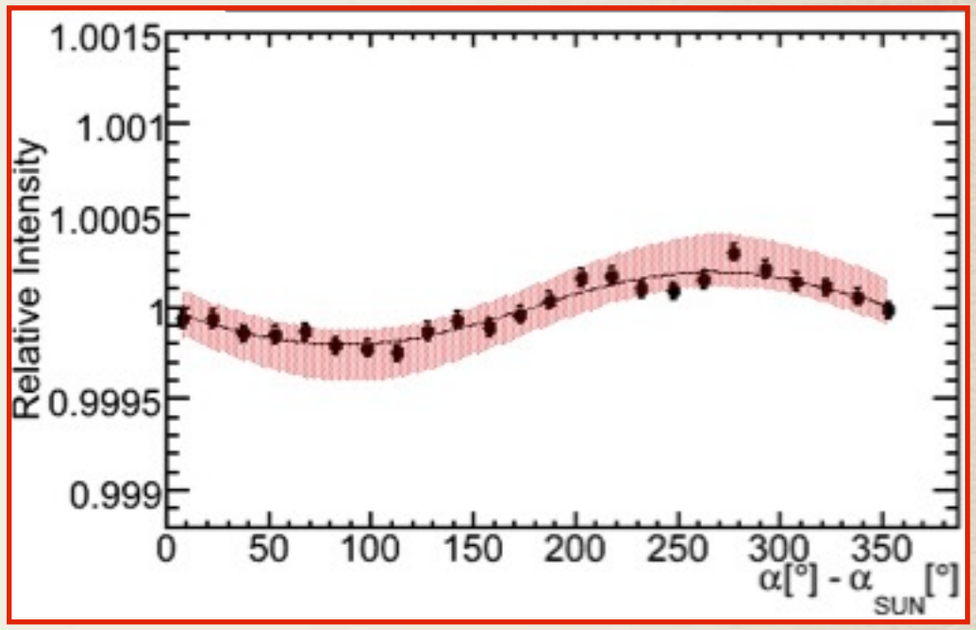

Preliminary

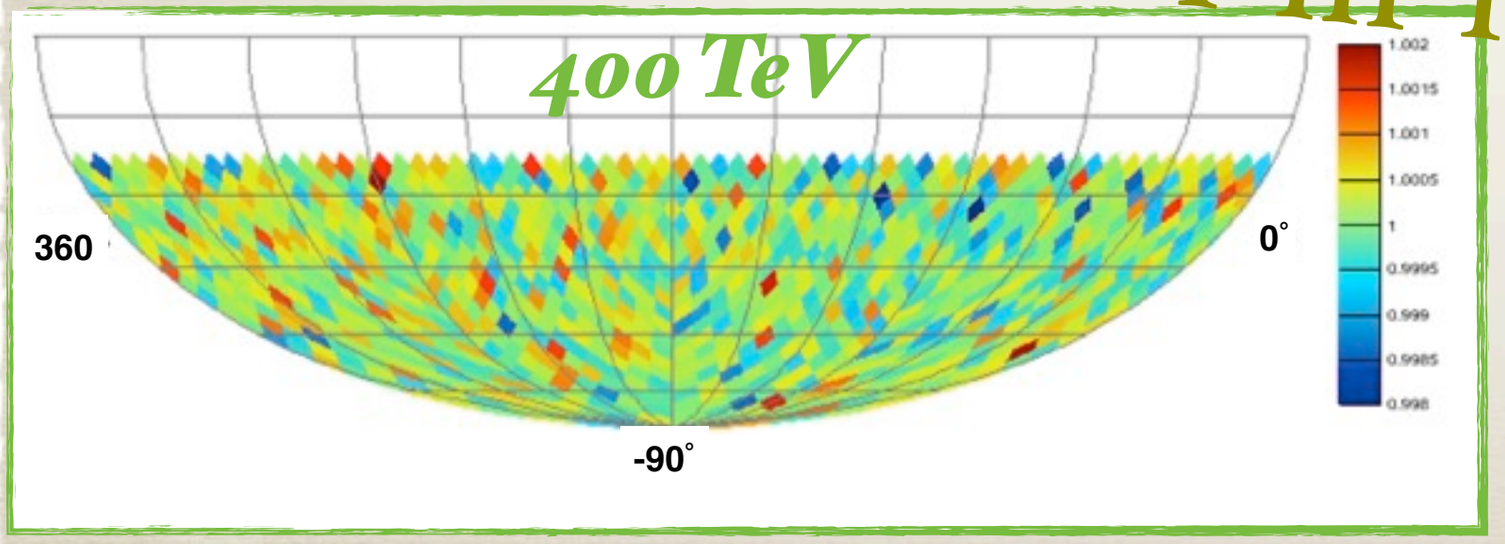

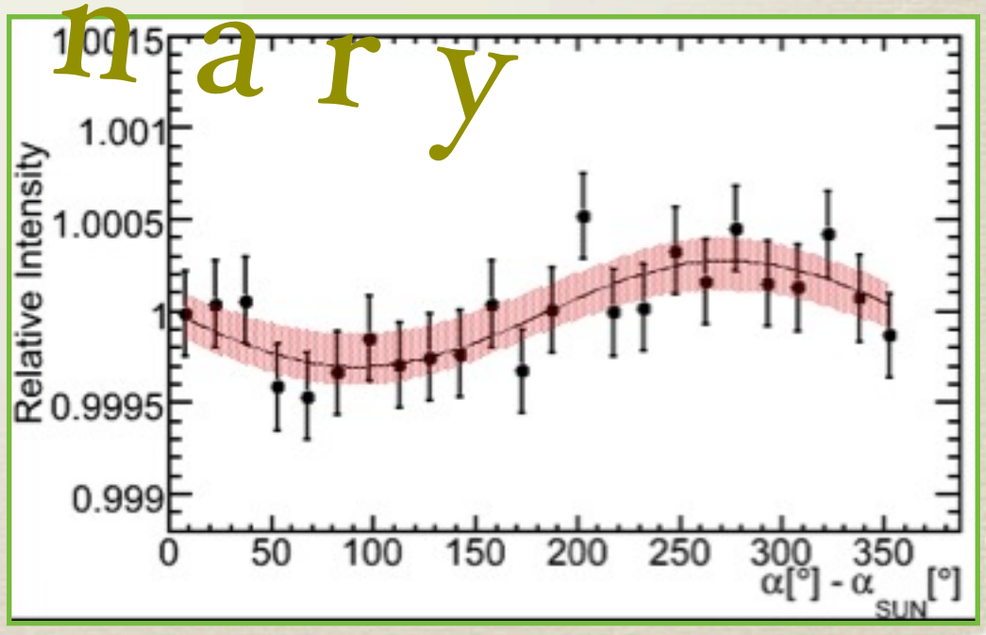

Small scale anisotropy

Several experiments have discovered anisotropies on scales of about 10°

✳ Milagro observes two localized regions with **significance > 10σ** in the total data set of 2.2 10^{11} events recorded over 7 years. The "hot" regions have fractional excesses of order several times **10^{-4}** relative to the background.

✳ Same structures observed by ARGO-YBJ.

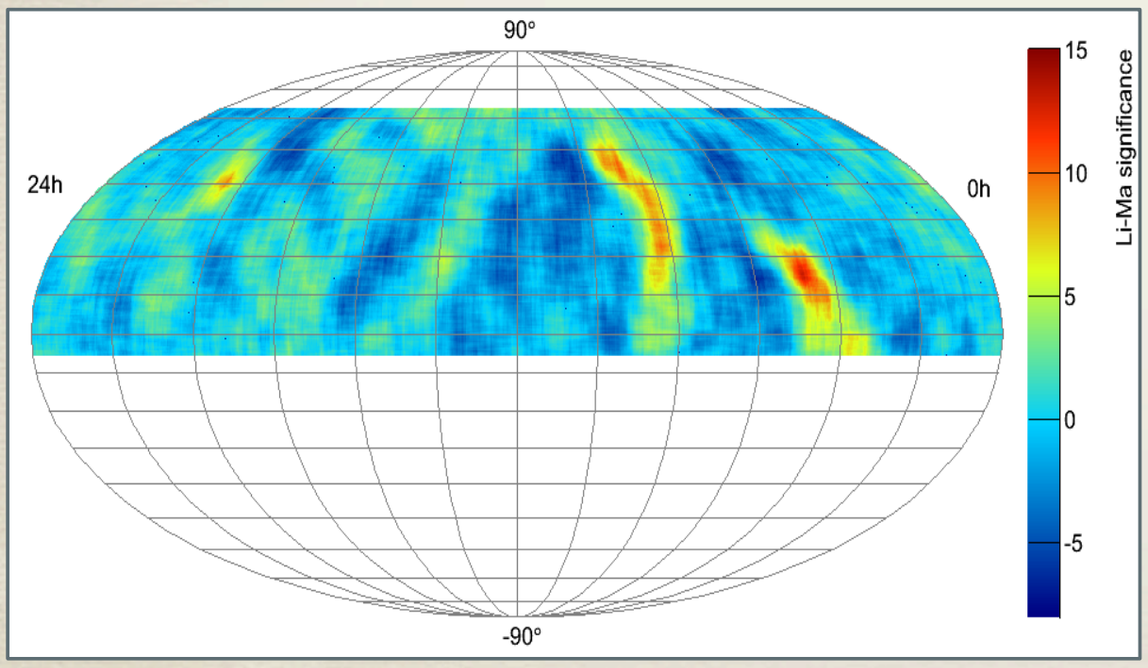

A. Abdo et al., PRL 101 (2008) 221101

Milagro

Median Energy: 1 TeV

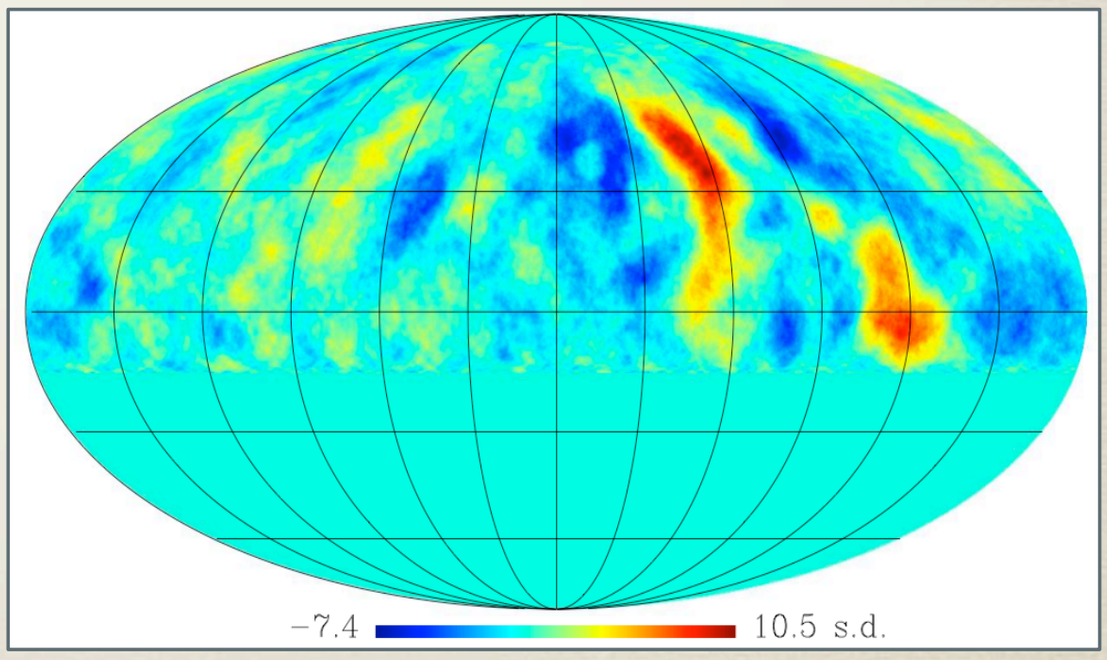

S. Vernetto, Proc. 31st ICRC, 2009

ARGO-YBJ

Median Energy: 2 TeV

Relative Intensity map

Equatorial sky maps in HEALPix: equal area pixel ***(size ~ 0.9°)***

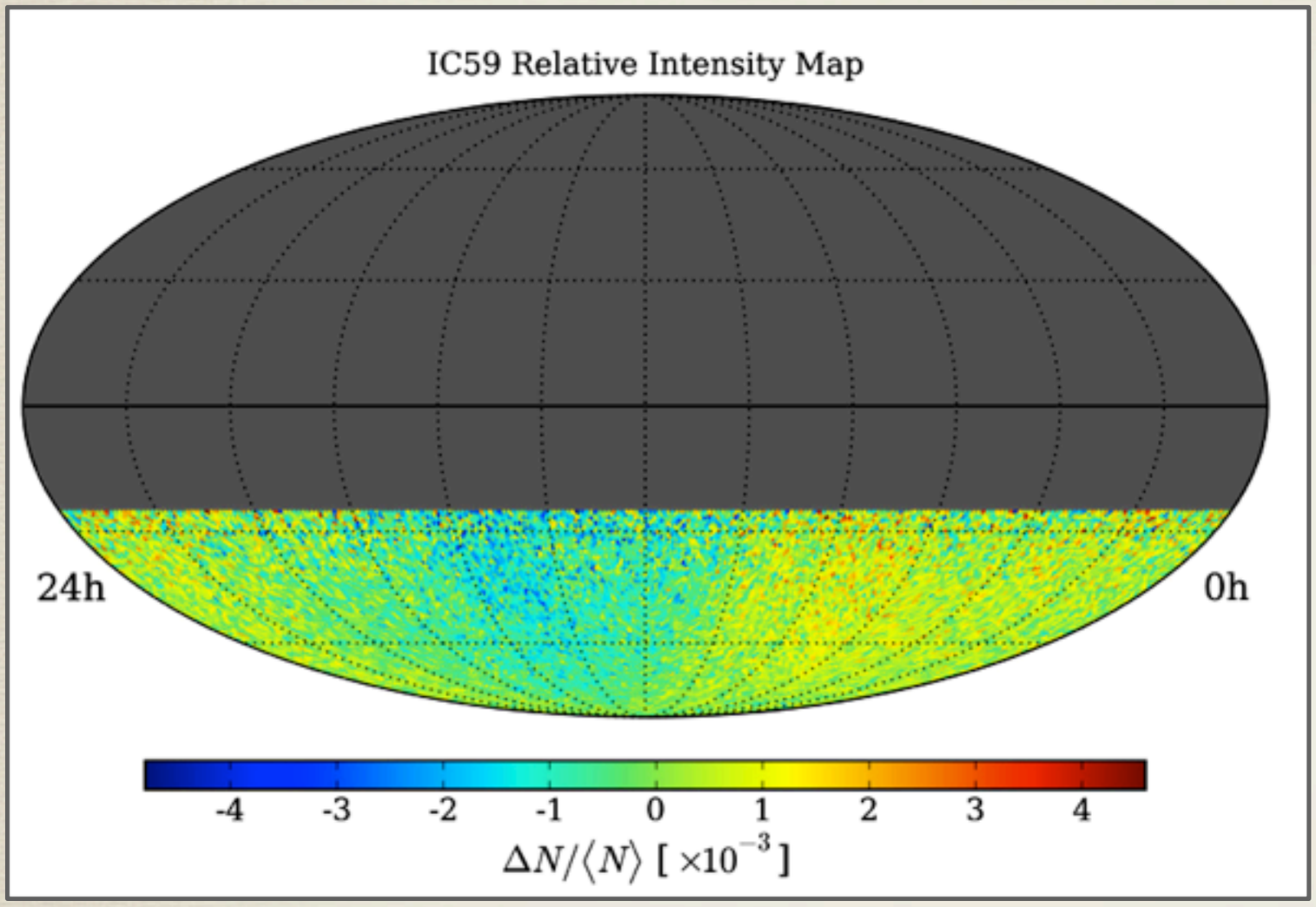

Sky map created using the background estimation technique from real data:

- N_i **:** number of data events in the i^{th} pixel.
- $\langle N_i \rangle$**:** expected number of events in an isotropic sky (time scrambling in 24 hr) in the i^{th} pixel.
- Relative Intensity:

$$\frac{\Delta N_i}{\langle N \rangle_i} = \frac{N_i(\alpha,\delta) - \langle N_i(\alpha,\delta)\rangle}{\langle N_i(\alpha,\delta)\rangle}.$$

Relative intensity map is *not isotropic*. In IceCube-59, the *strong large scale structure* already observed in IceCube-22 data is visible in the "raw" data.

Significance map

Significance calculation:

$$s = \sqrt{2}\left\{ N_{\rm on} \ln\left[\frac{1+\alpha}{\alpha}\left(\frac{N_{\rm on}}{N_{\rm on}+N_{\rm off}}\right)\right] + N_{\rm off} \ln\left[(1+\alpha)\left(\frac{N_{\rm off}}{N_{\rm on}+N_{\rm off}}\right)\right]\right\}^{1/2} \qquad \alpha = 1/20$$

Li, T., & Ma, Y. 1983, ApJ, 272, 317

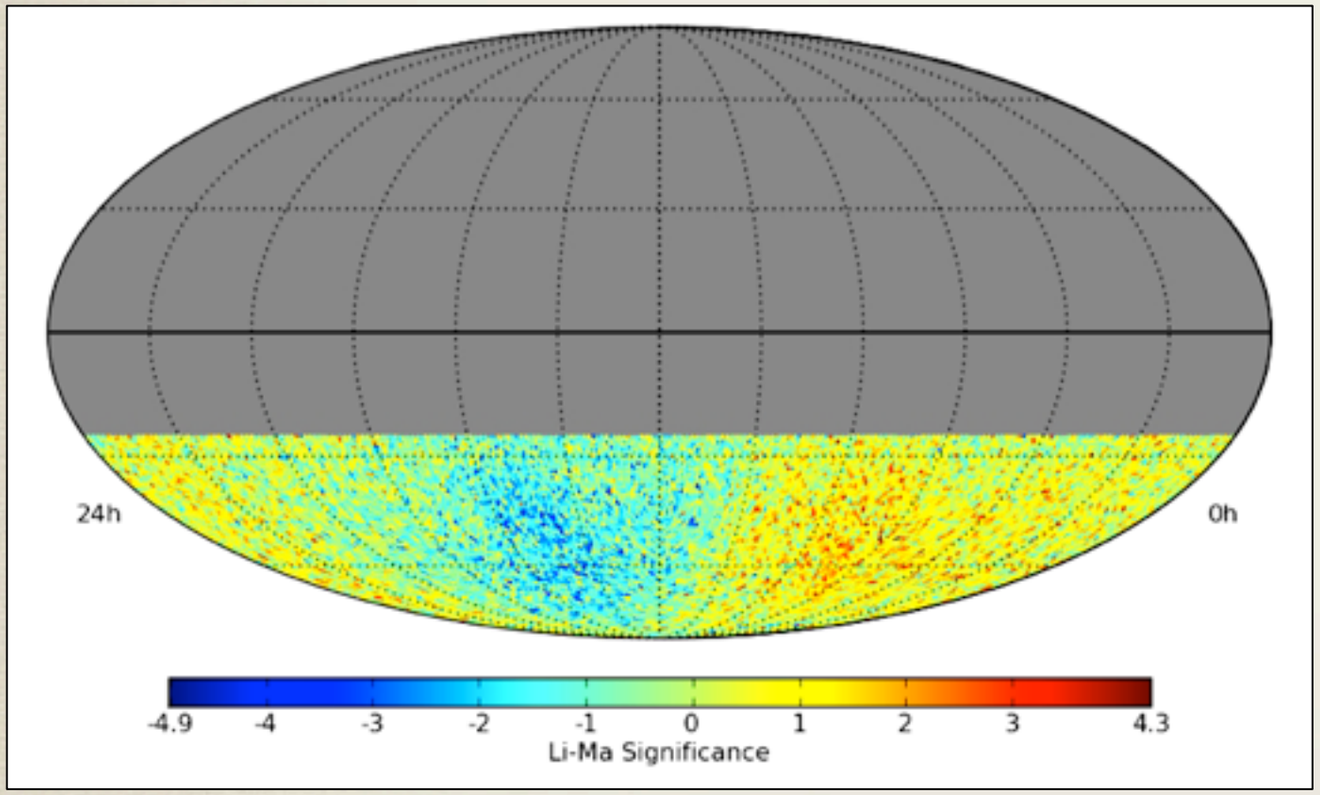

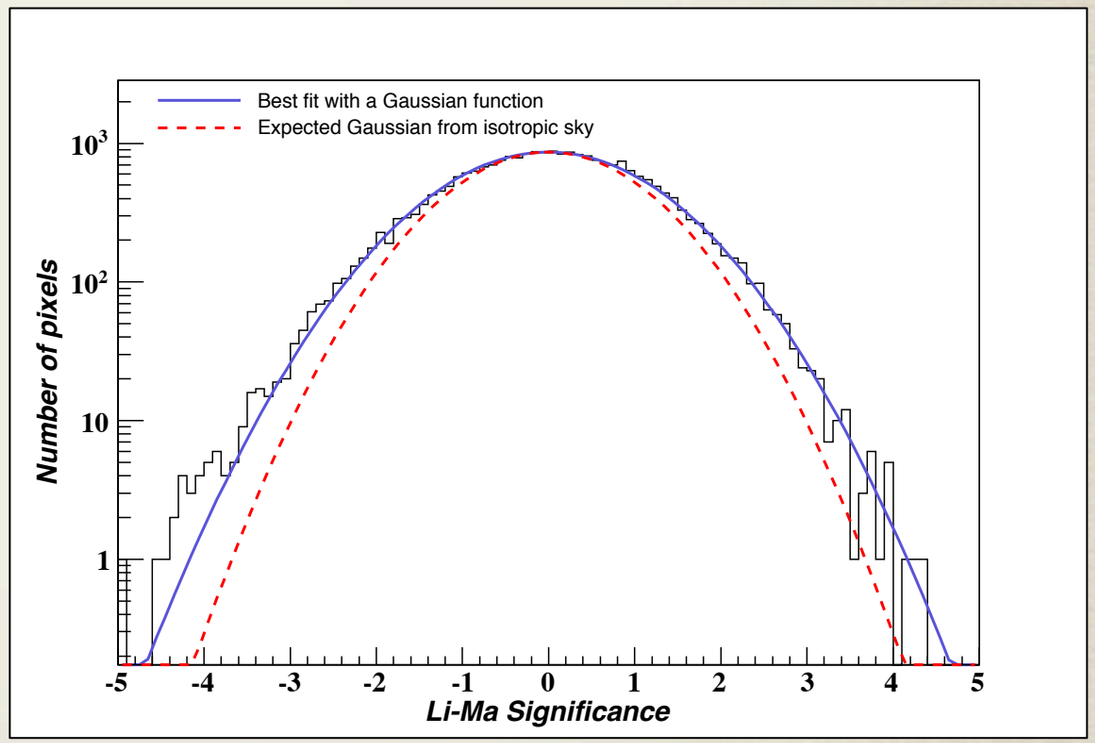

Power spectrum

Angular size $\theta \sim \dfrac{180^\circ}{\ell}$

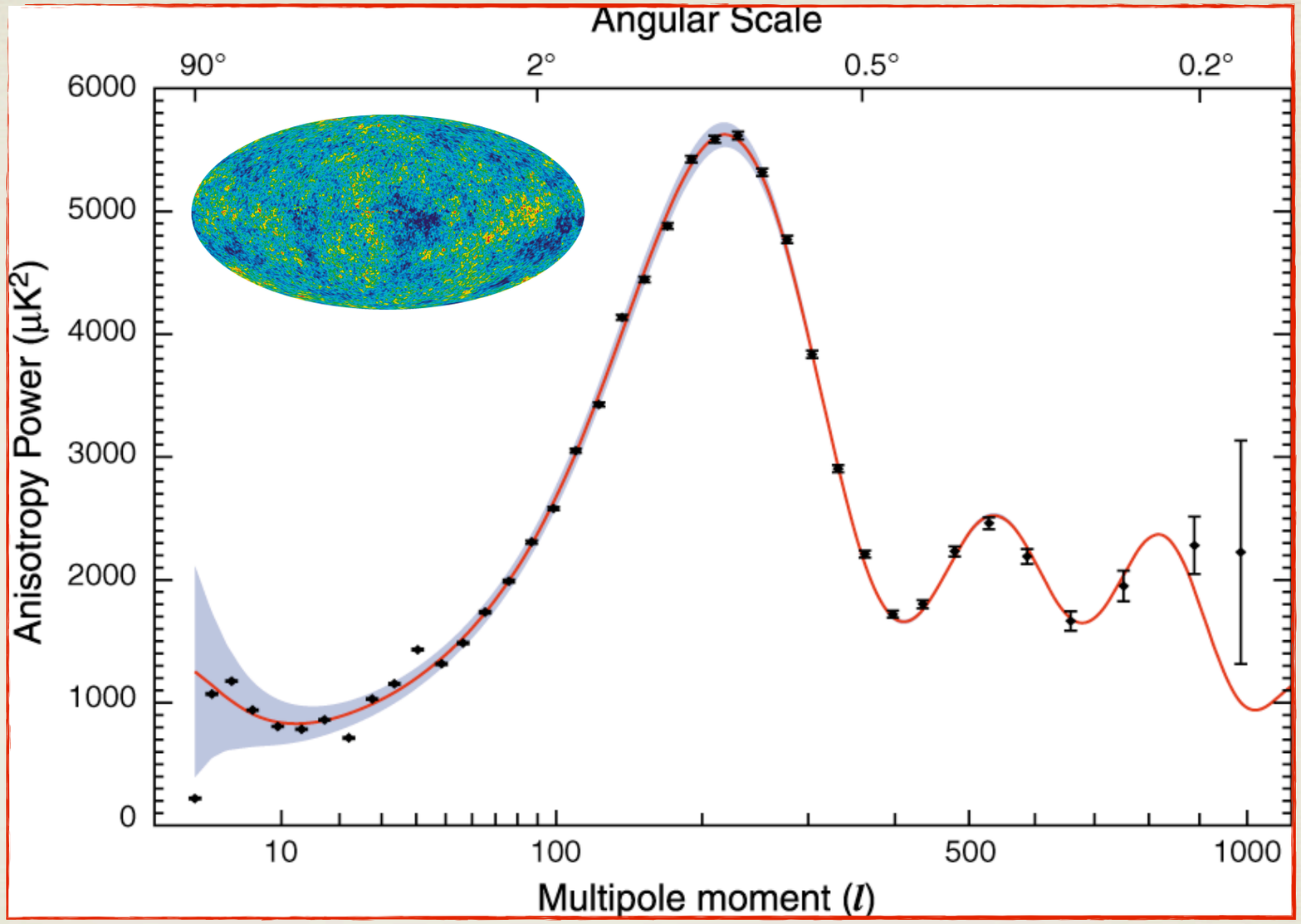

Multipole expansion: $\delta I(\mathbf{u}_i) = \sum_{\ell=1}^{\infty} \sum_{m=-\ell}^{\ell} a_{\ell m} Y_{\ell m}(\mathbf{u}_i)$ $\qquad C_\ell = \dfrac{1}{2\ell+1} \sum_m |a_{\ell m}|^2$

Power spectrum

Angular size $\theta \sim \frac{180^\circ}{\ell}$

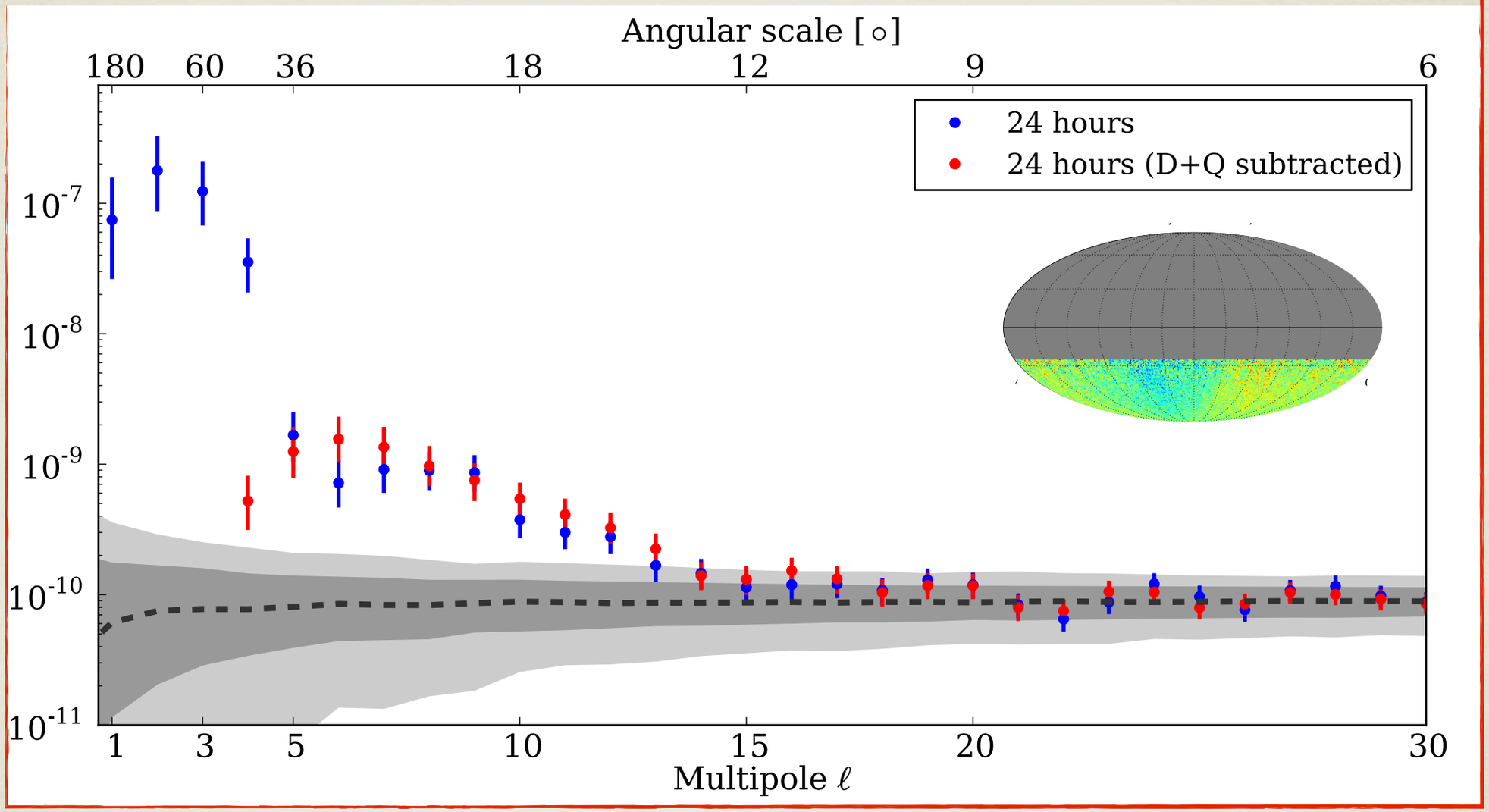

Multipole expansion: $\delta I(\mathbf{u}_i) = \sum_{\ell=1}^{\infty} \sum_{m=-\ell}^{\ell} a_{\ell m} Y_{\ell m}(\mathbf{u}_i)$ $\quad C_\ell = \frac{1}{2\ell+1} \sum_m |a_{\ell m}|^2$

Dipole and quadrupole fit

$$\delta I(\alpha,\delta) = m_0 \qquad \textbf{monopole}$$
$$+p_x \cos\delta\cos\alpha + p_y \cos\delta\sin\alpha + p_z \sin\delta \qquad \textbf{dipole}$$
$$+\frac{1}{2}Q_1(3\cos^2\delta - 1) + Q_2 \sin 2\delta\cos\alpha + Q_3 \sin 2\delta\sin\alpha + Q_4 \cos^2\delta\cos 2\alpha + Q_5 \cos^2\delta\sin 2\alpha \qquad \textbf{quadrupole}$$

Coefficient	Fit Value
m_0	0.320 ± 2.264
p_x	2.435 ± 0.707
p_y	-3.856 ± 0.707
p_z	0.548 ± 3.872
Q_1	0.233 ± 1.702
Q_2	-2.949 ± 0.494
Q_3	-8.797 ± 0.494
Q_4	-2.148 ± 0.200
Q_5	-5.268 ± 0.200

$$\chi^2/\mathrm{ndf} = 14743.4/14187$$
$$\Pr(\chi^2|\mathrm{ndf}) = 5.5 \times 10^{-4}$$

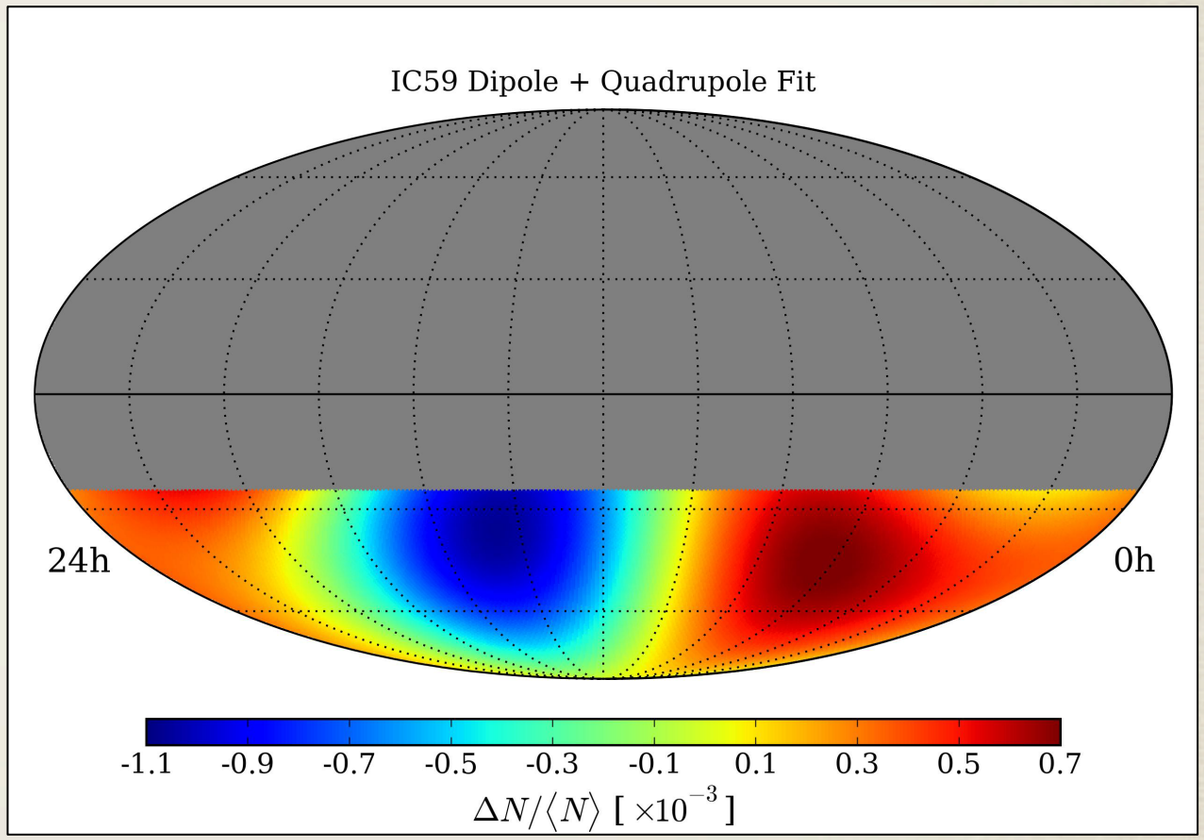

Residual map

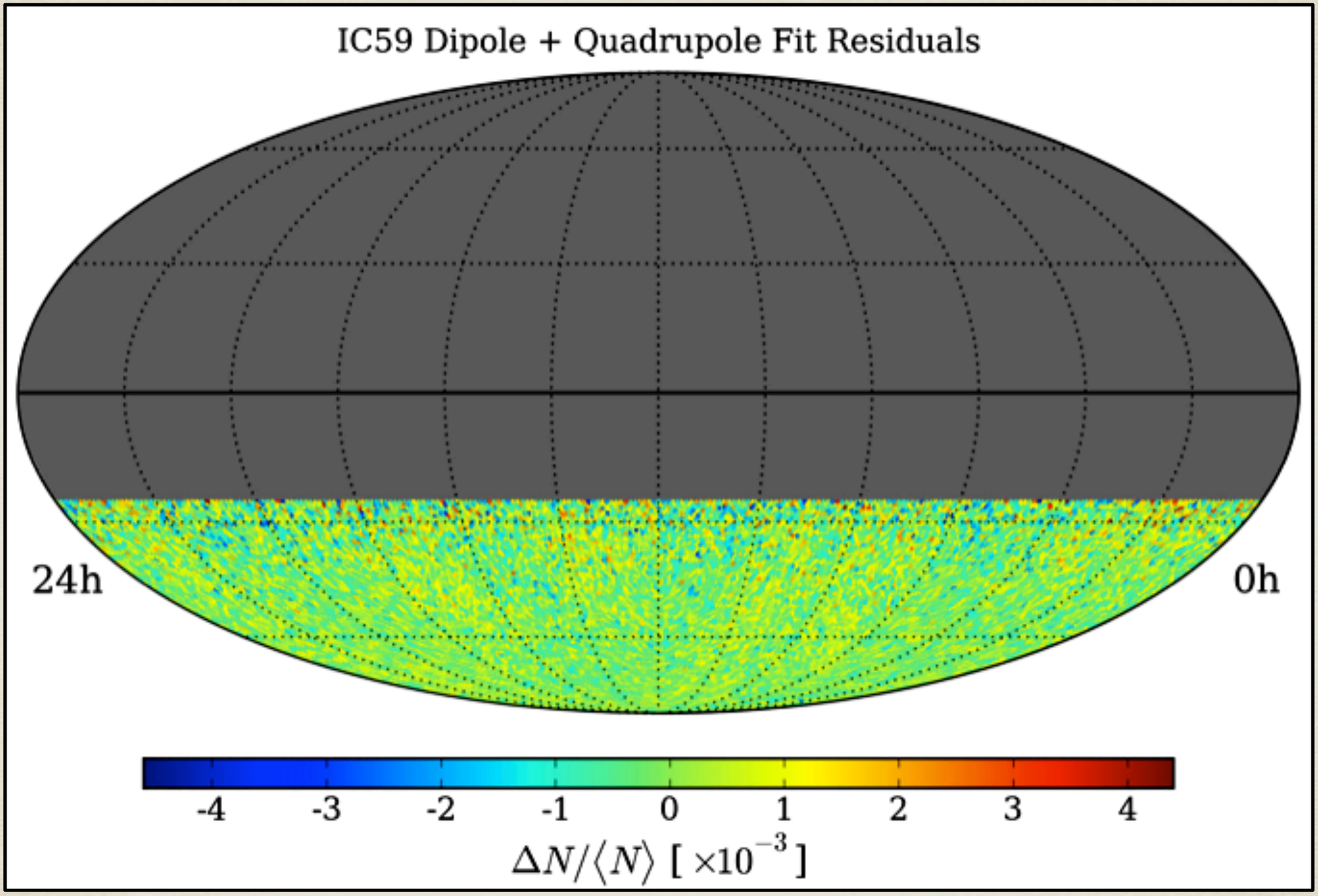

No structures seem to be present: we need to smooth the map.

MAP SMOOTHING SCAN

Scan from 1 - 30° in smoothing
Different regions have different optimal angular smoothing
Significances are pre-trial

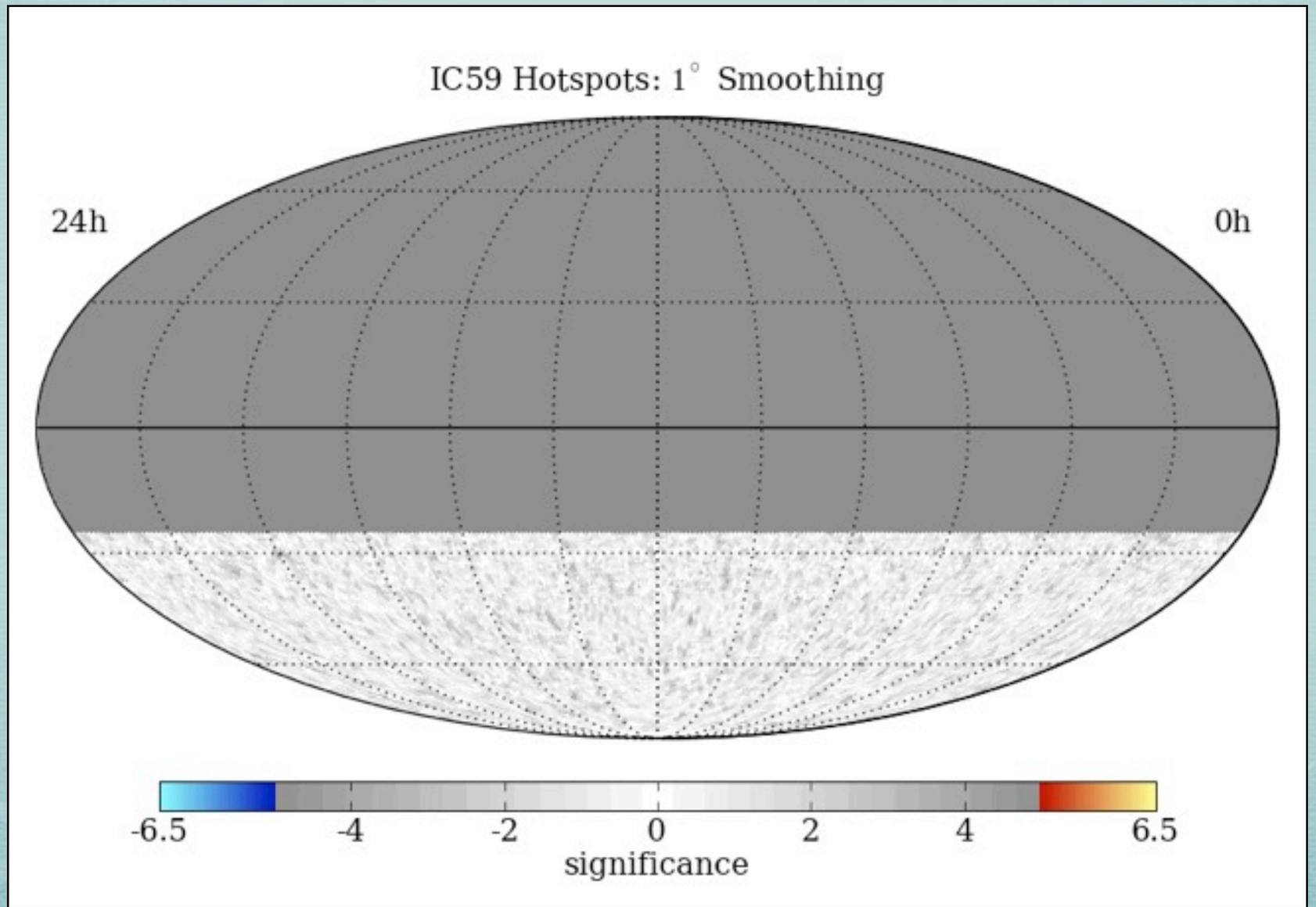

MAP SMOOTHING SCAN

Scan from 1 - 30° in smoothing
Different regions have different optimal angular smoothing
Significances are pre-trial

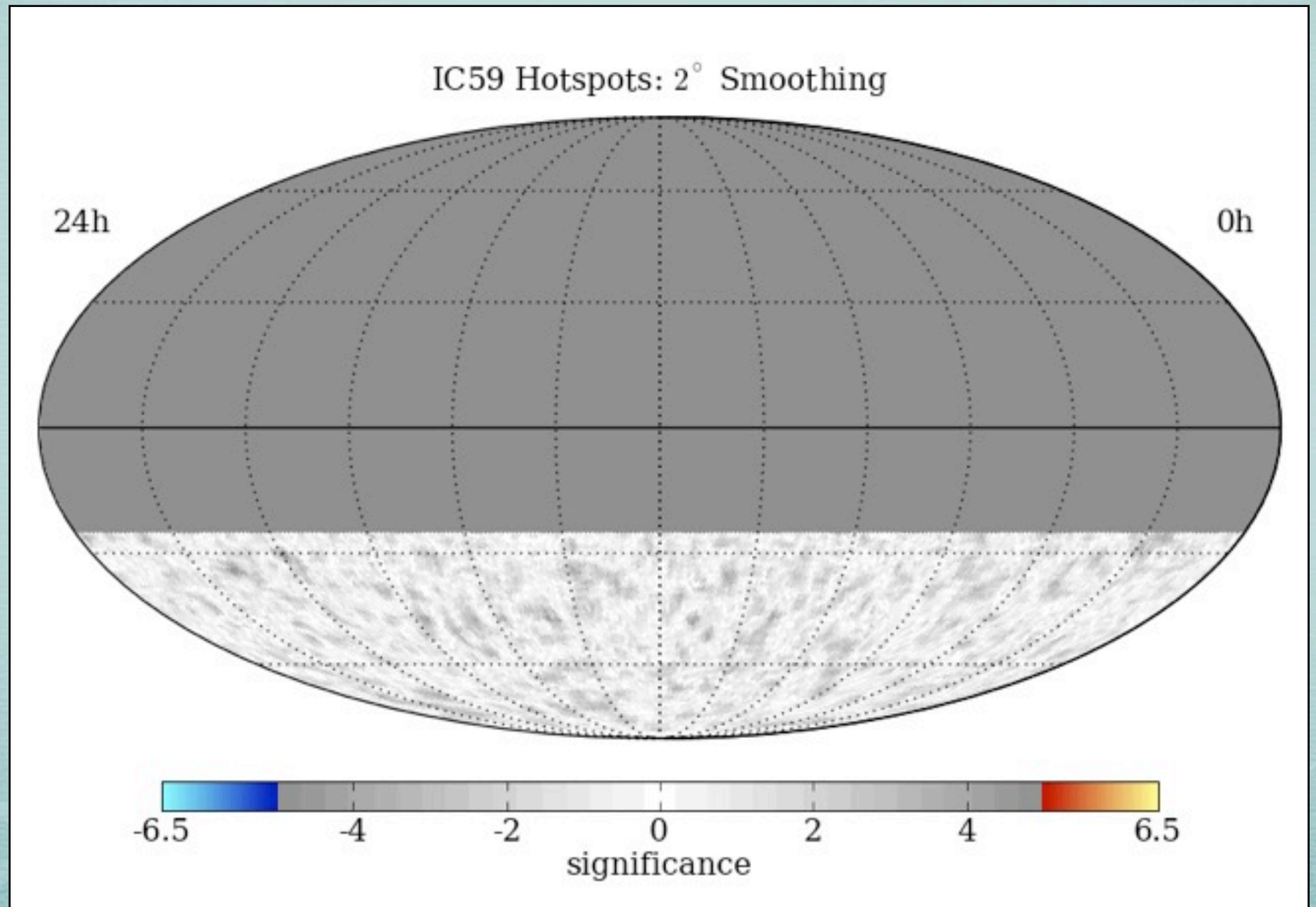

MAP SMOOTHING SCAN

Scan from 1 - 30° in smoothing
Different regions have different optimal angular smoothing
Significances are pre-trial

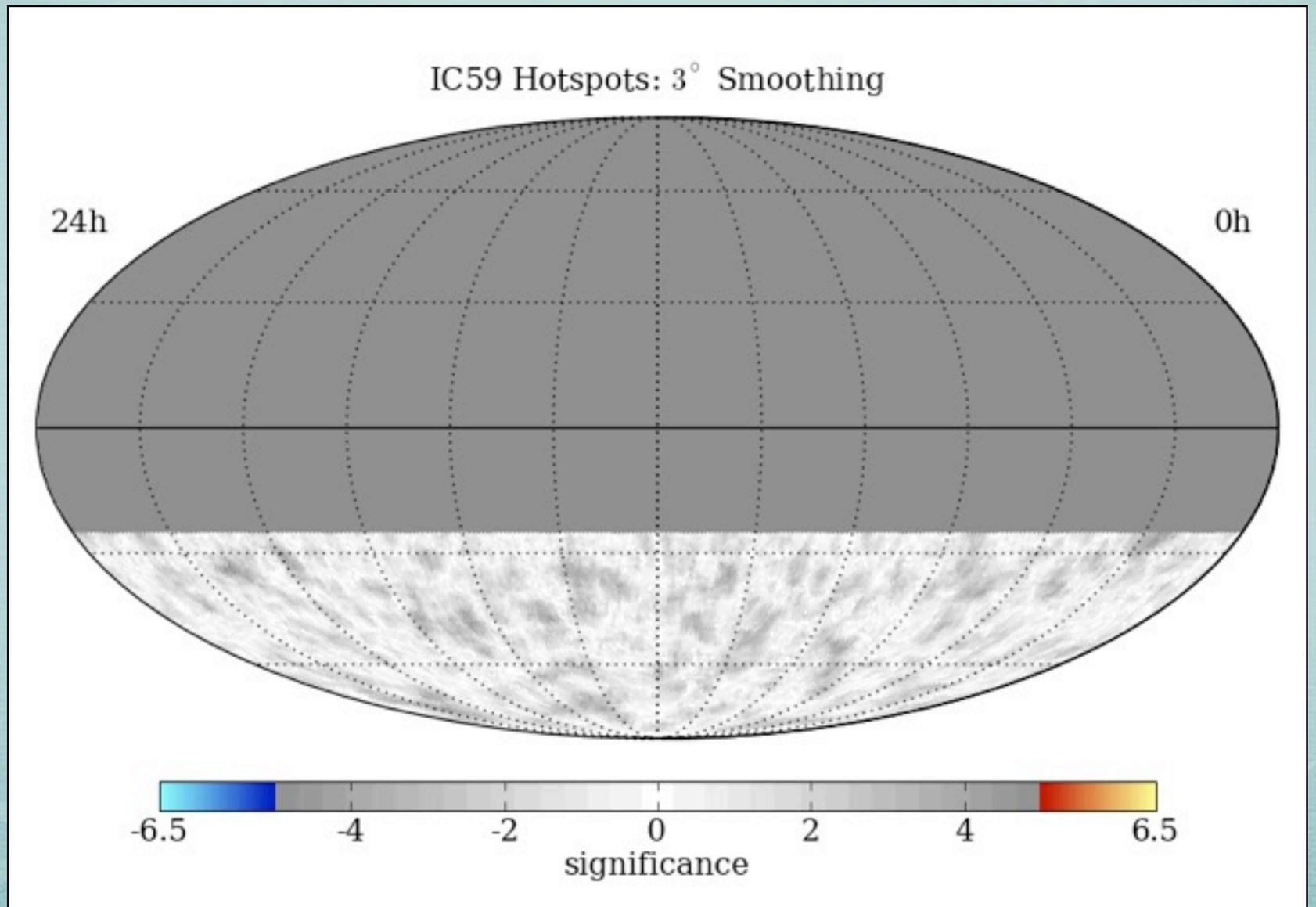

MAP SMOOTHING SCAN

Scan from 1 - 30° in smoothing
Different regions have different optimal angular smoothing
Significances are pre-trial

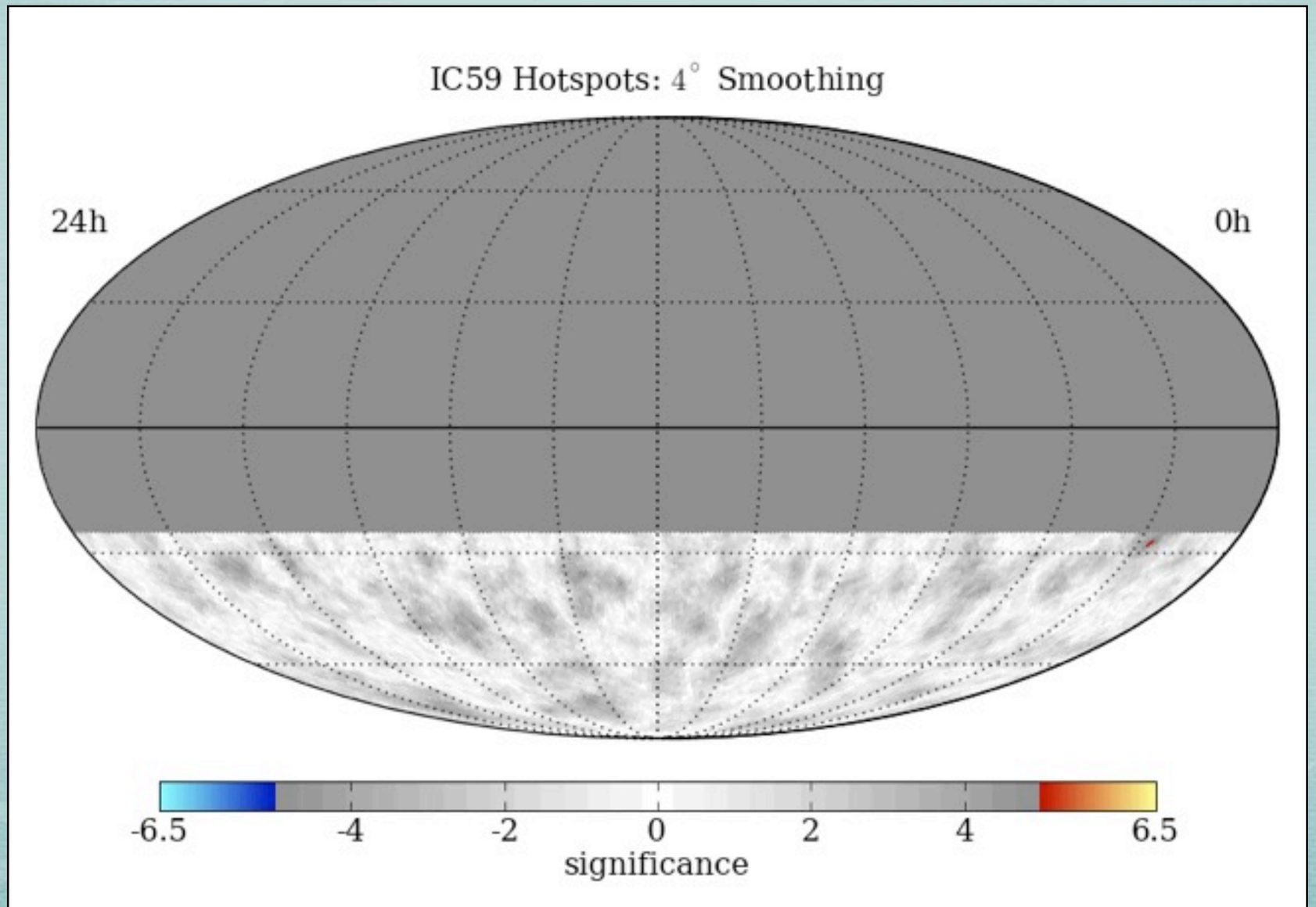

MAP SMOOTHING SCAN

Scan from 1 - 30° in smoothing
Different regions have different optimal angular smoothing
Significances are pre-trial

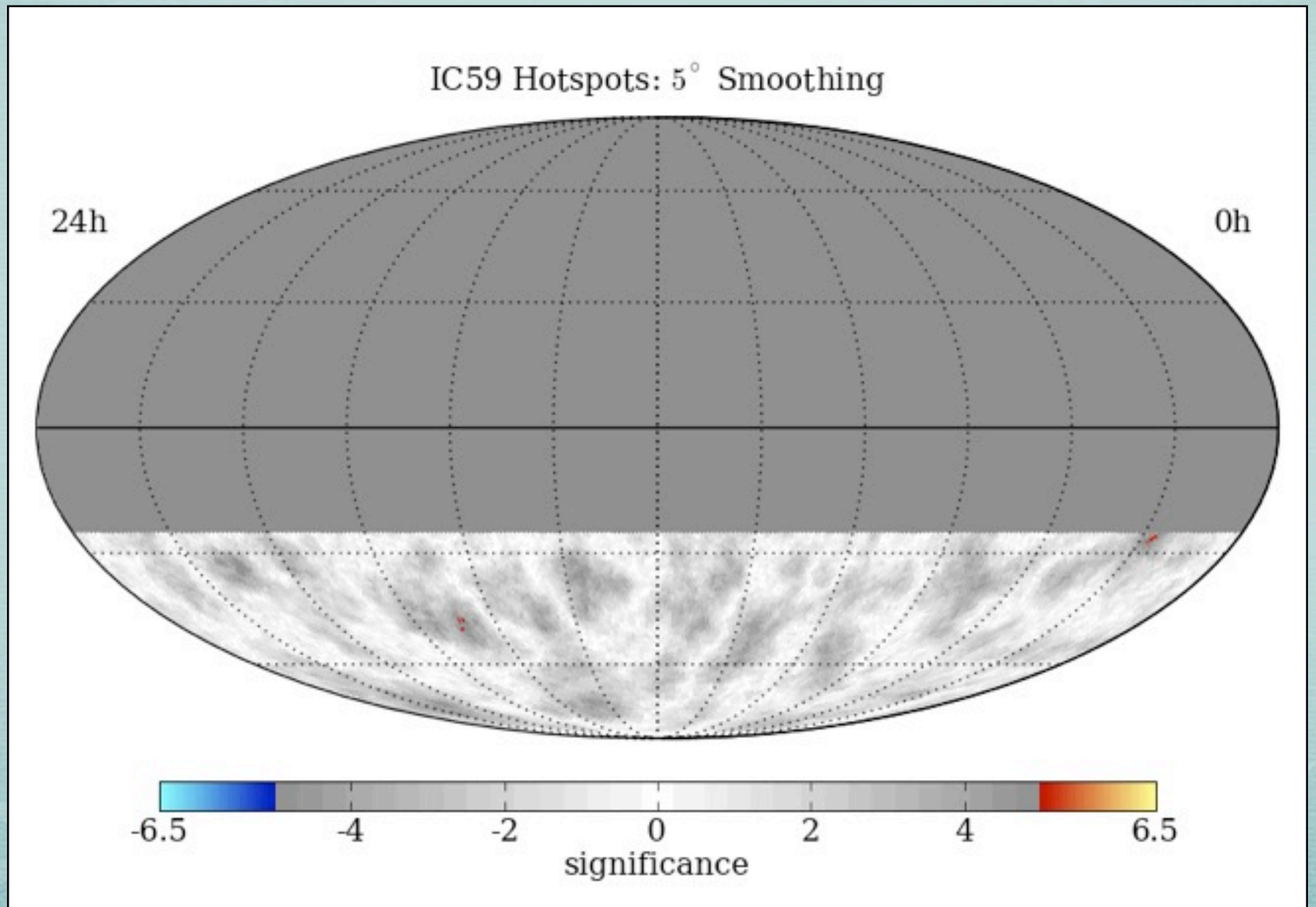

MAP SMOOTHING SCAN

Scan from 1 - 30° in smoothing
Different regions have different optimal angular smoothing
Significances are pre-trial

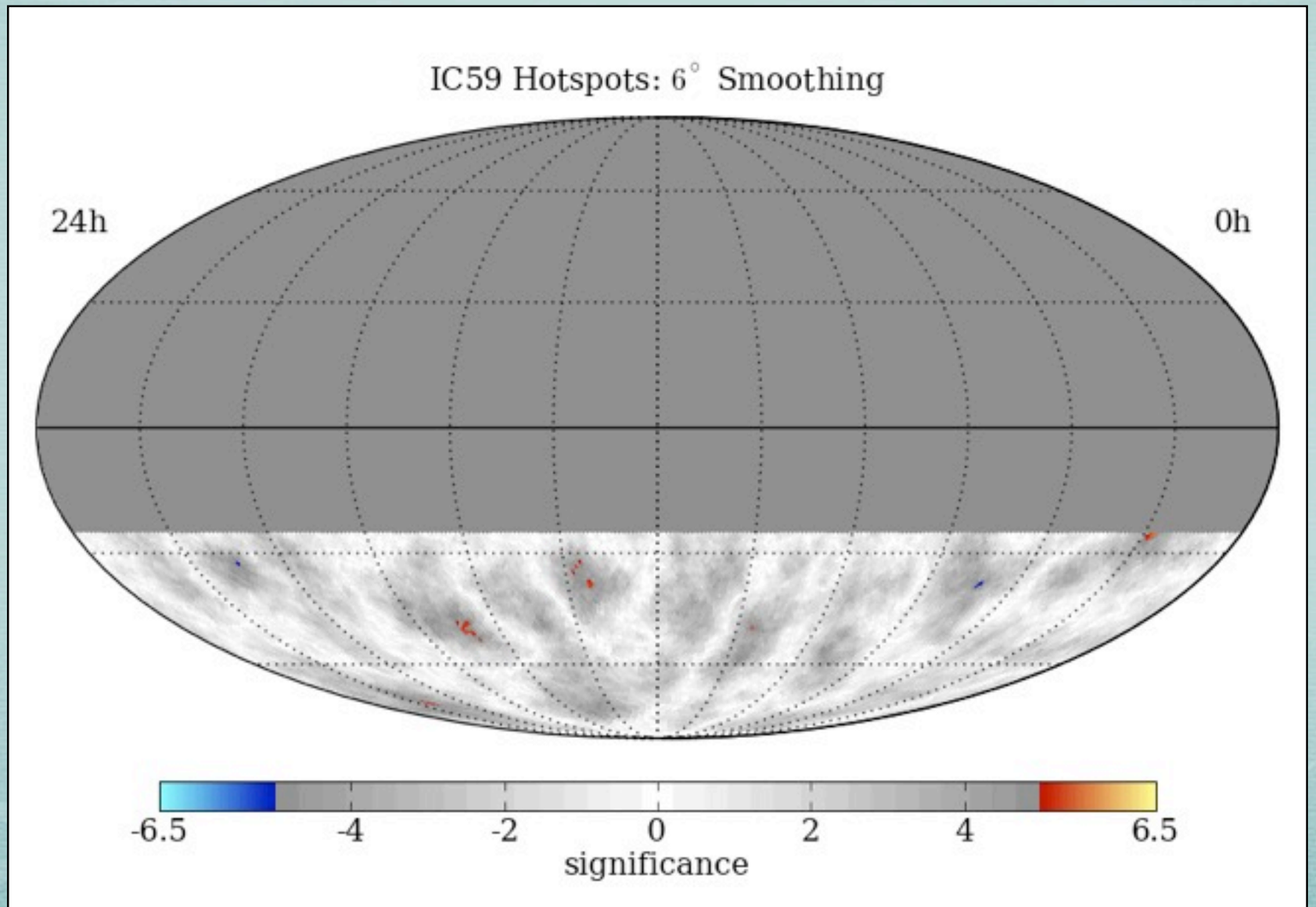

MAP SMOOTHING SCAN

Scan from 1 - 30° in smoothing
Different regions have different optimal angular smoothing
Significances are pre-trial

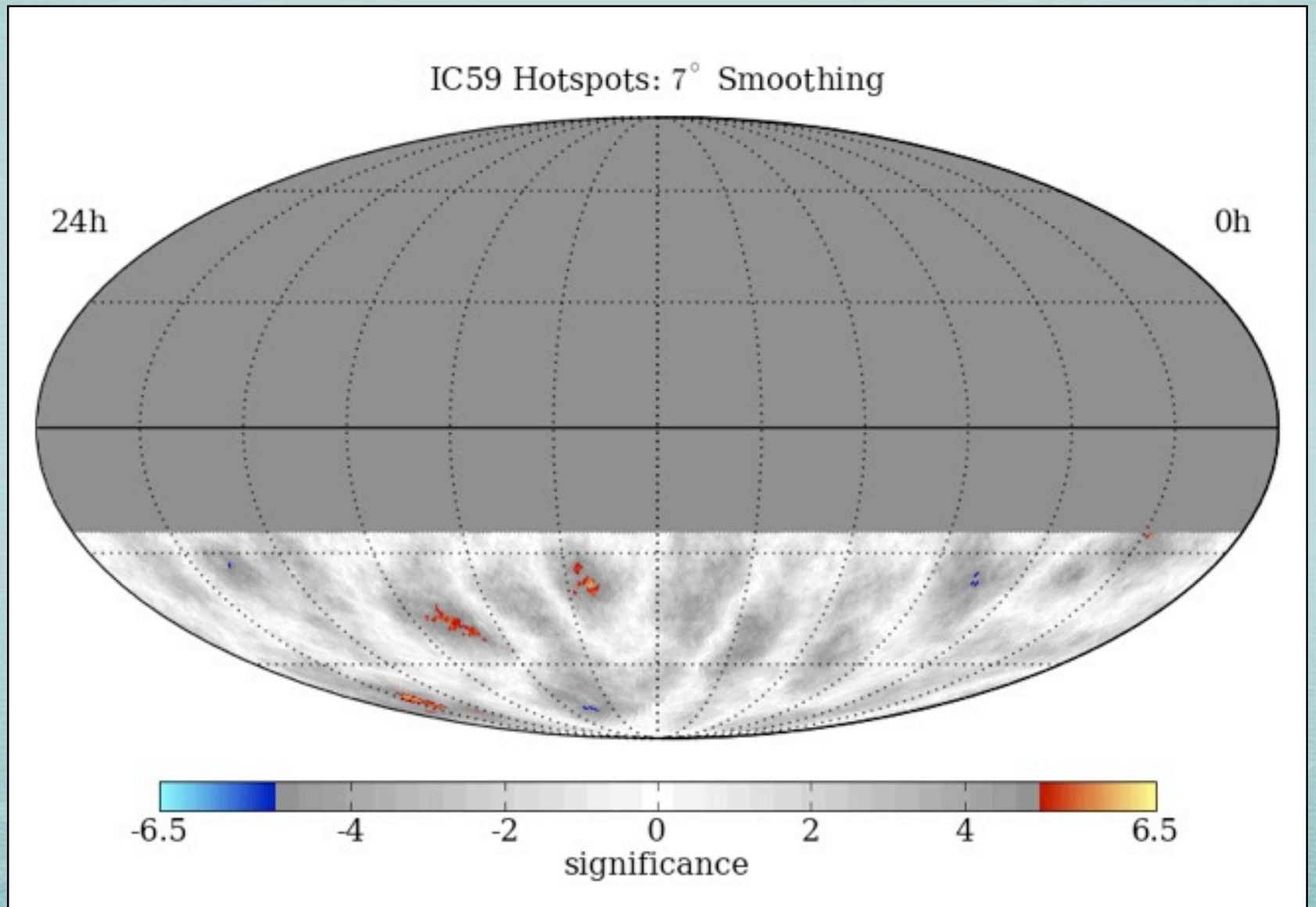

MAP SMOOTHING SCAN

Scan from 1 - 30° in smoothing
Different regions have different optimal angular smoothing
Significances are pre-trial

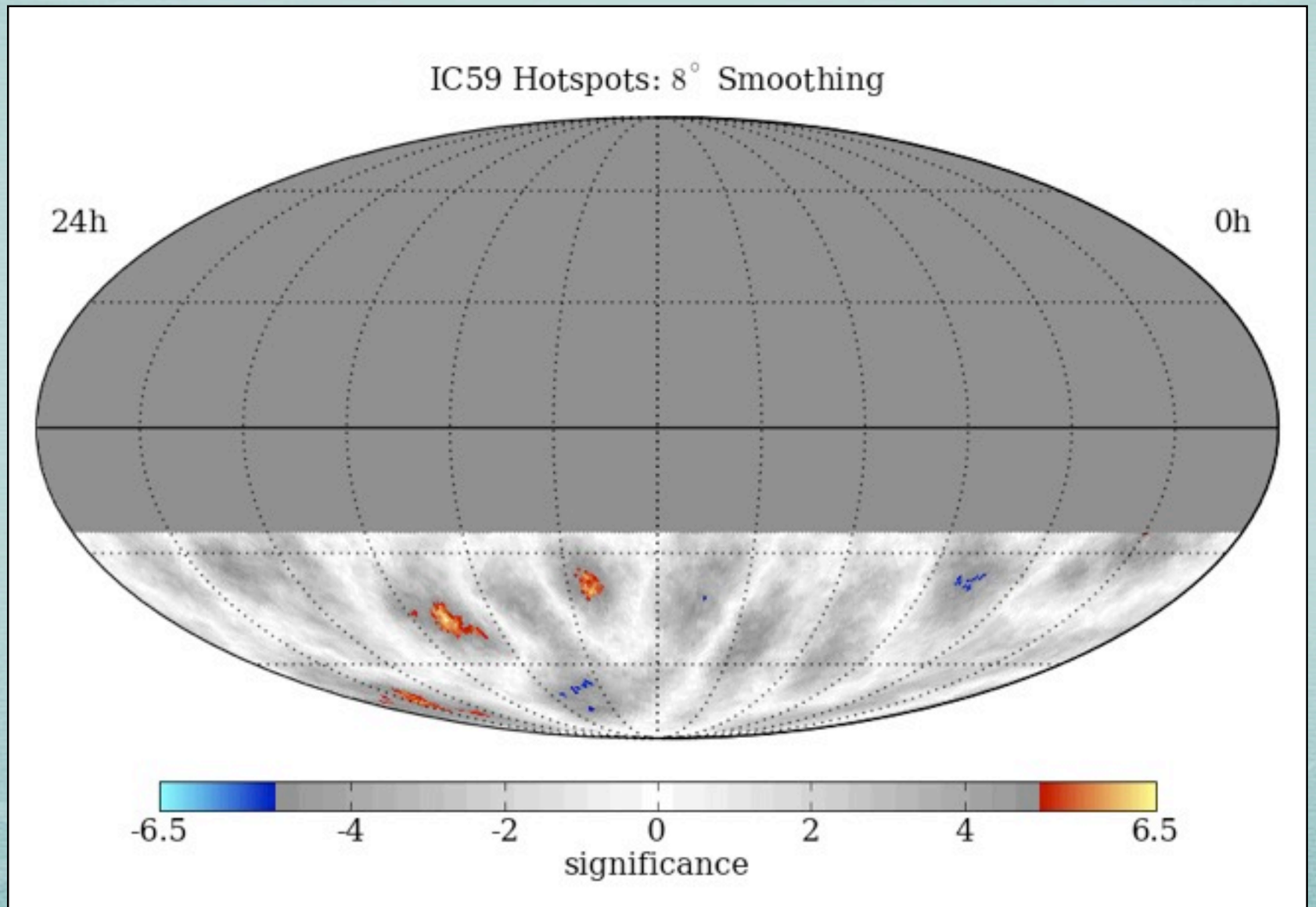

MAP SMOOTHING SCAN

Scan from 1 - 30° in smoothing
Different regions have different optimal angular smoothing
Significances are pre-trial

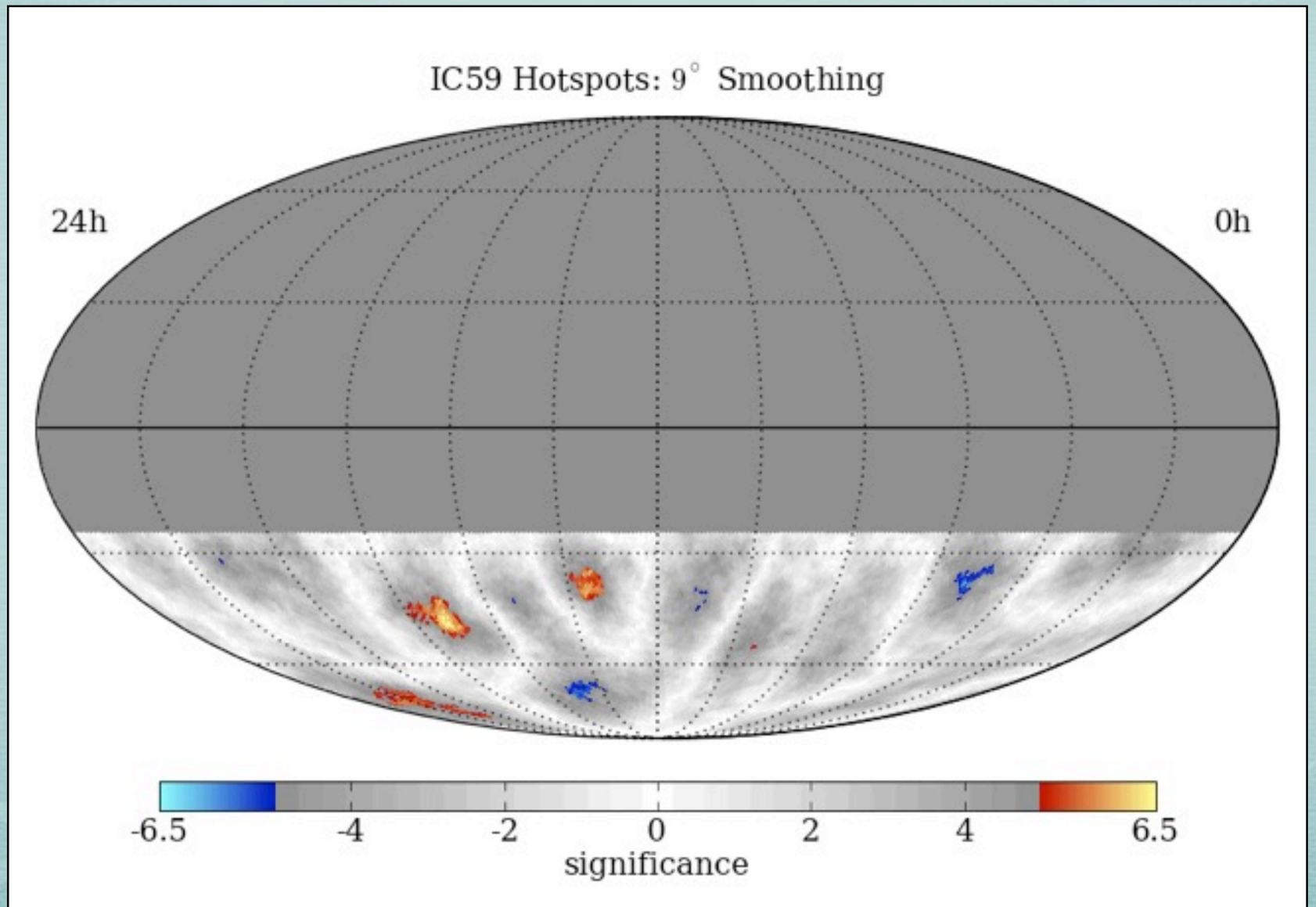

MAP SMOOTHING SCAN

Scan from 1 - 30° in smoothing
Different regions have different optimal angular smoothing
Significances are pre-trial

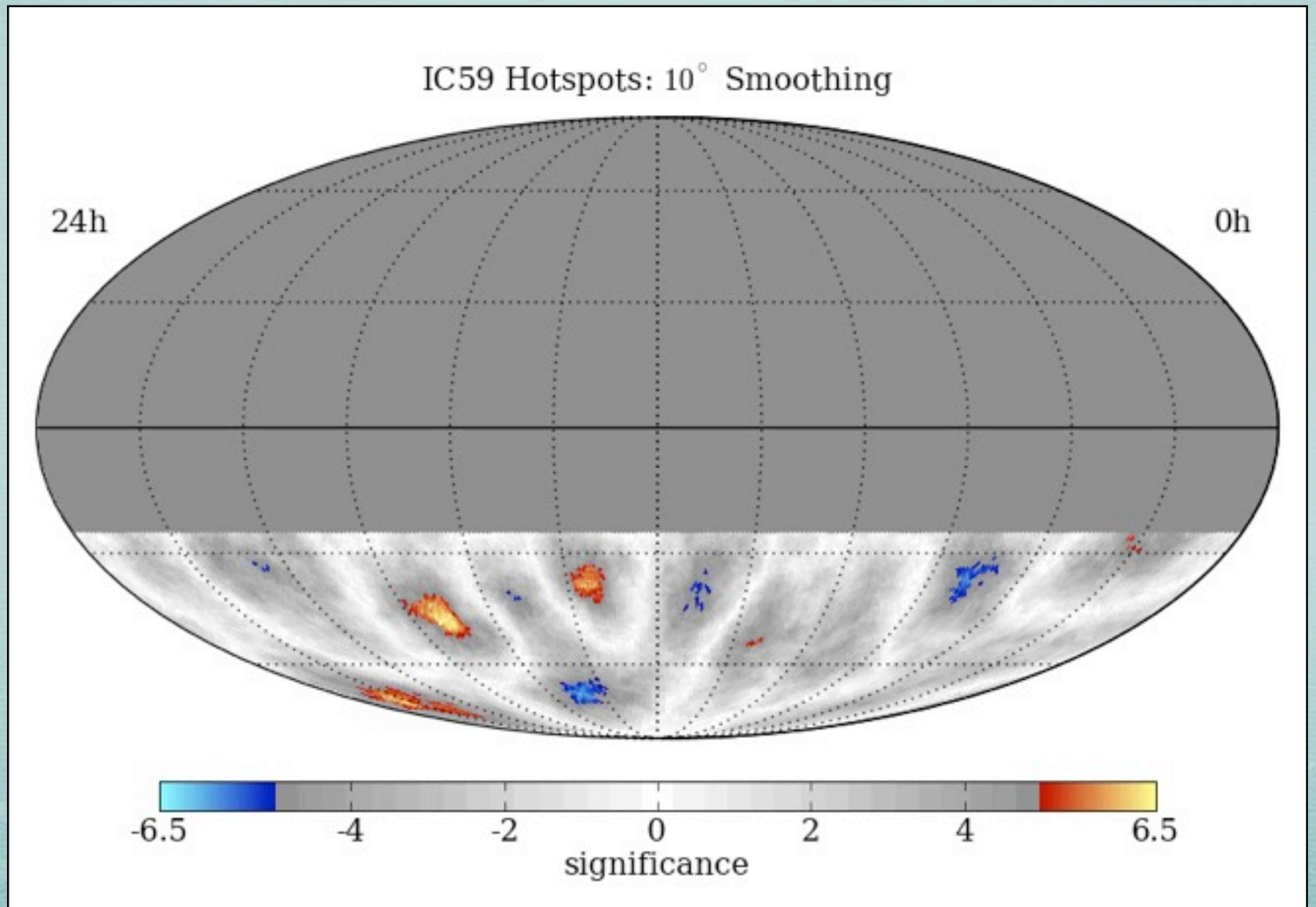

MAP SMOOTHING SCAN

Scan from 1 - 30° in smoothing
Different regions have different optimal angular smoothing
Significances are pre-trial

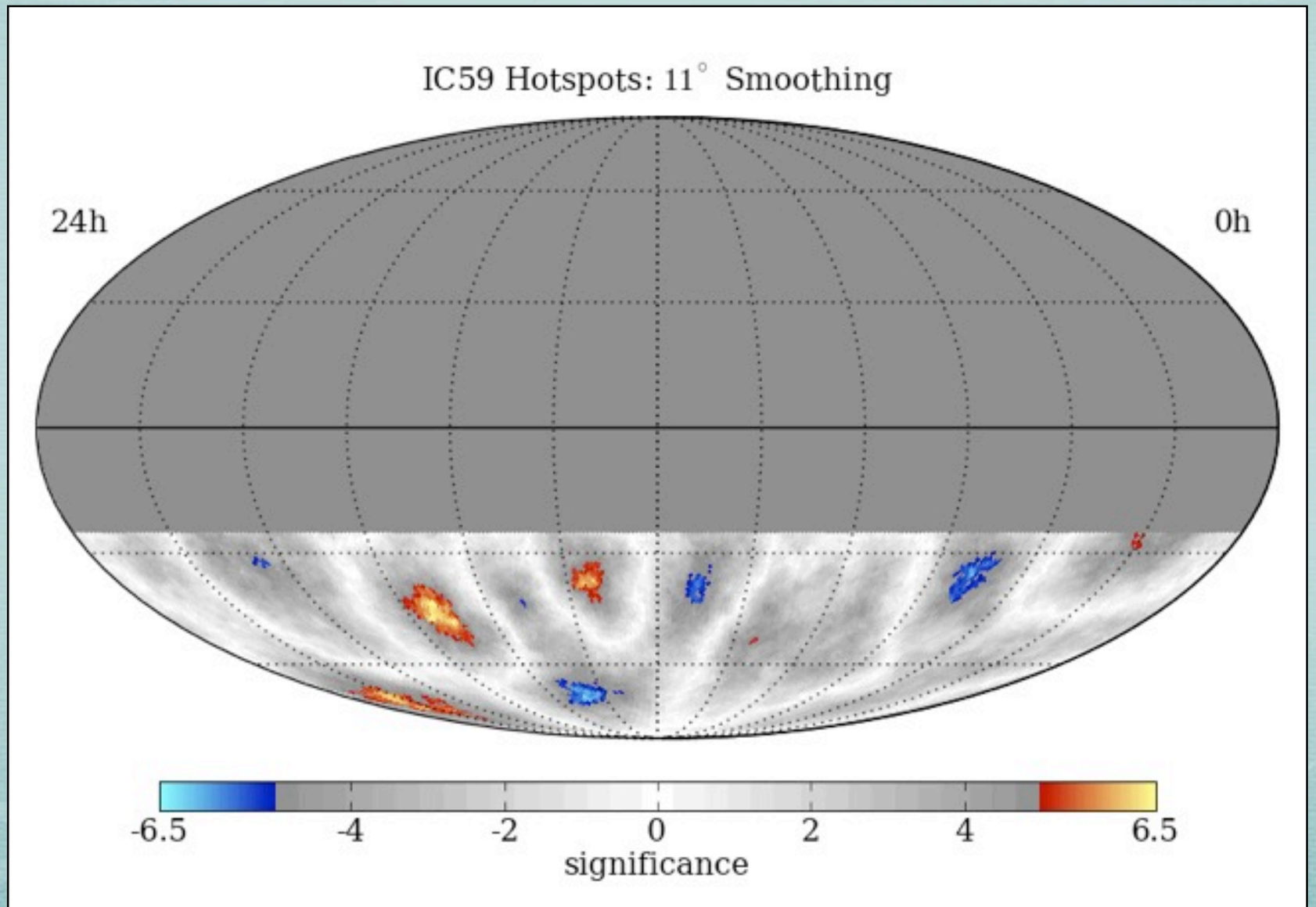

MAP SMOOTHING SCAN

Scan from 1 - 30° in smoothing
Different regions have different optimal angular smoothing
Significances are pre-trial

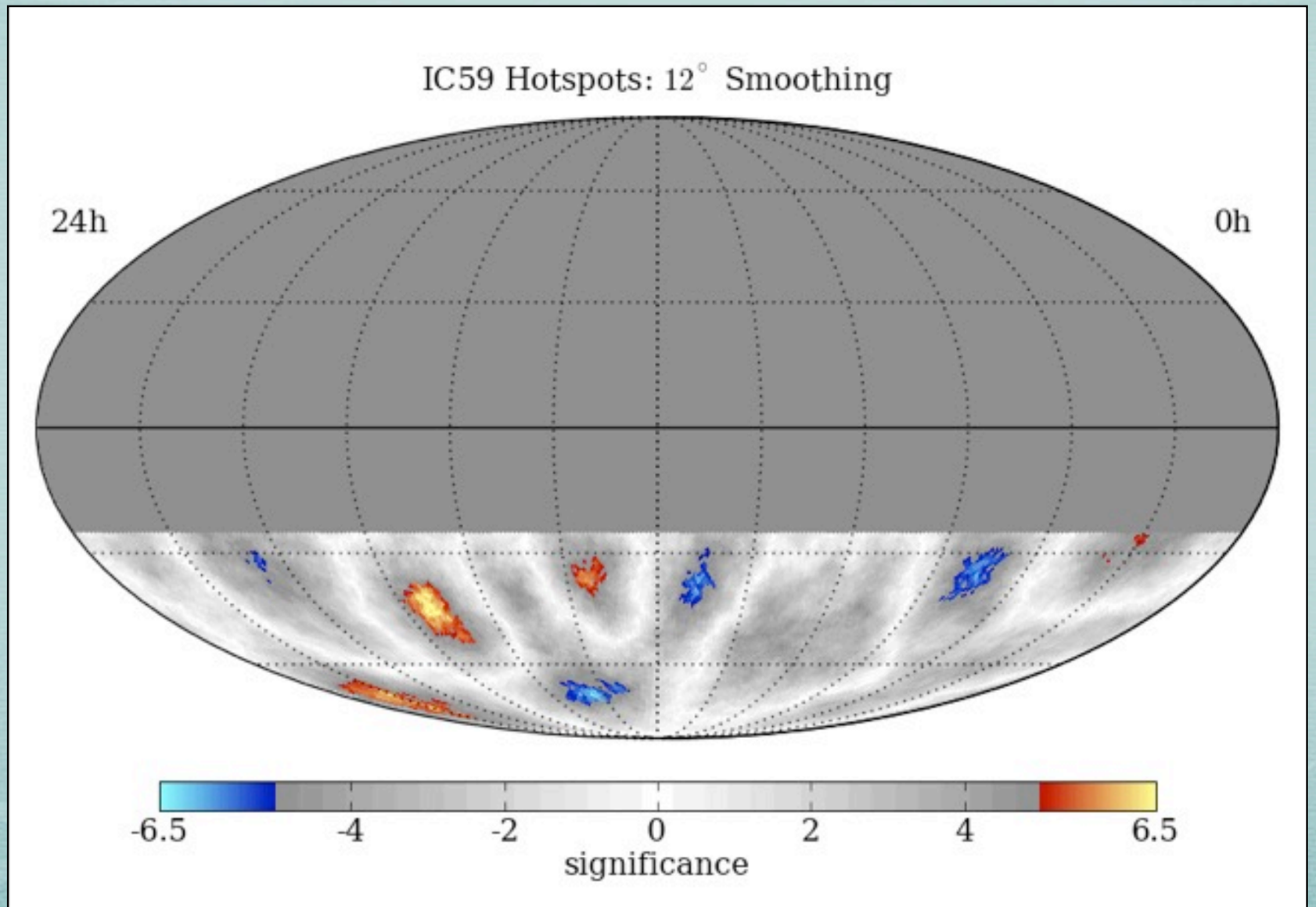

MAP SMOOTHING SCAN

Scan from 1 - 30° in smoothing
Different regions have different optimal angular smoothing
Significances are pre-trial

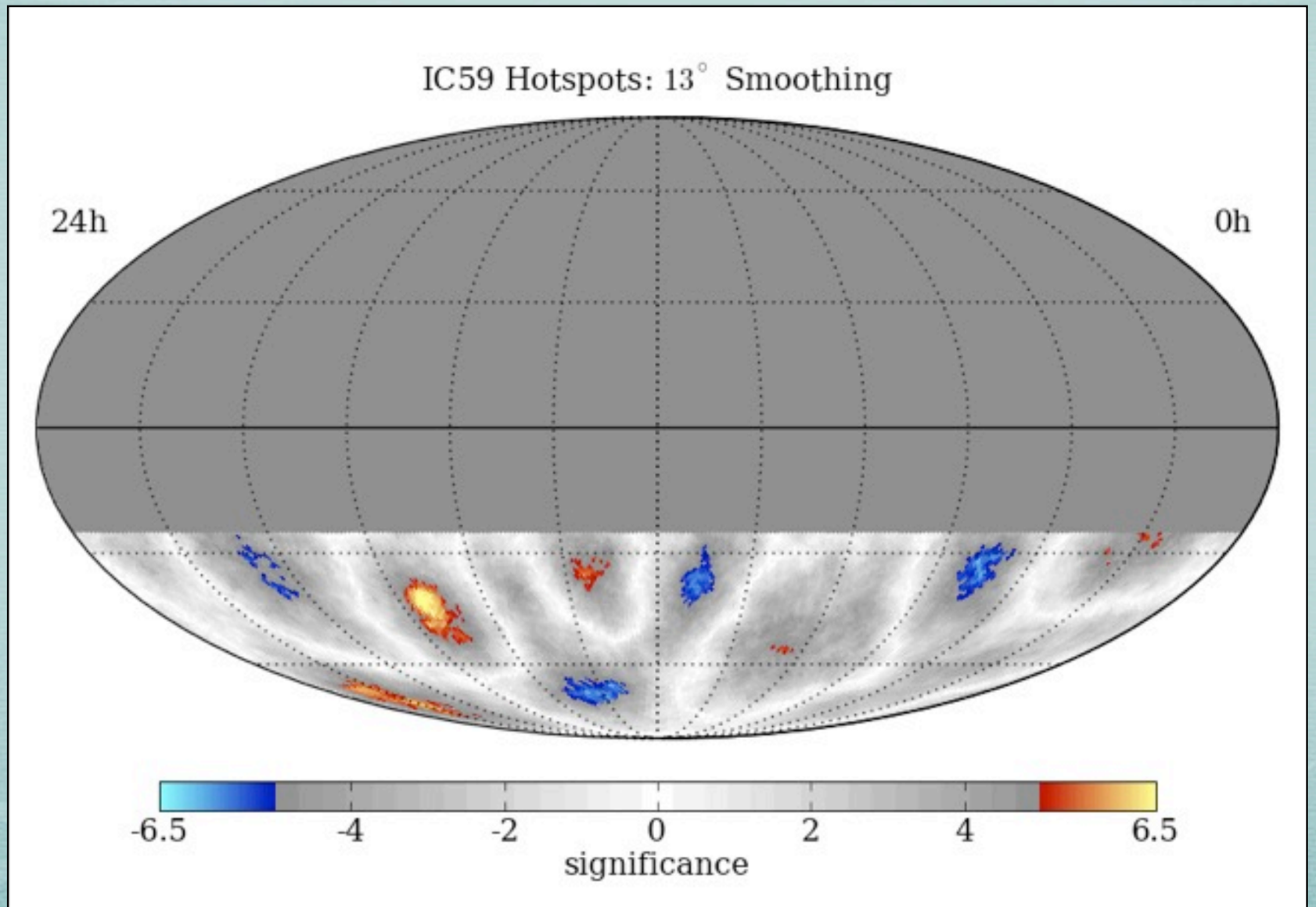

MAP SMOOTHING SCAN

Scan from 1 - 30° in smoothing
Different regions have different optimal angular smoothing
Significances are pre-trial

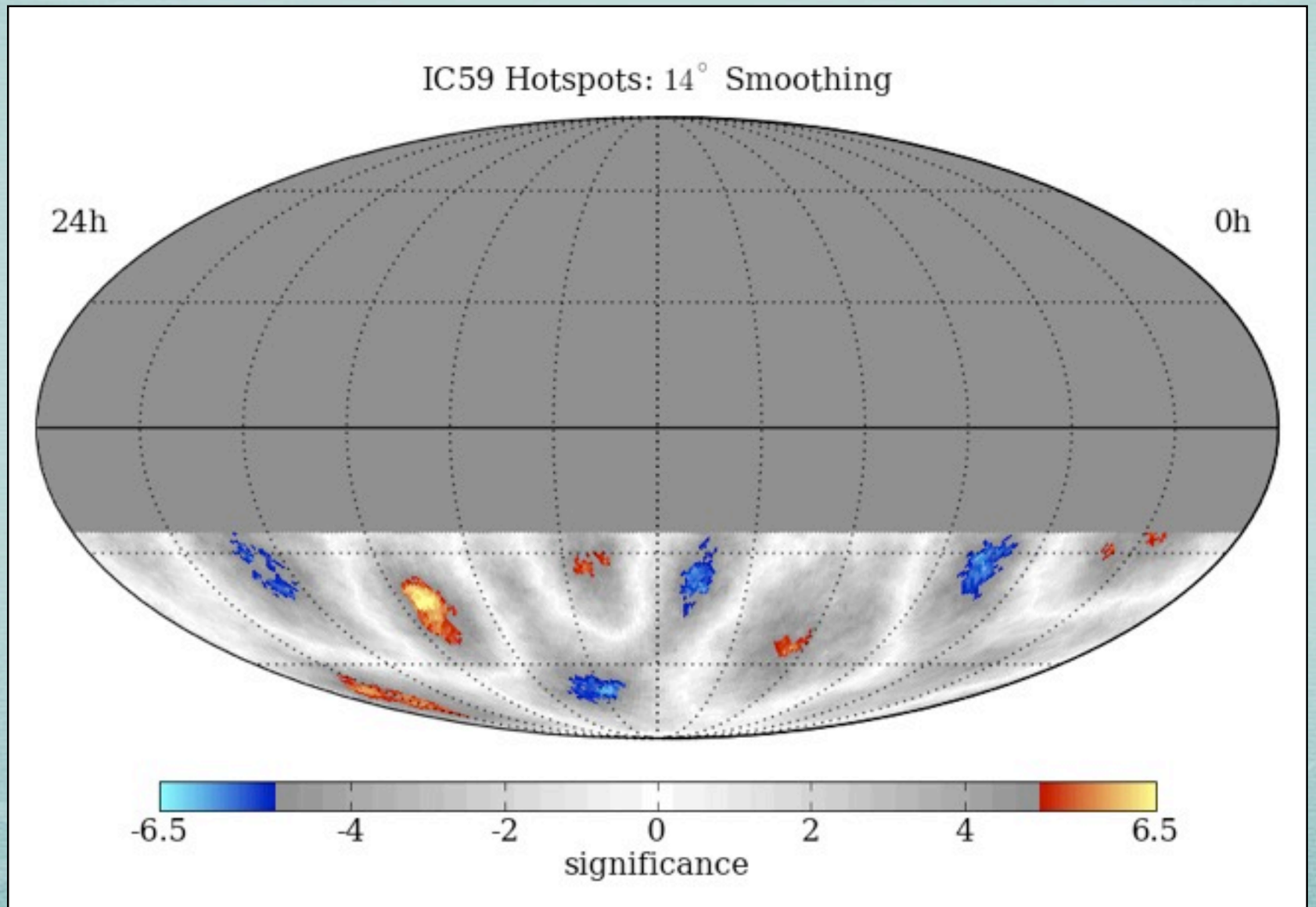

MAP SMOOTHING SCAN

Scan from 1 - 30° in smoothing
Different regions have different optimal angular smoothing
Significances are pre-trial

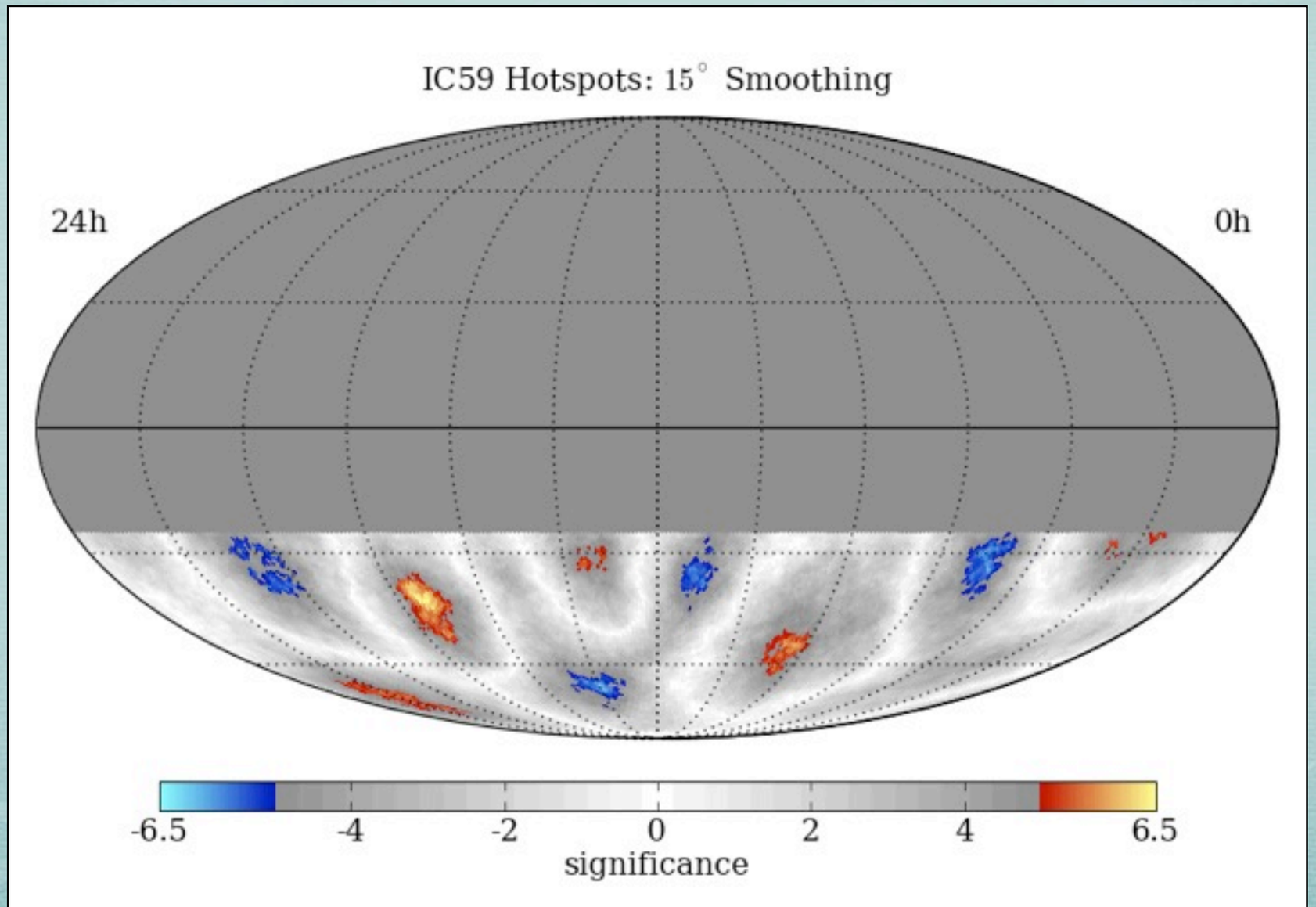

MAP SMOOTHING SCAN

Scan from 1 - 30° in smoothing
Different regions have different optimal angular smoothing
Significances are pre-trial

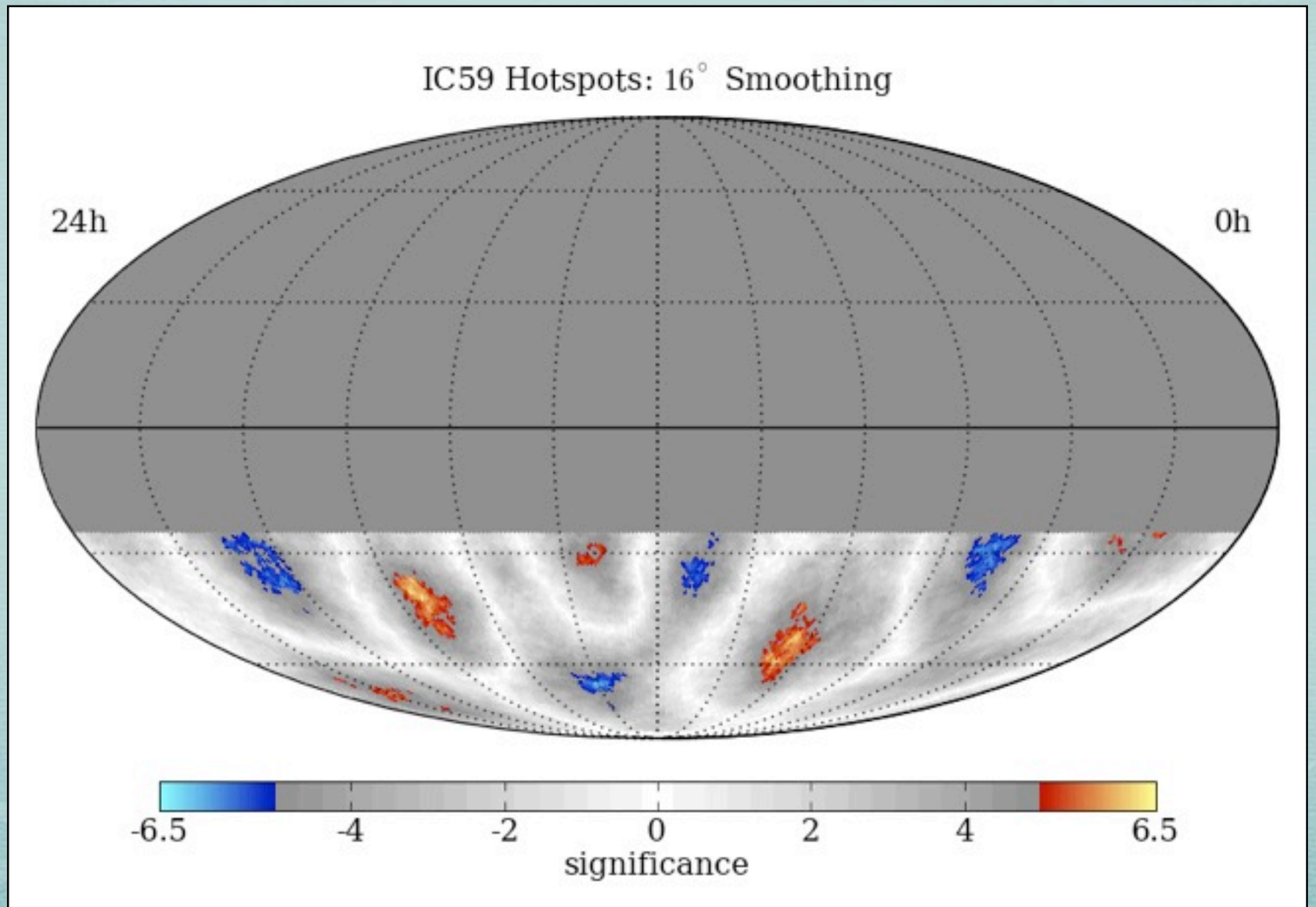

MAP SMOOTHING SCAN

Scan from 1 - 30° in smoothing
Different regions have different optimal angular smoothing
Significances are pre-trial

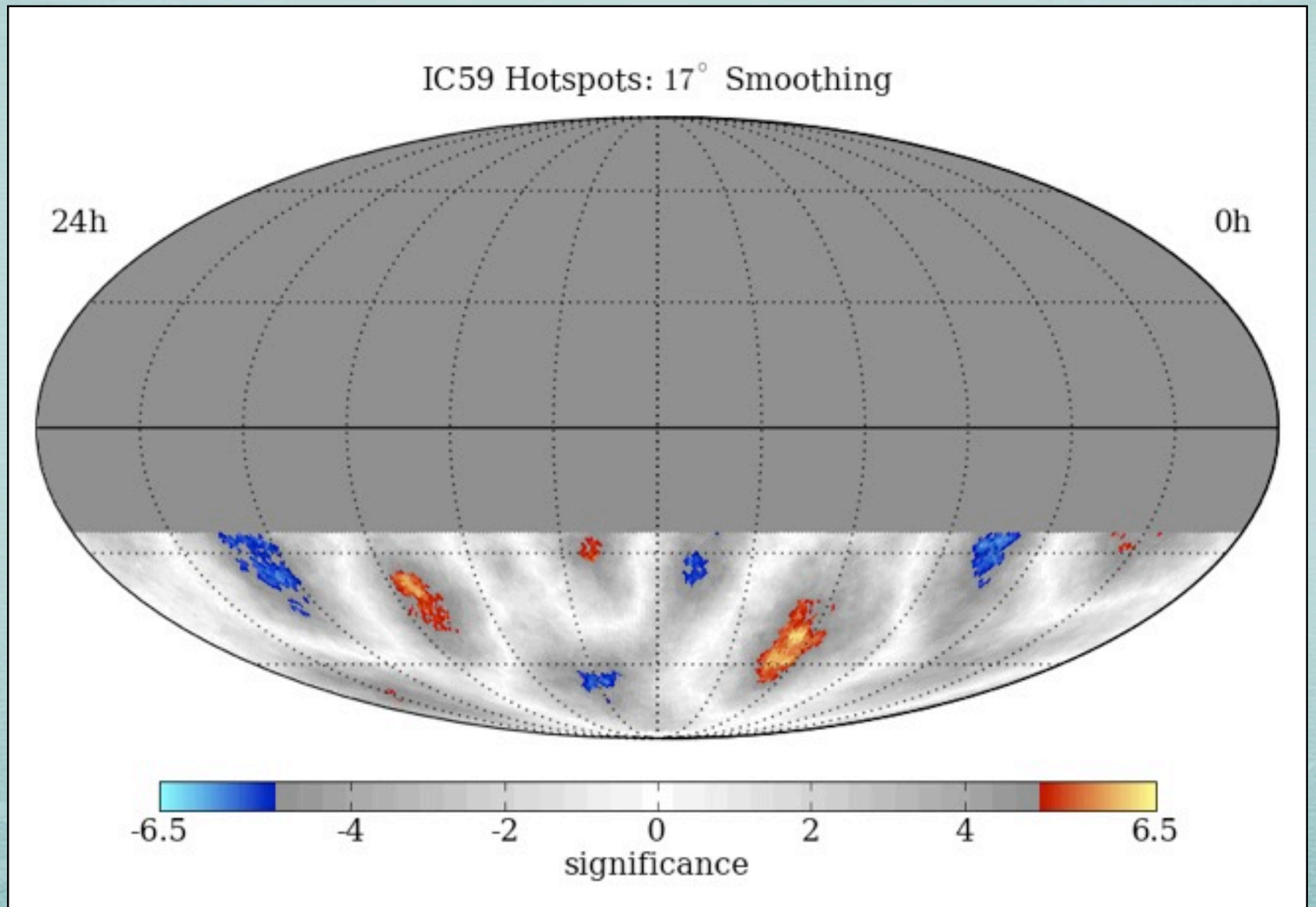

MAP SMOOTHING SCAN

Scan from 1 - 30° in smoothing
Different regions have different optimal angular smoothing
Significances are pre-trial

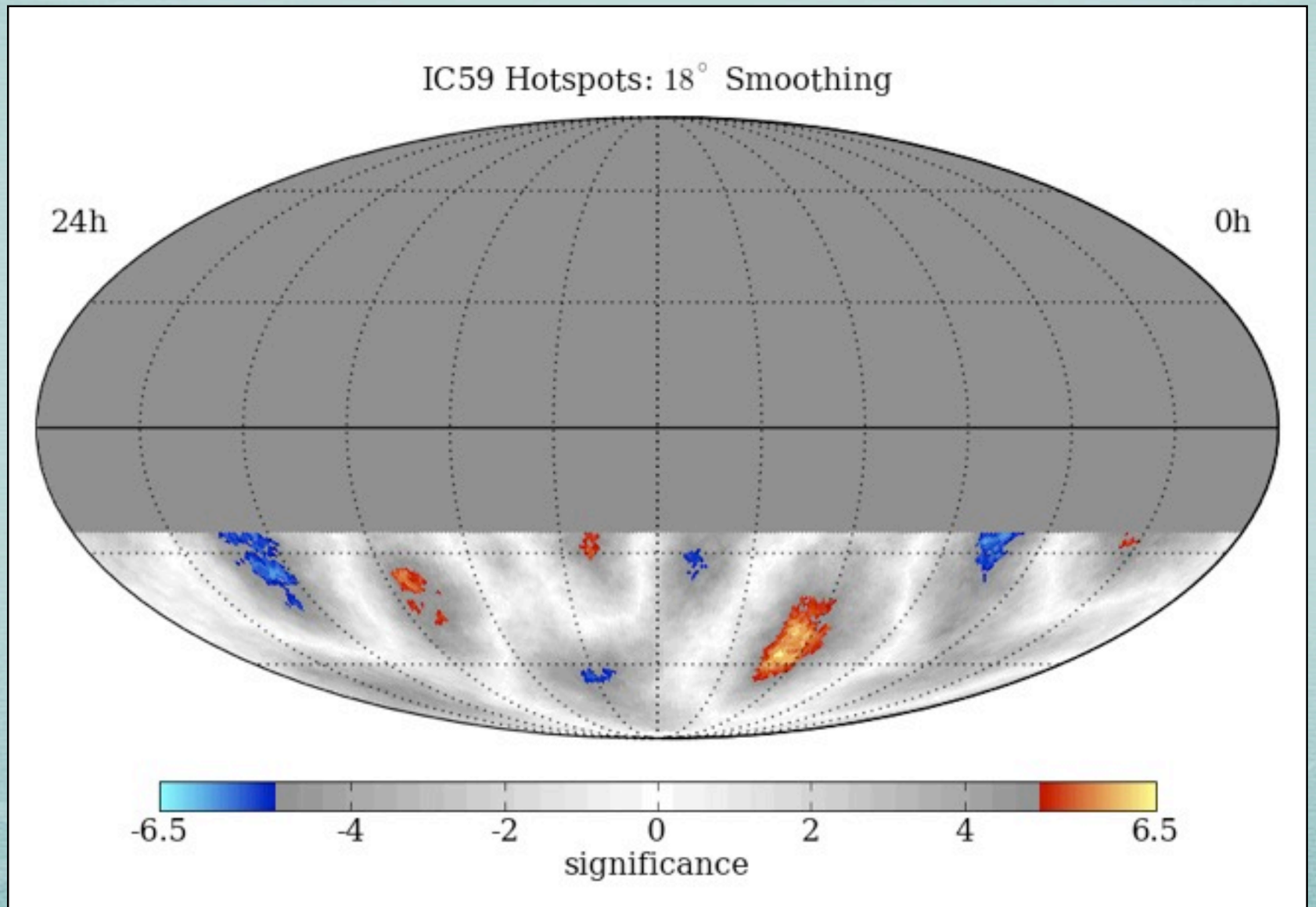

MAP SMOOTHING SCAN

Scan from 1 - 30° in smoothing
Different regions have different optimal angular smoothing
Significances are pre-trial

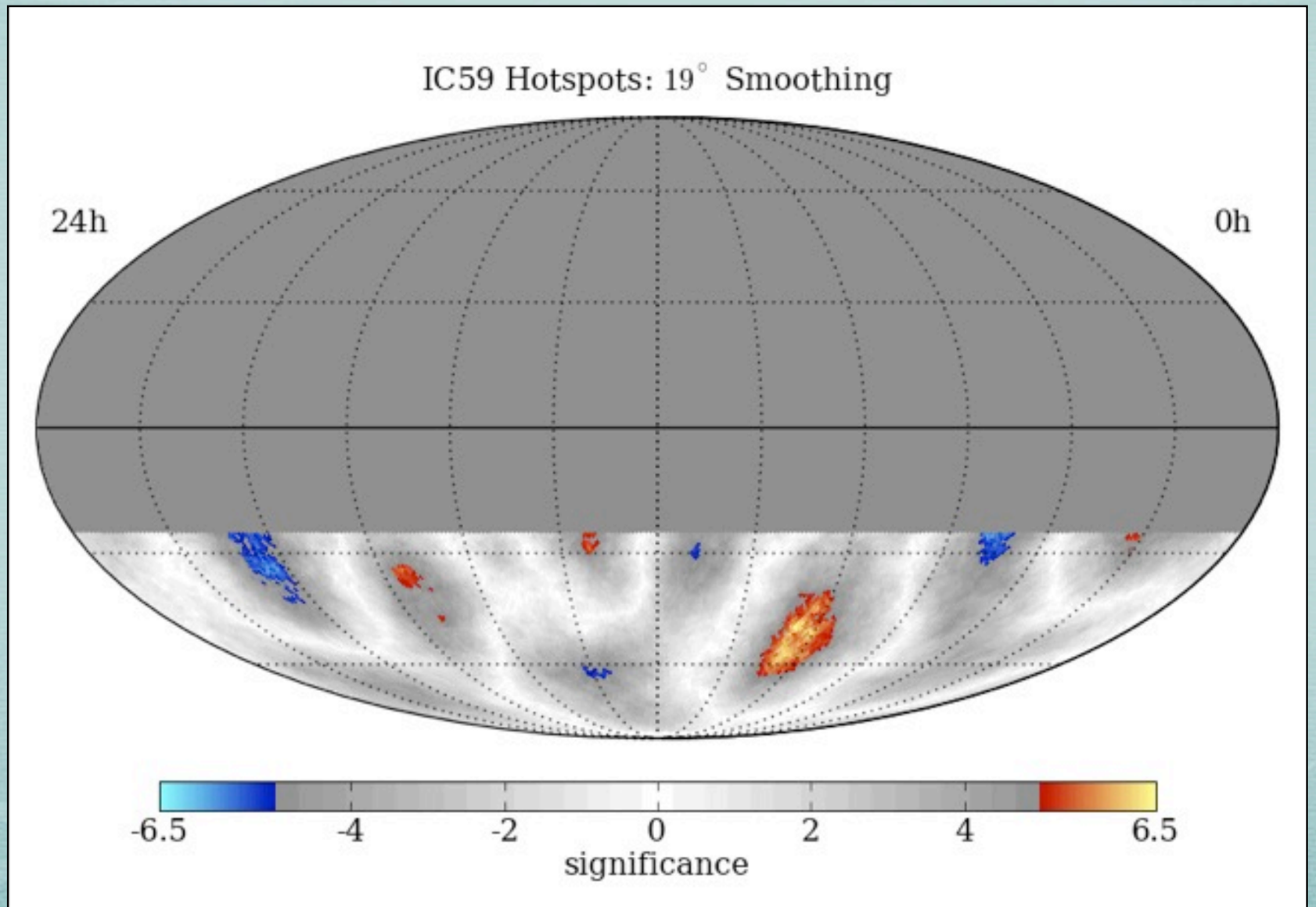

MAP SMOOTHING SCAN

Scan from 1 - 30° in smoothing
Different regions have different optimal angular smoothing
Significances are pre-trial

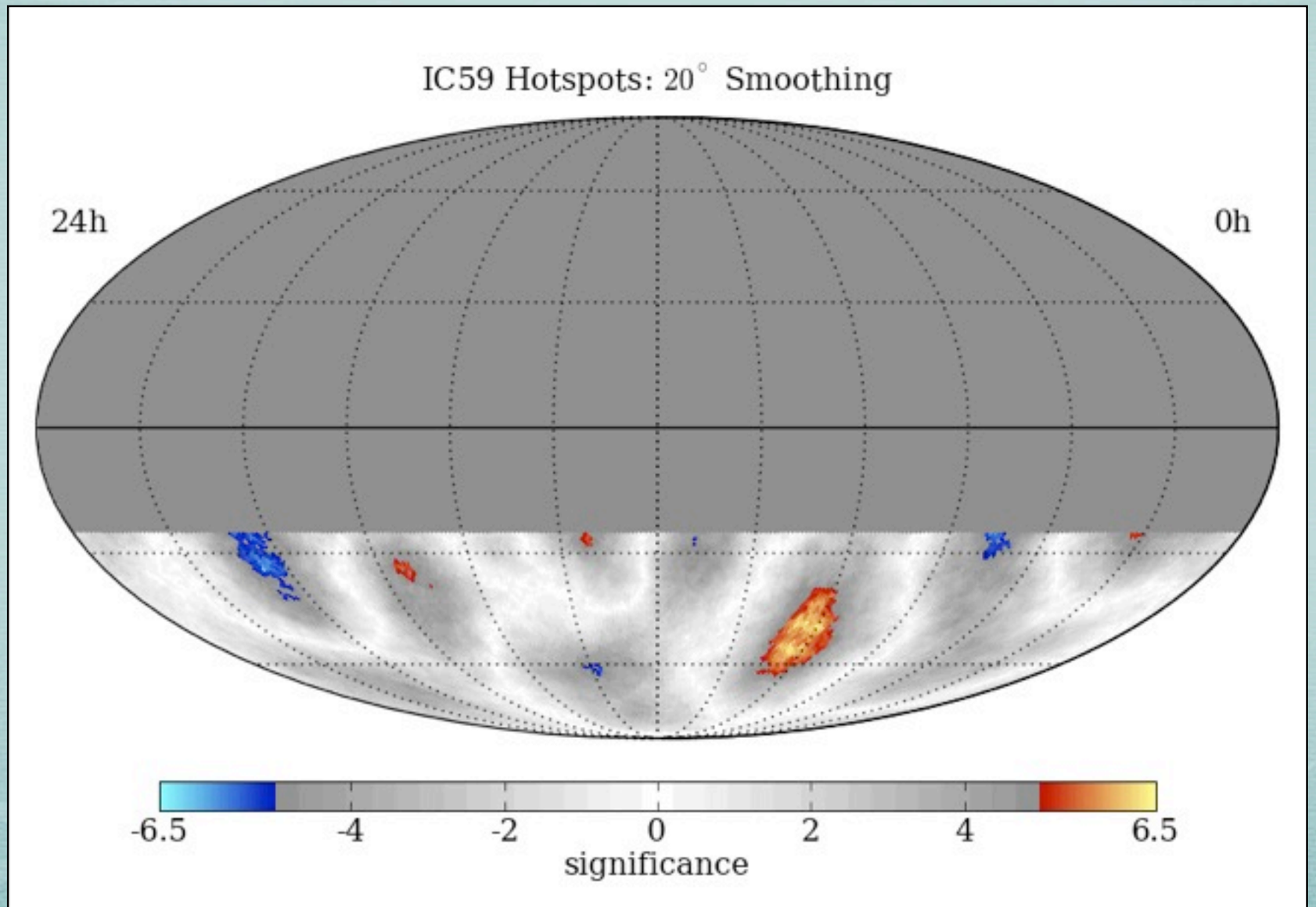

MAP SMOOTHING SCAN

Scan from 1 - 30° in smoothing
Different regions have different optimal angular smoothing
Significances are pre-trial

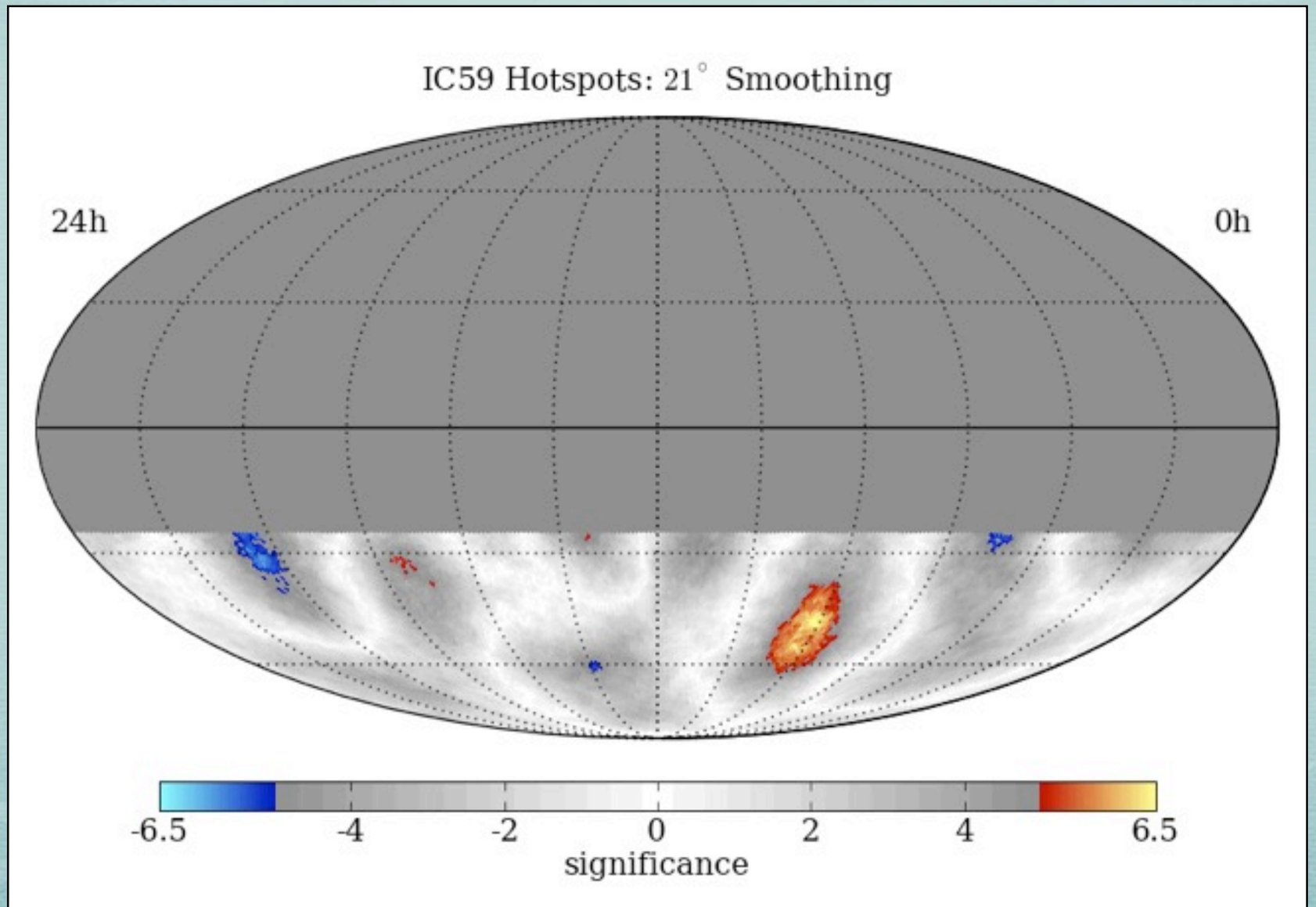

MAP SMOOTHING SCAN

Scan from 1 - 30° in smoothing
Different regions have different optimal angular smoothing
Significances are pre-trial

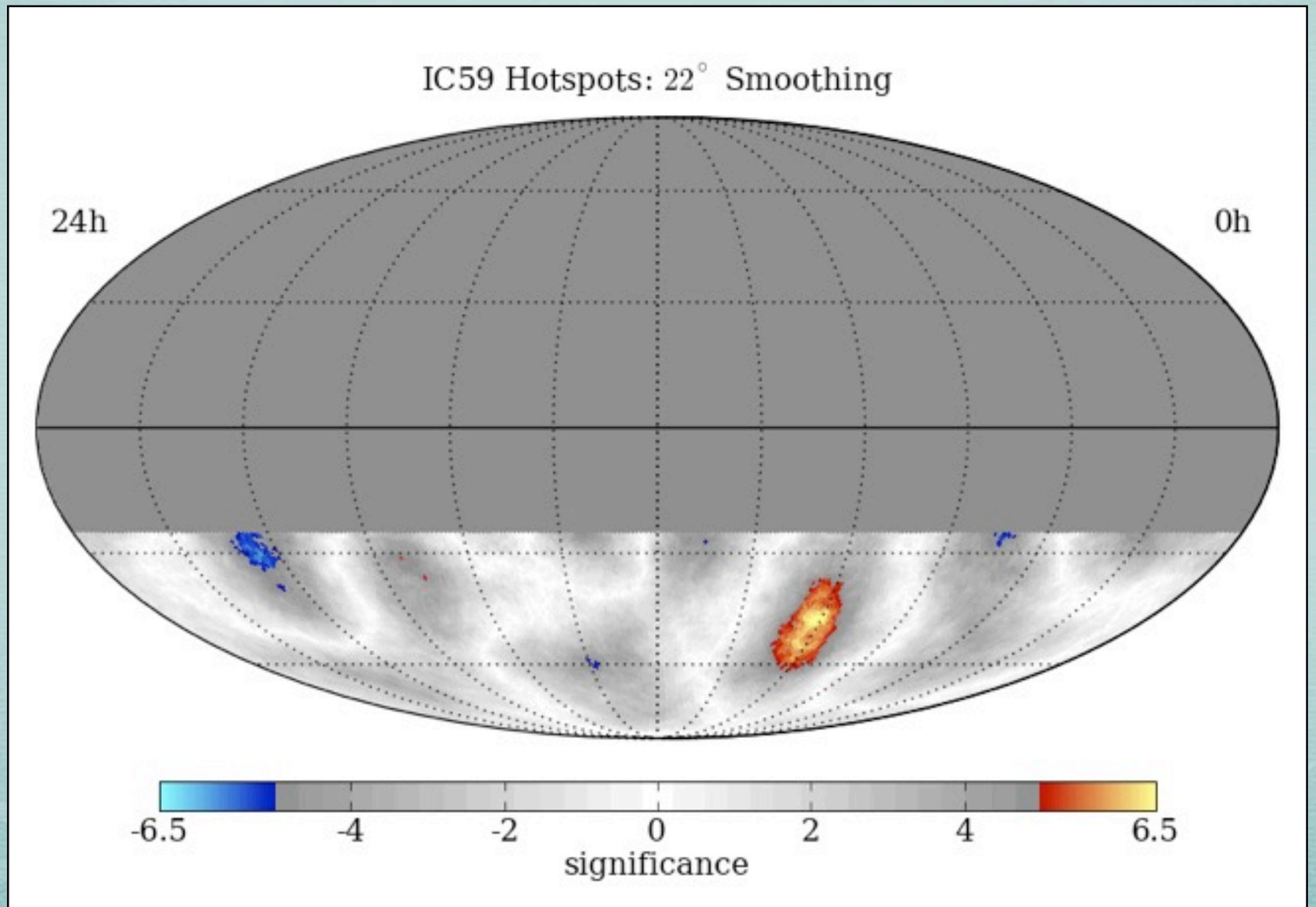

MAP SMOOTHING SCAN

Scan from 1 - 30° in smoothing
Different regions have different optimal angular smoothing
Significances are pre-trial

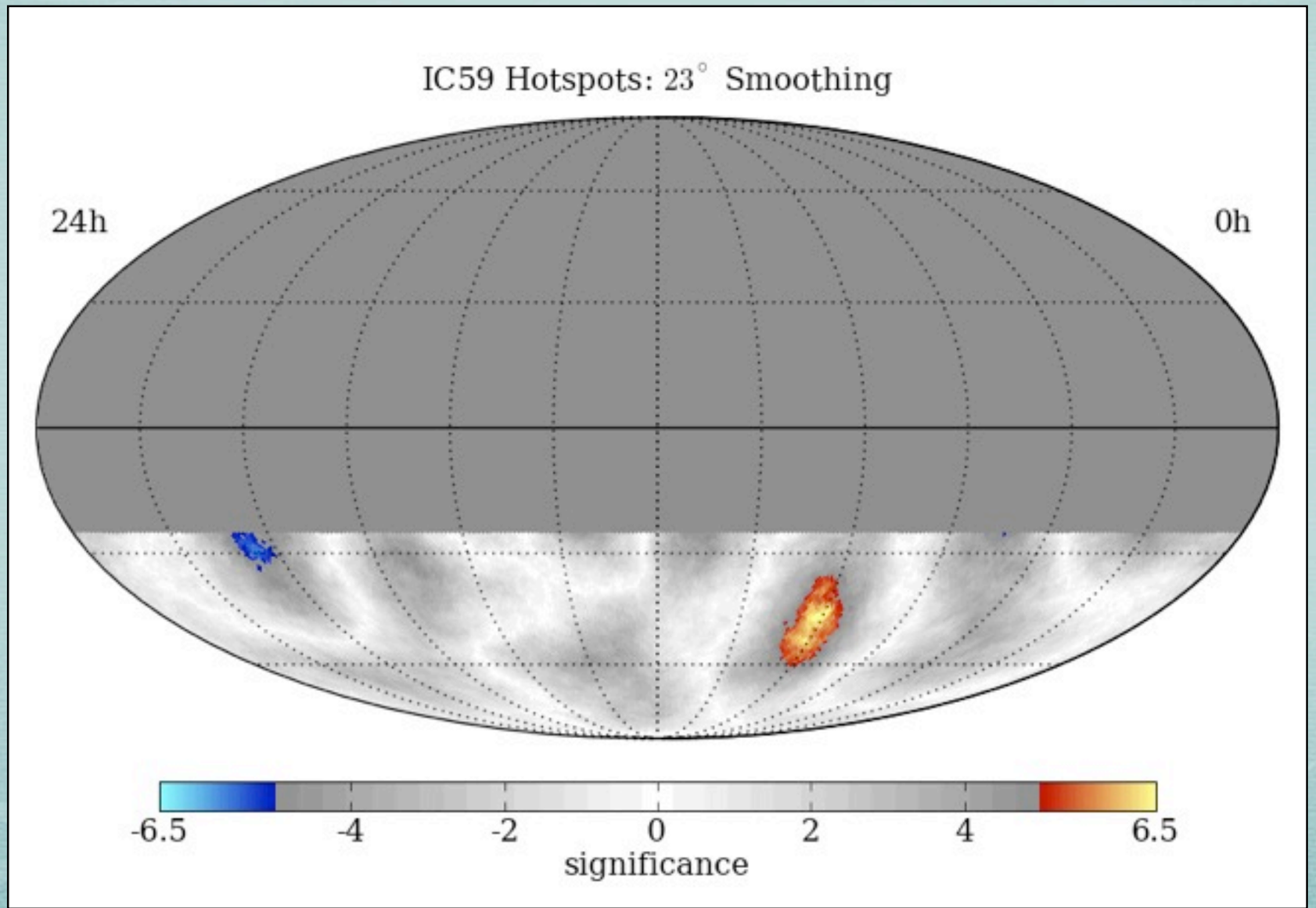

MAP SMOOTHING SCAN

Scan from 1 - 30° in smoothing
Different regions have different optimal angular smoothing
Significances are pre-trial

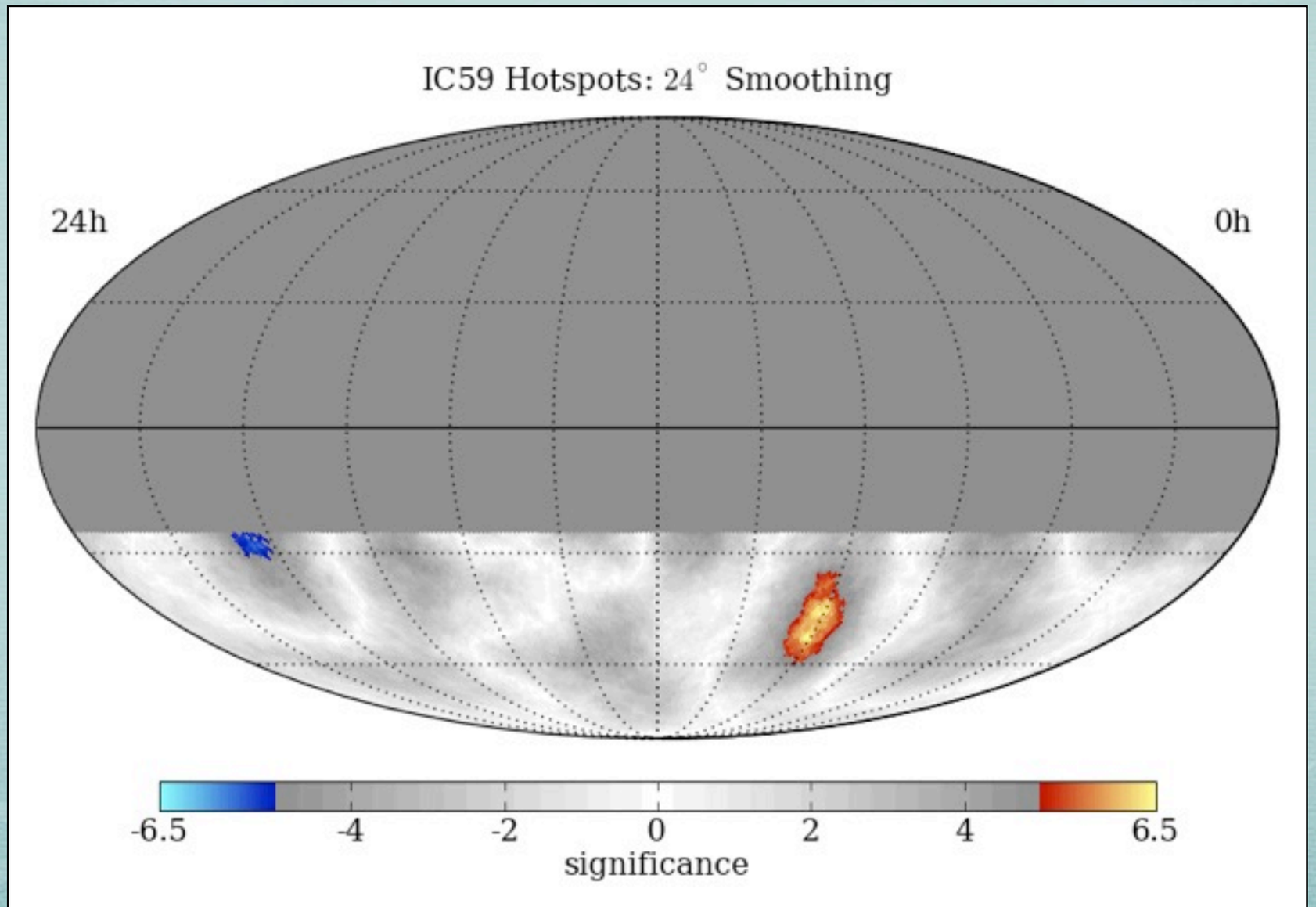

MAP SMOOTHING SCAN

Scan from 1 - 30° in smoothing
Different regions have different optimal angular smoothing
Significances are pre-trial

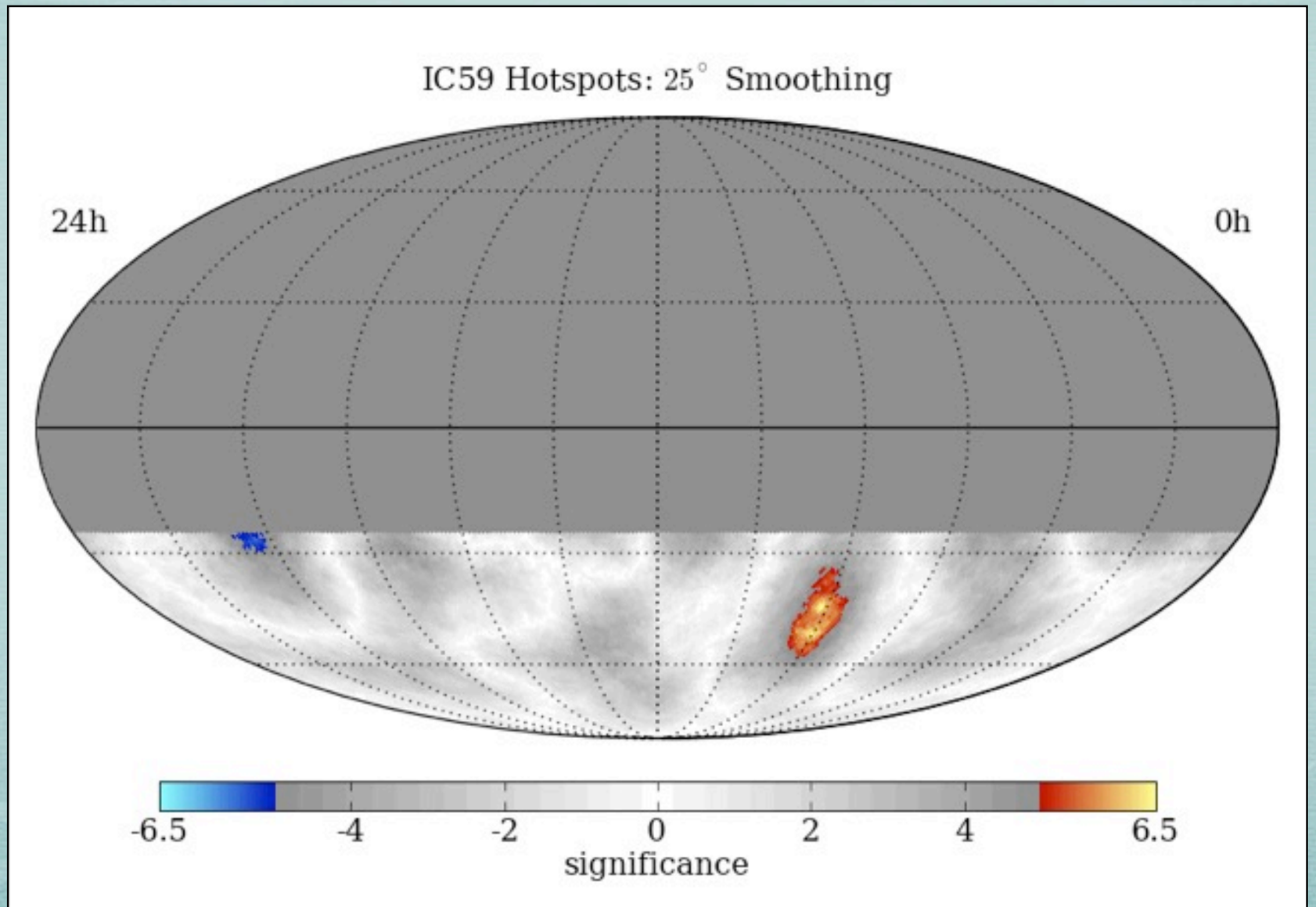

MAP SMOOTHING SCAN

Scan from 1 - 30° in smoothing
Different regions have different optimal angular smoothing
Significances are pre-trial

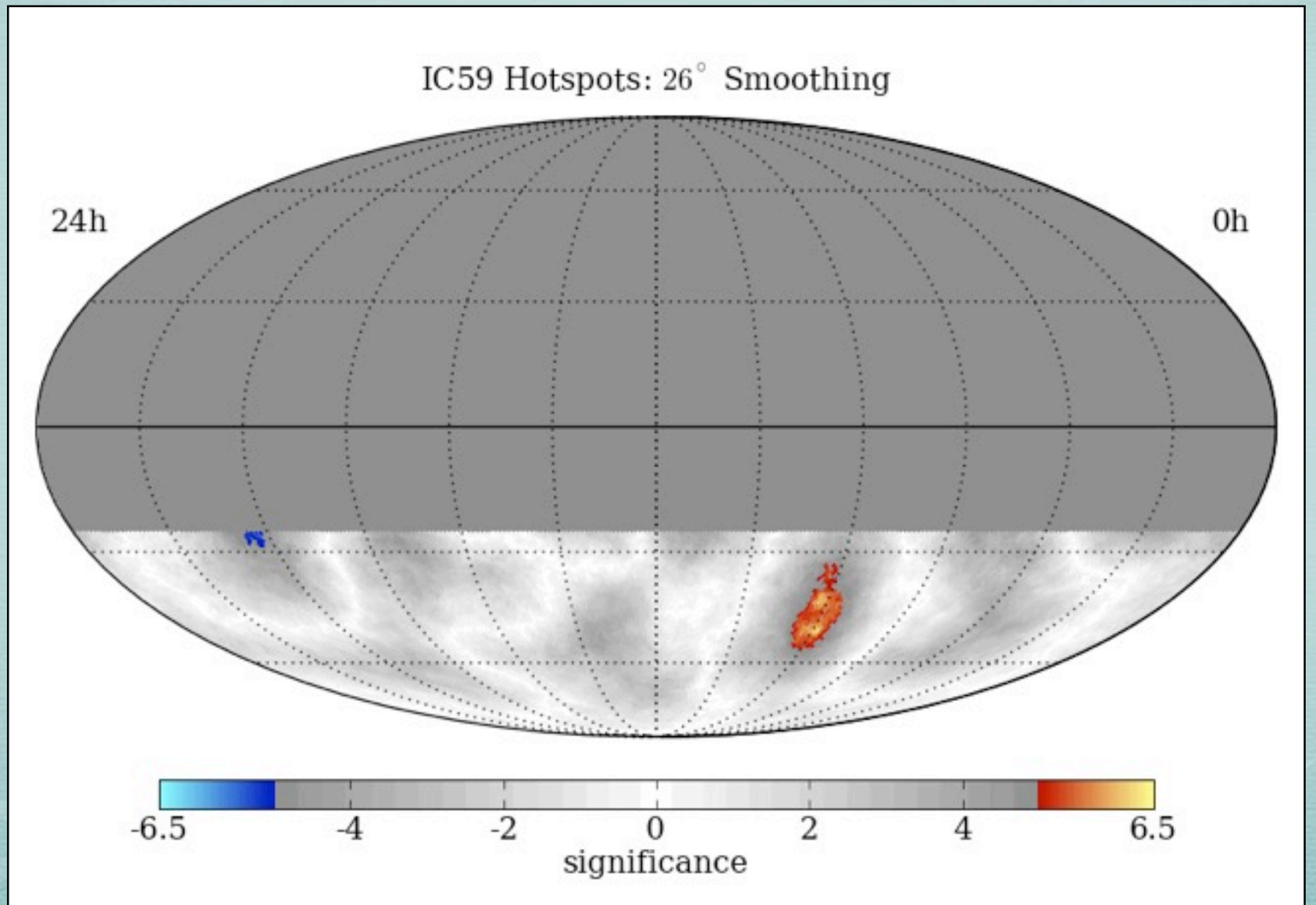

MAP SMOOTHING SCAN

Scan from 1 - 30° in smoothing
Different regions have different optimal angular smoothing
Significances are pre-trial

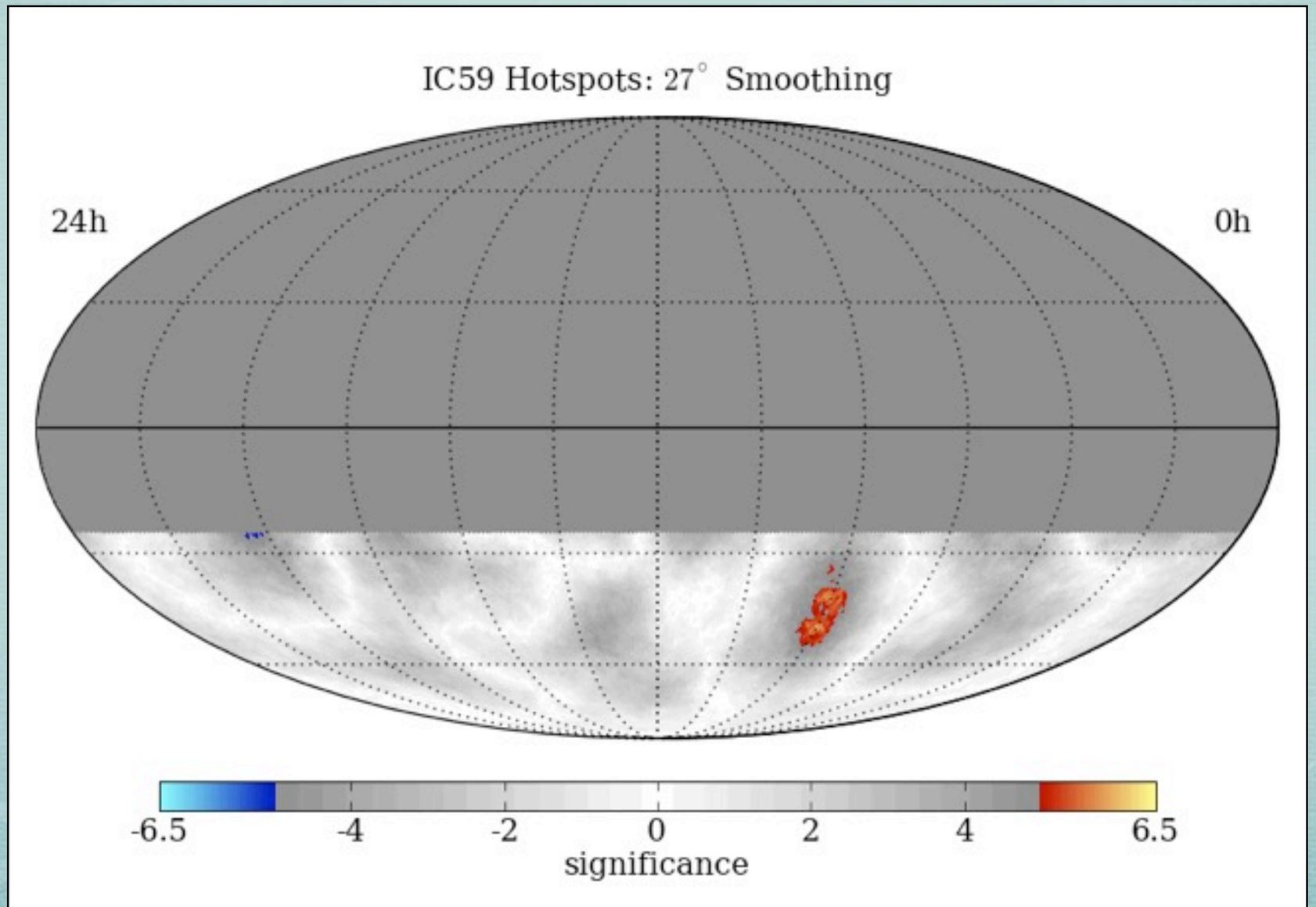

MAP SMOOTHING SCAN

Scan from 1 - 30° in smoothing
Different regions have different optimal angular smoothing
Significances are pre-trial

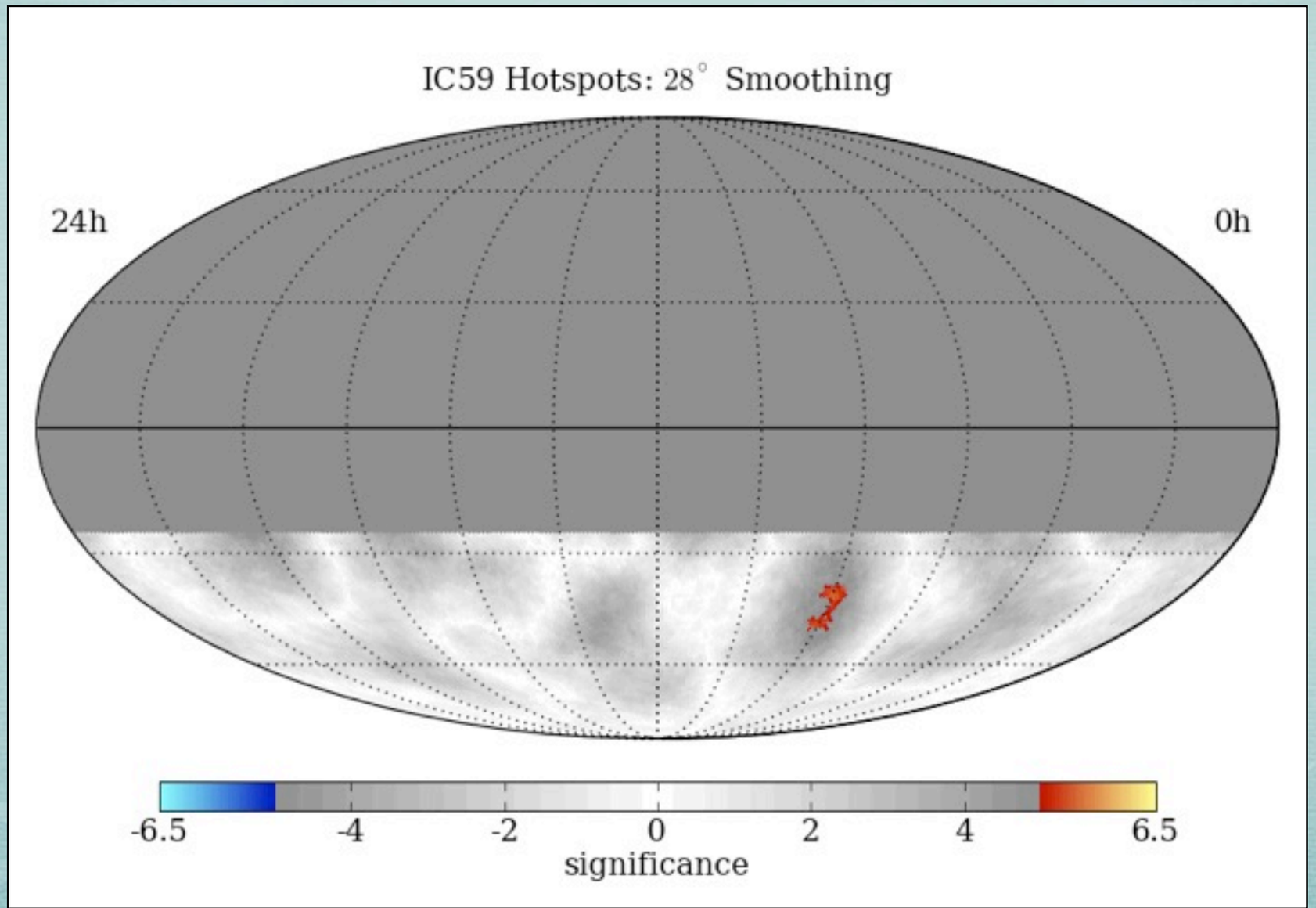

MAP SMOOTHING SCAN

Scan from 1 - 30° in smoothing
Different regions have different optimal angular smoothing
Significances are pre-trial

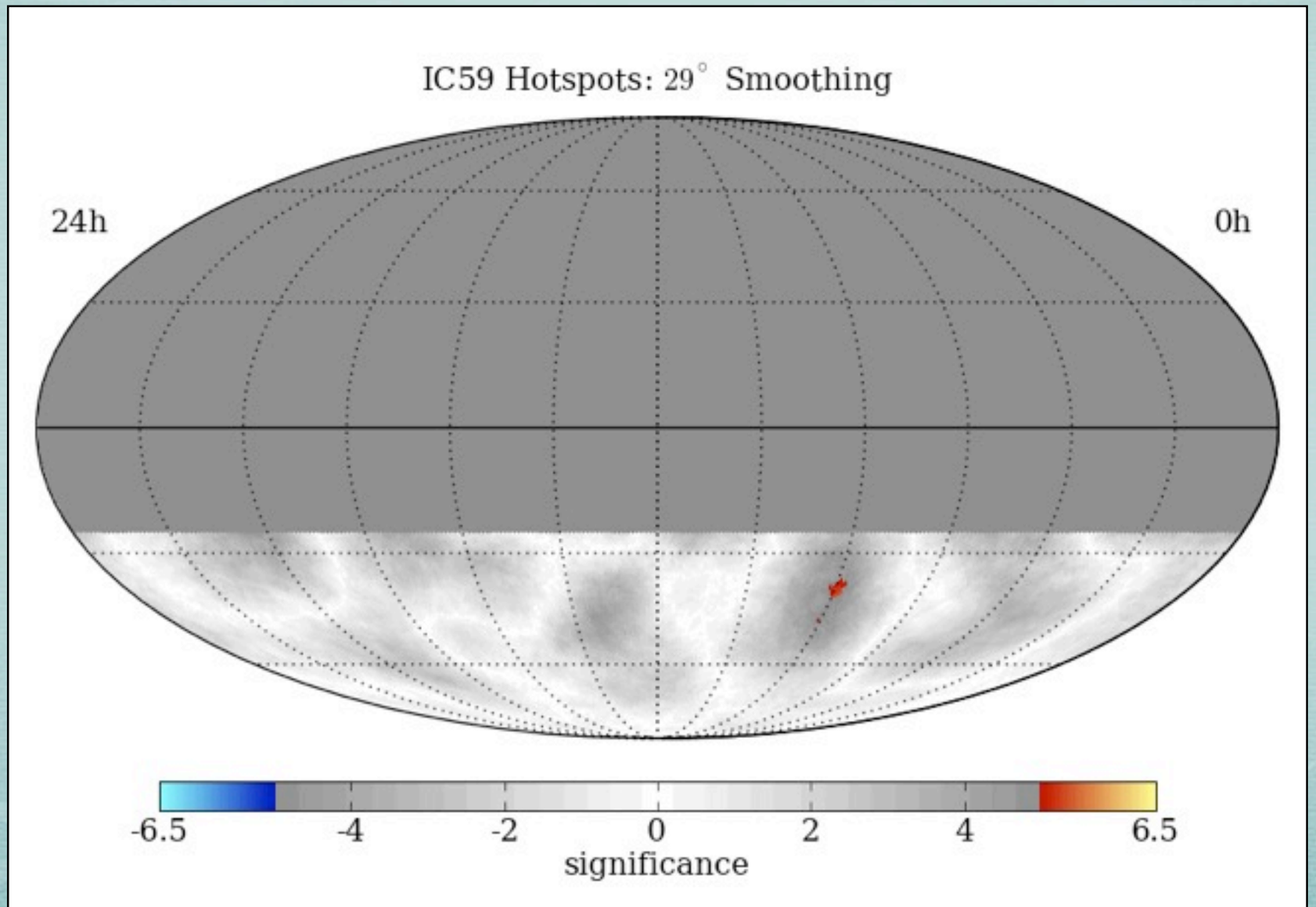

MAP SMOOTHING SCAN

Scan from 1 - 30° in smoothing
Different regions have different optimal angular smoothing
Significances are pre-trial

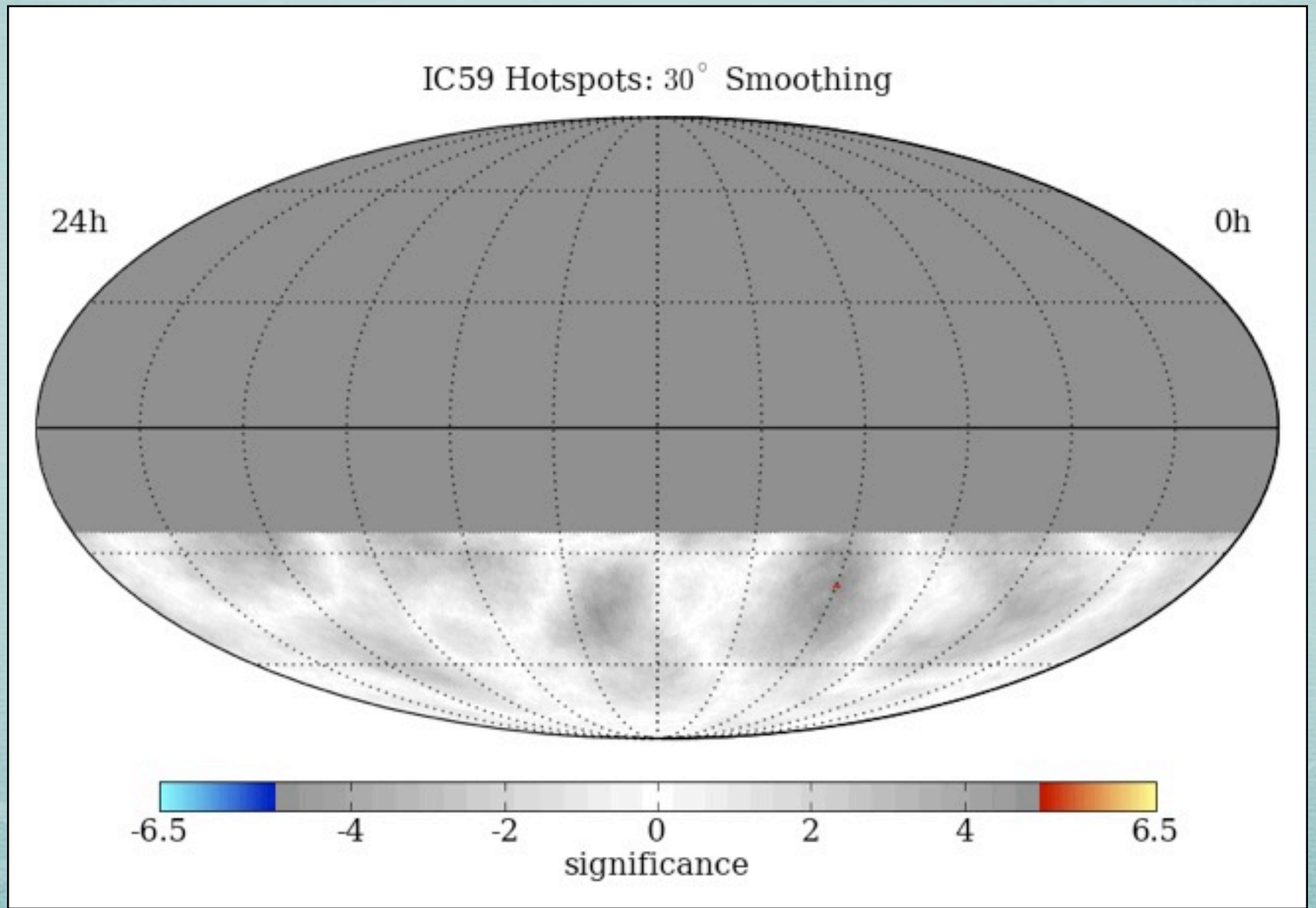

Identification of significant structures

region	right ascension	declination	optimal scale	peak significance	post-trials
1	$(122.4^{+4.1}_{-4.7})^\circ$	$(-47.4^{+7.5}_{-3.2})^\circ$	22°	7.0σ	5.3σ
2	$(263.0^{+3.7}_{-3.8})^\circ$	$(-44.1^{+5.3}_{-5.1})^\circ$	13°	6.7σ	4.9σ
3	$(201.6^{+6.0}_{-1.1})^\circ$	$(-37.0^{+2.2}_{-1.9})^\circ$	11°	6.3σ	4.4σ
4	$(332.4^{+9.5}_{-7.1})^\circ$	$(-70.0^{+4.2}_{-7.6})^\circ$	12°	6.2σ	4.2σ
5	$(217.7^{+10.2}_{-7.8})^\circ$	$(-70.0^{+3.6}_{-2.3})^\circ$	12°	-6.4σ	-4.5σ
6	$(77.6^{+3.9}_{-8.4})^\circ$	$(-31.9^{+3.2}_{-8.6})^\circ$	13°	-6.1σ	-4.1σ
7	$(308.2^{+4.8}_{-7.7})^\circ$	$(-34.5^{+9.6}_{-6.9})^\circ$	20°	-6.1σ	-4.1σ
8	$(166.5^{+4.5}_{-5.7})^\circ$	$(-37.2^{+5.0}_{-5.7})^\circ$	12°	-6.0σ	-4.0σ

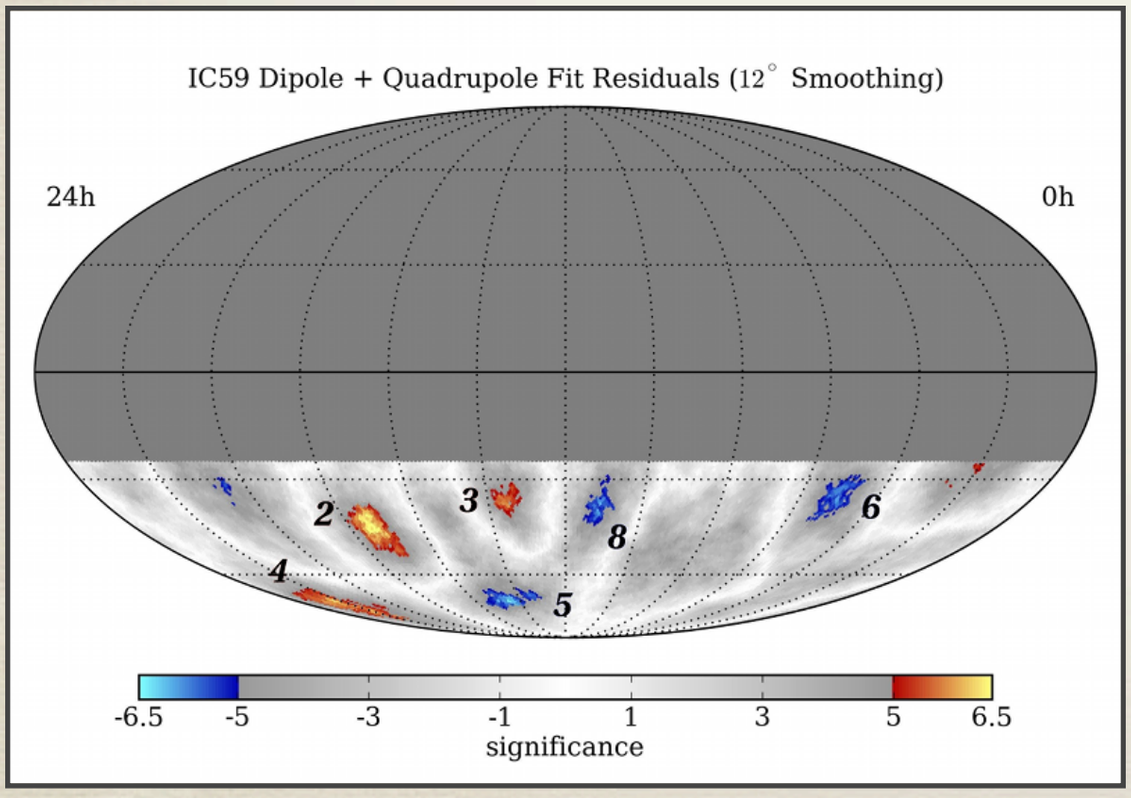

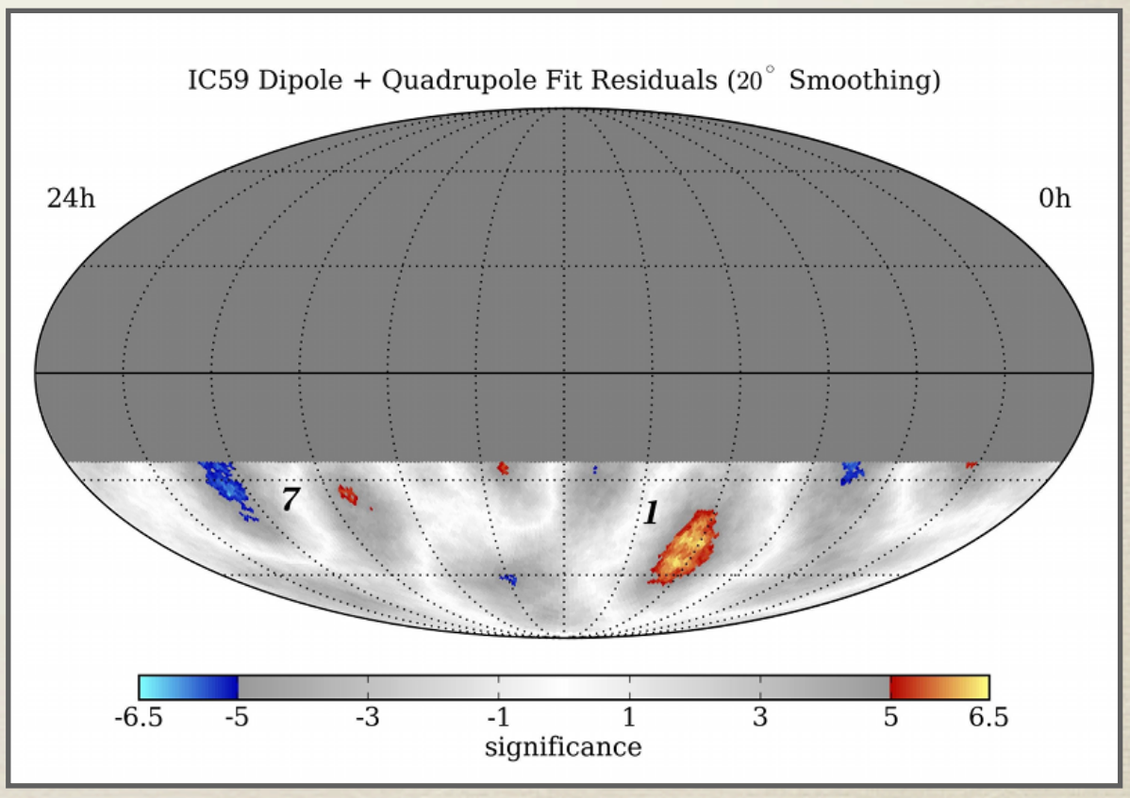

Systematics: previous data sets

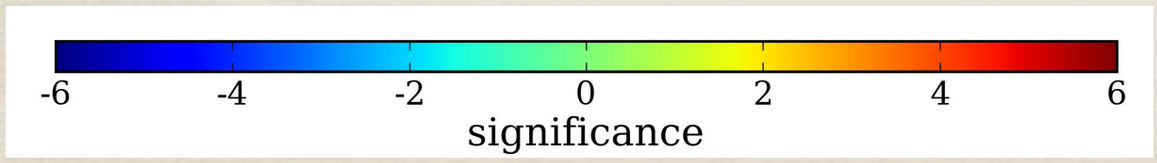

Different geometries, same structure

Signal grows with statistics

Systematics: previous data sets

IC22

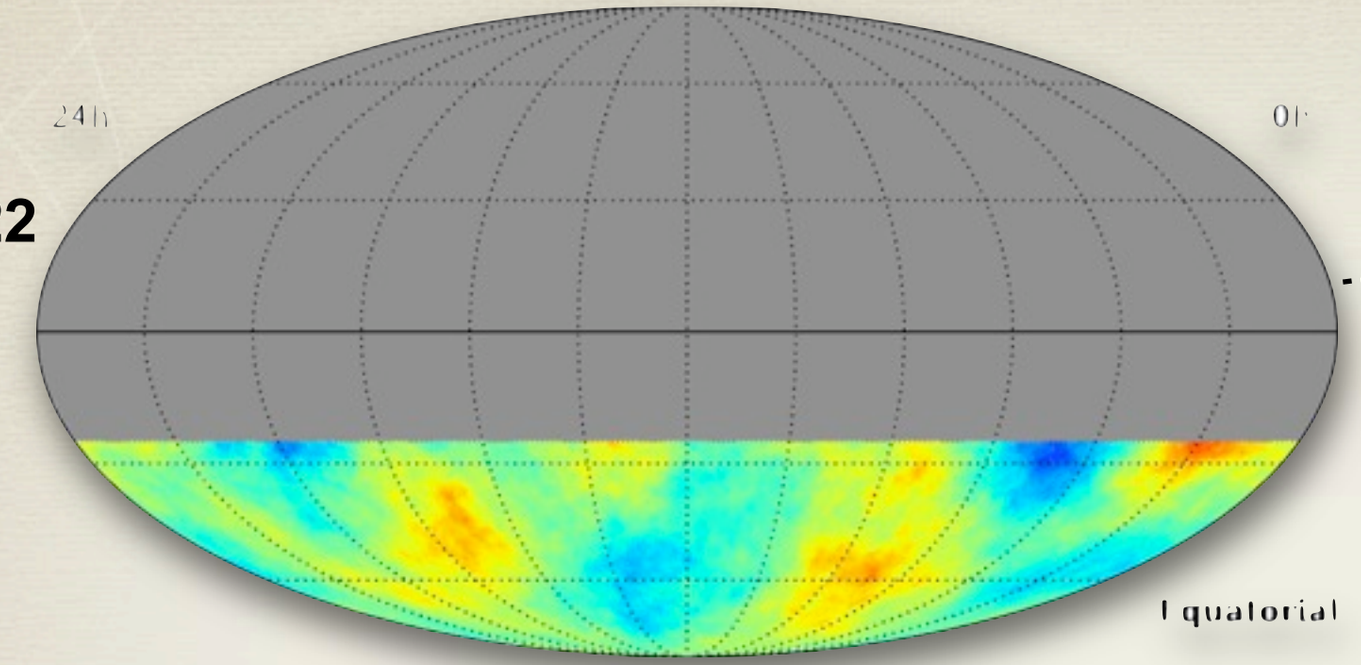

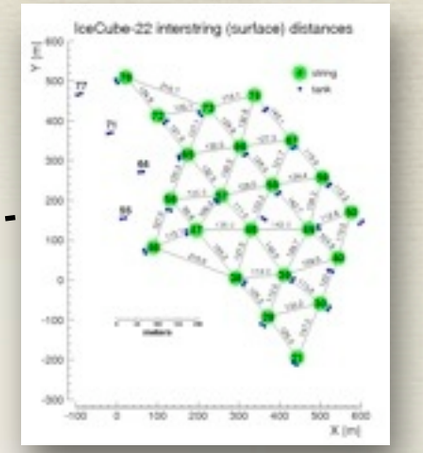

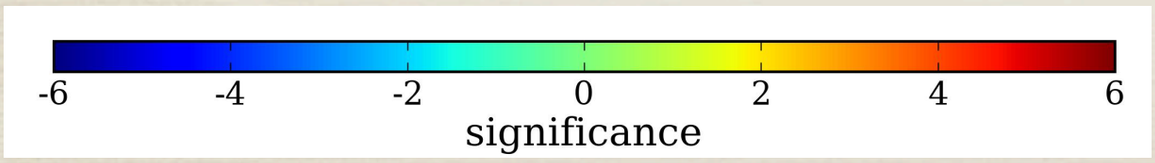

Different geometries, same structure

Signal grows with statistics

Systematics: previous data sets

IC22

IC40

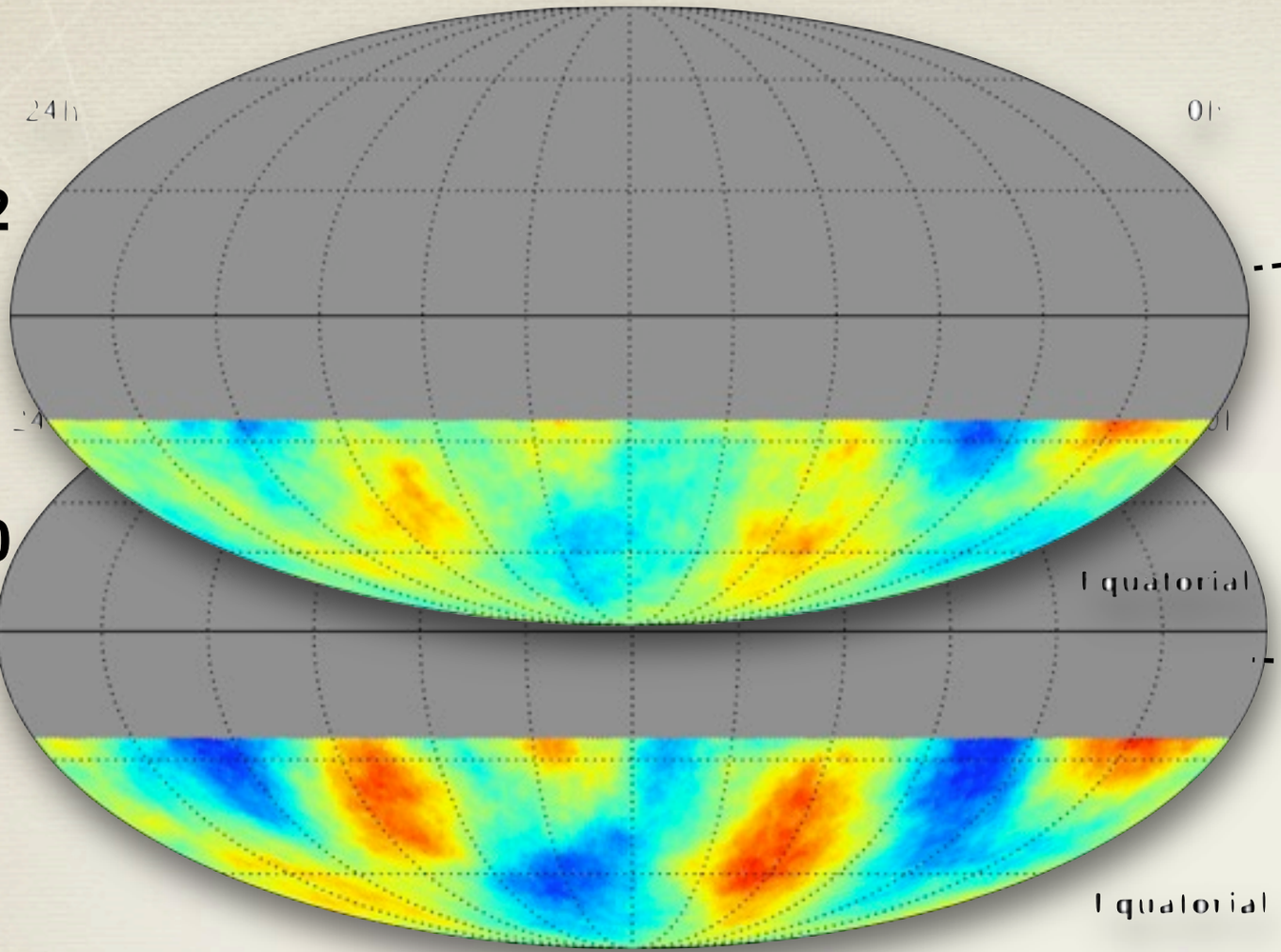

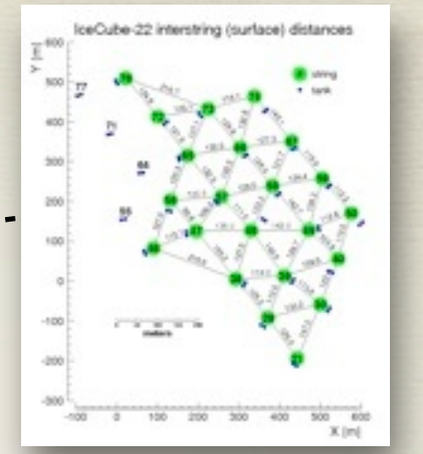

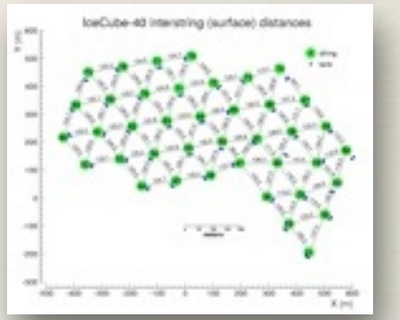

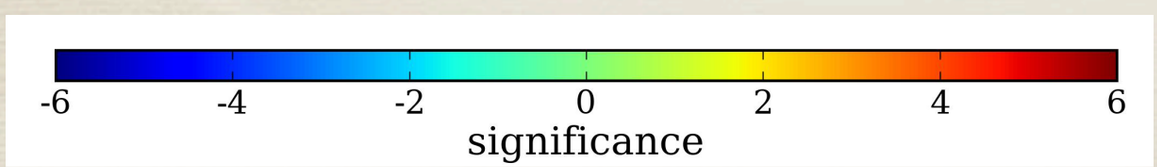

Different geometries, same structure

Signal grows with statistics

Systematics: previous data sets

IC22

IC40

IC59

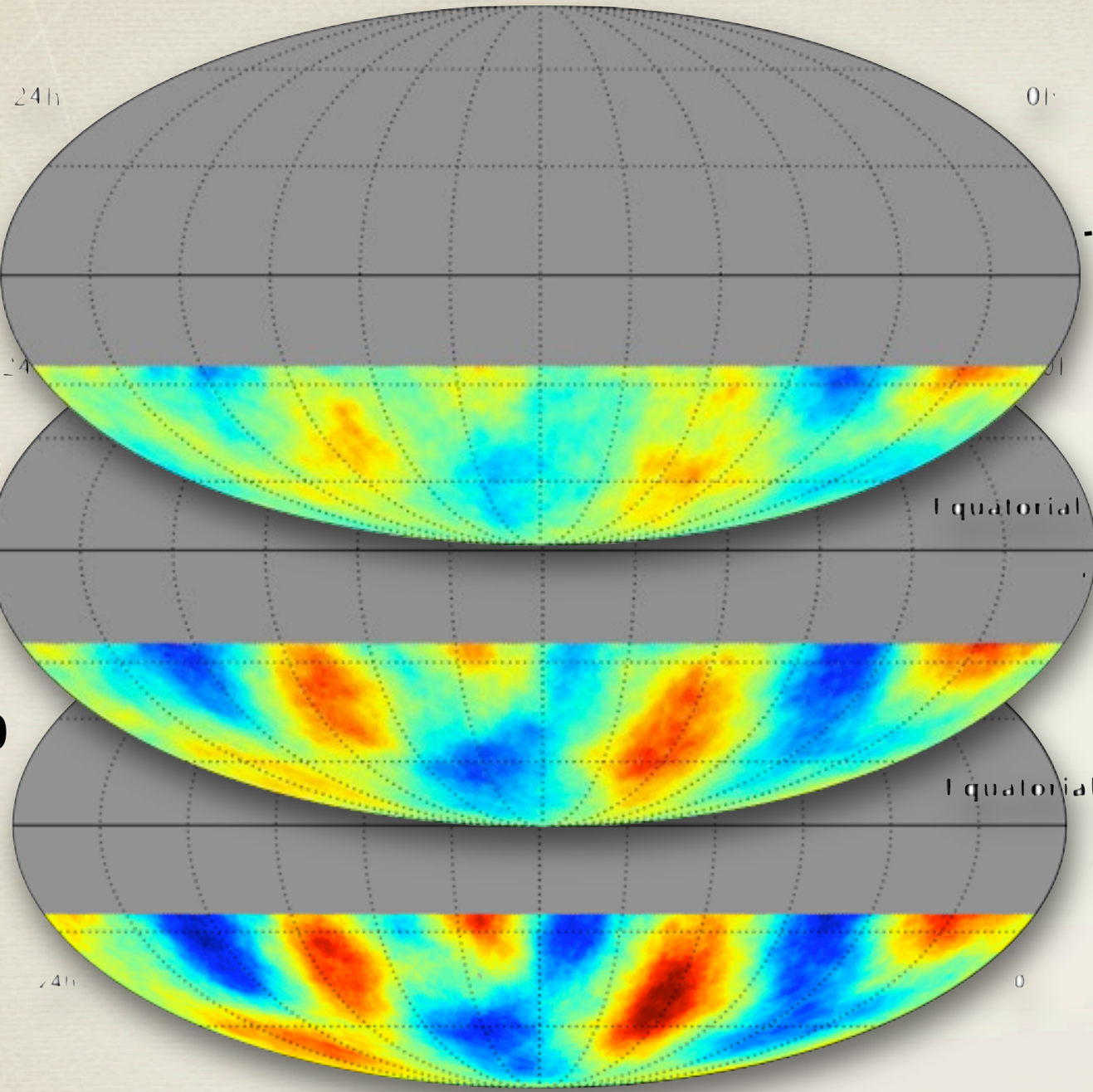

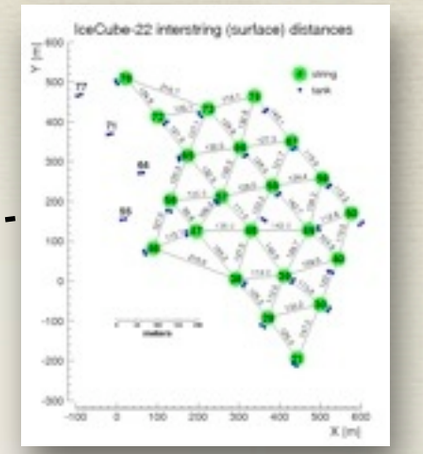

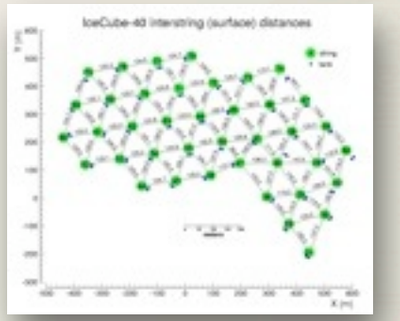

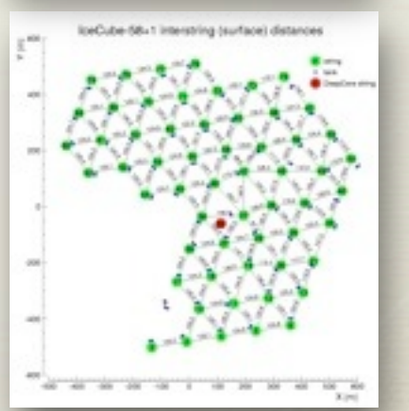

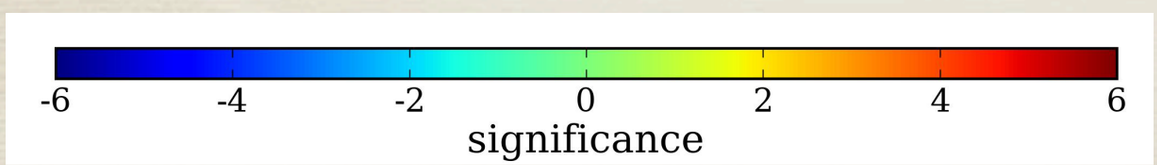

Different geometries, same structure

Signal grows with statistics

Milagro + IceCube combined map

IceCube map contains all data from IC22, IC40 and IC59 data sets

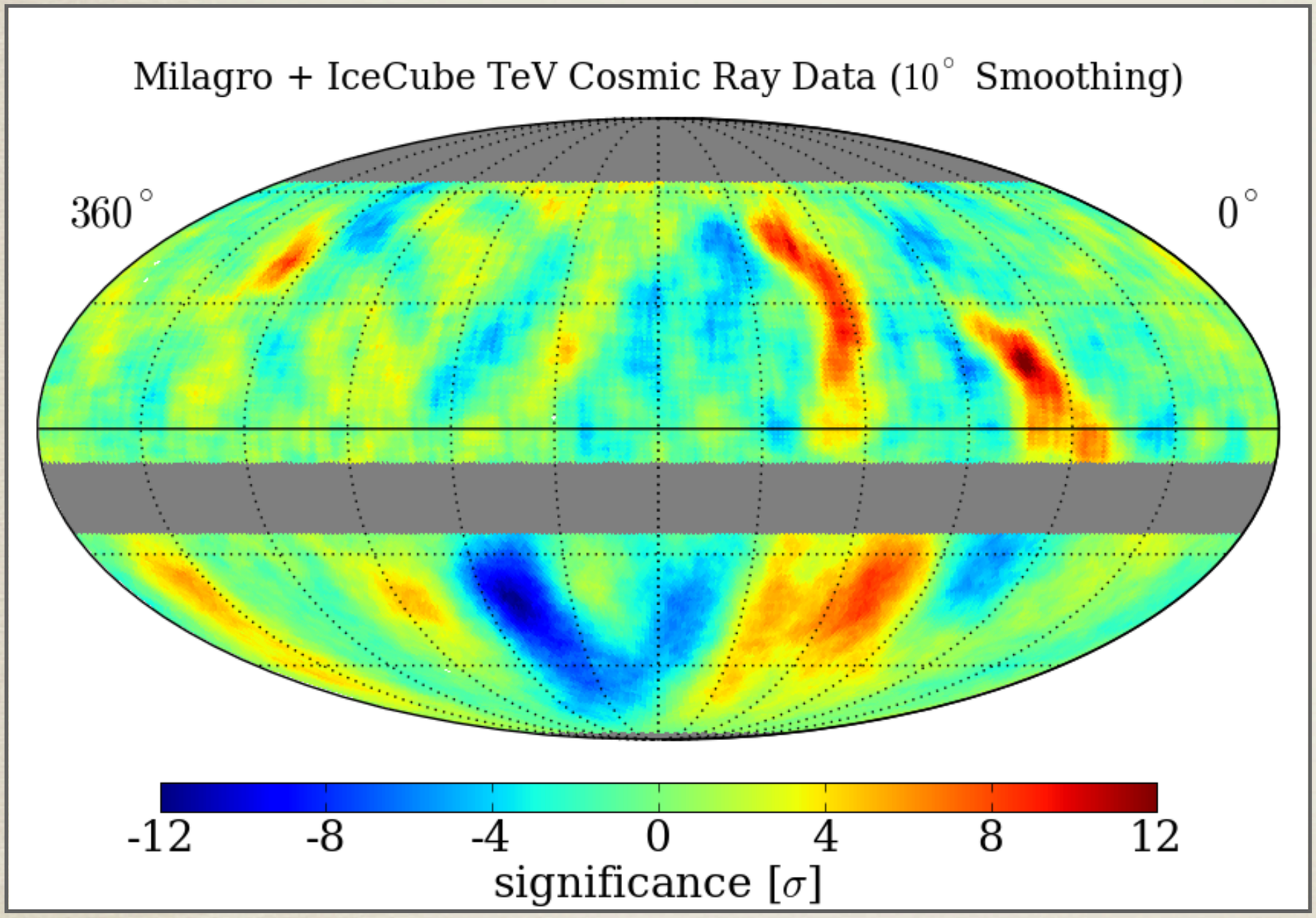

Milagro map:

[Abdo, A. A., et al. 2008, Phys. Rev. Lett., 101, 221101]

- **2.2 x 10^{11}** events
- time scrambling (2 hr)
- 10° smoothing
- median energy **1 TeV**

IceCube map:

- **5.6x10^{10}** events
- time scrambling (4 hr)
- 10° smoothing
- median energy **20 TeV**

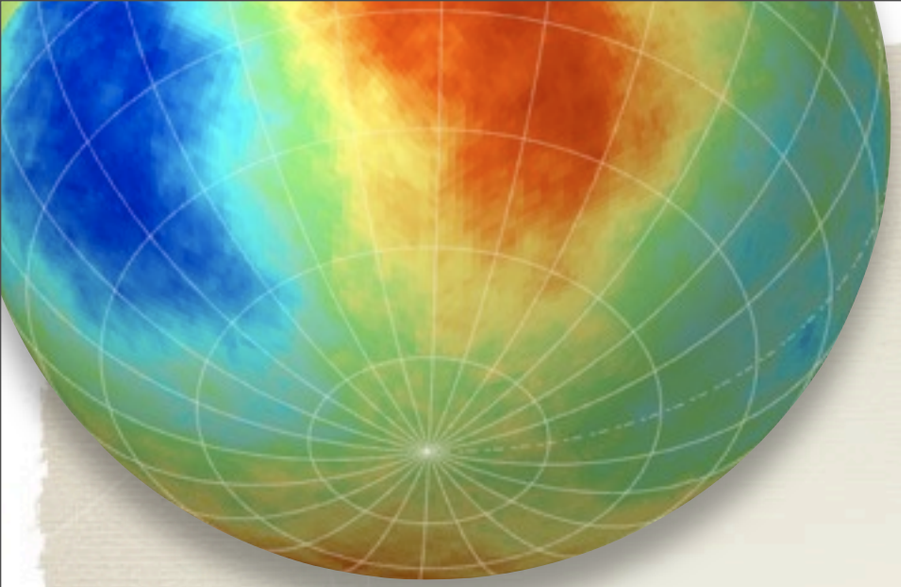

Conclusions

- **IceCube** detector was **completed in December 2010** and is now taking data in its final configuration (86 strings).
- **Large scale anisotropy**:
  - First observation of sidereal anisotropy @ 400 TeV in southern hemisphere.
  - Sidereal anisotropy at 20 TeV confirms previous observation.
  - Indication of a persistence of anisotropy @ 400 TeV: evidence of a "dip".
- **Small and medium scale** structures:
  - Southern sky in TeV cosmic rays shows significant anisotropy across a wide range of angular scales (10-180 degrees).
- **The origin of the anisotropy is still unknown.**